LEVEL (2)

AD A068971

AFFDL-TR-76-55
Volume II

20000726133

Aerodynamic Stability Technology for Maneuverable Missiles. Vol. II. Asymmetric Vortex Effects Computer Program

Martin Marietta Corporation
Orlando Division
P. O. Box 5837
Orlando, Florida 32805

March 1979

Technical Report AFFDL-TR-76-55, Vol. II
Final Report for period February 1975 - December 1976

Approved for public release; distribution unlimited

PREPARED FOR:

Air Force Flight Dynamics Laboratory
Air Force Wright Aeronautical Laboratories
Air Force Systems Command
Wright-Patterson Air Force Base, Ohio 45433

015

NOTICE

When Government drawings, specifications, or other data are used for any purpose other than in connection with a definitely related Government procurement operation, the United States Government thereby incurs no responsibility nor any obligation whatsoever; and the fact that the government may have formulated, furnished, or in any way supplied the said drawings, specifications, or other data, is not to be regarded by implication or otherwise as in any manner licensing the holder or any other person or corporation, or conveying any rights or permission to manufacture, use, or sell any patented invention that may in any way be related thereto.

This report has been reviewed by the Information Office (OI) and is releasable to the National Technical Information Service (NTIS). At NTIS, it will be available to the general public, including foreign nations.

This technical report has been reviewed and is approved for publication.

William H. Lane
WILLIAM H. LANE
Project Engineer
Control Dynamics Branch

R. O. Anderson
R. O. ANDERSON, Chief
Control Dynamics Branch
Flight Control Division

FOR THE COMMANDER

James R. Stanley
J. R. STANLEY, Col, USAF
Chief, Flight Control Division
Air Force Flight Dynamics Laboratory

"If your address has changed, if you wish to be removed from our mailing list, or if the addressee is no longer employed by your organization please notify AFFDL/FGC ,W-PAFB, OH 45433 to help us maintain a current mailing list".

Copies of this report should not be returned unless return is required by security considerations, contractual obligations, or notice on a specific document.

UNCLASSIFIED

SECURITY CLASSIFICATION OF THIS PAGE (When Data Entered)

14 **REPORT DOCUMENTATION PAGE**

READ INSTRUCTIONS BEFORE COMPLETING FORM

1. REPORT NUMBER 18 AFFDL TR-76-55, Vol-II	2. GOVT ACCESSION NO.	3. RECIPIENT'S CATALOG NUMBER
4. TITLE (and Subtitle) 6 Aerodynamic Stabil·ty Technology for Maneuverable Missiles. ~~Vol~~. II. Asymmetric Vortex Effects Computer Program		5. TYPE OF REPORT & PERIOD COVERED Final Report, February 1975 to December 1976
		6. PERFORMING ORG. REPORT NUMBER 14 OR-14,828
7. AUTHOR(s) 10 Gennaro F./Aiello Michael C./Bateman		8. CONTRACT OR GRANT NUMBER(s) 15 F33615-75-C-3052 new
9. PERFORMING ORGANIZATION NAME AND ADDRESS Martin Marietta Corporation Orlando Division, PO Box 5837 Orlando, FL 32805		10. PROGRAM ELEMENT, PROJECT, TASK AREA & WORK UNIT NUMBERS 12 96p.
11. CONTROLLING OFFICE NAME AND ADDRESS U.S. Air Force Flight Dynamics Laboratory Wright-Patterson Air Force Base Dayton, Ohio		12. REPORT DATE 11 Mar[illegible]79
		13. NUMBER OF PAGES 90
14. MONITORING AGENCY NAME & ADDRESS (if different from Controlling Office) 9 Final rept. Feb 75-Dec 76		15. SECURITY CLASS. (of this report) Unclassified
		15a. DECLASSIFICATION/DOWNGRADING SCHEDULE

16. DISTRIBUTION STATEMENT (of this Report)

Approved for public release; distribution unlimited

17. DISTRIBUTION STATEMENT (of the abstract entered in Block 20, if different from Report)

18. SUPPLEMENTARY NOTES

19. KEY WORDS (Continue on reverse side if necessary and identify by block number)

Asymmetric lee-side vortices
High angles of attack
Slender missile configurations
Induced side forces and yawing moments

20. ABSTRACT (Continue on reverse side if necessary and identify by block number)

A procedure for estimating the effects of asymmetric lee-side vortices on slender missile configurations with and without tails is developed, using both theoretical and empirical inputs. A computerized model of the procedure which calculates induced side forces, yawing moments, tail forces and rolling moments is presented. Program flow charts, input instructions and sample cases are provided. Comparisons between experimental data and program calculations show acceptable preliminary design level accuracies.

DD FORM 1 JAN 73 1473 EDITION OF 1 NOV 65 IS OBSOLETE

403 238

JOB

UNCLASSIFIED

SECURITY CLASSIFICATION OF THIS PAGE (When Data Entered)

FOREWORD

This report was prepared for the U.S. Air Force Flight Dynamics Laboratory, Wright-Patterson Air Force Base, Ohio, under Contract Number F33615-75-C-3052.

The work reported herein was performed at the Orlando Division of Martin Marietta Aerospace as a part of Project 8219, "Stability and Control for Aerospace Vehicles", Work Unit 82190117, "Aerodynamic Stability Technology for Maneuverable Missiles".

This work was performed during the period February 1975 to December 1976. The principal investigators were J. E. Fidler and G. F. Aiello. The technical monitor for AFFDL was Mr. William H. Lane.

TABLE OF CONTENTS

LIST OF ILLUSTRATIONS

LIST OF SYMBOLS

A	Reference area
a	Body radius
AR	Tail aspect ratio
C_A	Axial force coefficient
C_{dc}	Crossflow drag coefficient
CETAMC	Yawing moment coefficient
C_L	Lift coefficient
C_ℓ	Rolling moment coefficient
C_N	Normal force coefficient
C_n	Yawing moment coefficient
C_Y	Side force coefficient
d	Missile body diameter
e	Axial extent of base influence
F	Vorticity flux
g	Axial distance over which boundary layer is shed to form vortex
h	Vortex street lateral dimension
K	Coefficient in vortex strength equation
l	length
ℓ	Vertical distance between vortices of like sign
M	Mach number
m	Number of vortices in wake at a given axial location on the body
n	Frequency with which vortices of like sign are shed
p	Spanwise distance from tail root to tip
$\bar{R}$	Radial limit of vortex influence on a body

LIST OF SYMBOLS (CONT'D)

R_e	Reynolds number
r	Radial distance from center of body
S	Strouhal number = nd/Vsinα
U_s	Circumferential velocity at edge of boundary layer at separation
V	Freestream velocity
v	Velocity induced normal to tail leading edge in the y direction
x	Axial distance along body
Y	Side force
y	Lateral distance normal to body axis
z	Distance above and normal to body axis
α	Angle of attack
δ	Nose hald angle
σ	Angle between growing vortex cores and body axis
θ_s	Circumferential separation point angular orientation
ξ	Angle between street vortex cores and body axis
Γ	Vortex strength
Γ(x)	Local value of strength in a growing vortex
Γ/Vdsinα	Vortex dimensionless strength parameter
ρ	Freestream density
ϕ	Roll angle
χ	Separation angle parameter
λ	Tail taper ratio

SUBSCRIPTS

a	Axial direction
B	Body
c	Crossflow
i	Induced, vortex indicator
L, R	Left and right sides of body, respectively
o	Initial condition
s	Denotes vortices, starting with third from missile nose
T	Tail
x	Denotes conditions at axial station x
1, 2	First and second vortices, respectively

SUMMARY

A computerized engineering model is presented for estimating the effects of asymmetric lee-side vortices on slender missile configurations. The procedure was developed using both empirically determined quantities and theoretical techniques. Empirical inputs define both vortex locations and street vortex strengths; whereas, potential flow considerations guide in the definition of initial vortex strengths and induced forces and moments. The procedure is applicable to bodies with and without tails. Calculable effects are: induced side forces, yawing moments, tail forces, and rolling moments. The procedure was applied to a number of different combinations of geometries and flow conditions and the results compared against experimental data. These comparisons, while not exact, have shown the procedure to be suitably accurate for preliminary design purposes. Using this procedure, a user can estimate the magnitude but not necessarily the direction of vortex induced forces and moments and the angle of attack at which they first appear. Uncertainity in direction is attributed to the randomness associated with formation and subsequent shedding of the initial pair of vortices. Nose geometry irregularities greatly influence the side of the body from which the initial vortex separates.

A users manual for this computerized procedure is also provided. The manual includes user instructions, a program listing, sample inputs, and sample outputs.

1.0 INTRODUCTION

In recent years, increased maneuverability requirements for air-to-air missiles have dictated corresponding increases in angles of attack, particularly for those vehicles which perform slewing maneuvers. Maximum angles for such missiles can now reach 180 degrees. As a result of these developments, the flow fields with which the aerodynamicist has to deal are much more complex, and traditional methods for predicting aerodynamic characteristics are inadequate to deal with all the problems involved. One example of method deficiency is found in the angle of attack range 25-50 degrees. Here, steady, asymmetric vortex patterns usually develop in the body wake and can induce large side forces and yawing and rolling moments which are detrimental to missile controllability. Few methods are currently available for predicting these forces and moments or for analyzing the complex flow fields which produce them. The effects are particularly acute in the subsonic-transonic speed range. At Mach numbers greater than about 1.5, however, they tend to diminish rapidly.

The flow phenomena involved and their effects have received considerable attention recently,[1-9] although wake vortex effects and asymmetry have been reported by earlier authors.[10-13] Among the earliest studies were those of Allen and Perkins [10] and Perkins and Jorgensen,[11] in which some of the basic flow structure in the wake was investigated and the onset of vortex asymmetry observed. More recent work by Thomson and Morrison[1] and Thomson [2,8] determined details of the wake flow field and the associated vortex characteristics through direct flow probing. In that work, attention was drawn to the strong similarities between the three-dimensional asymmetric wake and its two-dimensional counterpart, the von Karman vortex street.

Measurements were made of vortex strengths, spacing and shedding frequency. The data of Reference 1 have often formed the basis for follow-on work to determine vortex effects on slender missiles[5,8] or for the computation of wake flow characteristics.[6] The measurements form part of the basis for the present work, with suitable modifications for various flow parameter changes.

Recent wind tunnel investigations performed by Martin Marietta showed marked evidence of asymmetric vortex effects. The magnitudes of typical induced quantities are shown in Figures 1 and 2. In Figure 1, pitch and yaw plane moment data up to 60 degrees angle of attack are shown for an isolated body composed of an ogive-cylinder of 10:1 total slenderness ratio. Beginning around 25 degrees angle of attack, considerable yawing moments were induced due to asymmetries. The addition of tails to the body (Figure 2) results in the generation of yawing moments which are almost as large as the pitching moments. In addition to the problem of magnitudes is that of unpredicatable sign.[1,3,4] Random changes in direction of forces and moments have been observed, sometimes related to changing flow conditions, but often interpreted to be caused by small manufacturing imperfections near the missile nose[1,3,4]. In fact, significant changes in induced force and moment magnitudes and signs can be produced by rotation of all or parts of the body.[1,3,4] This has further, serious implications for missile controllability.

It is clear that techniques are required for calculating the forces and moments induced by asymmetric vortex wakes. Some work has already been done in this area[8,9] for slender bodies at subcritical crossflow Reynolds number. The procedure presented in this document deals with that case also, but goes further in considering supercritical crossflow Reynolds and Mach

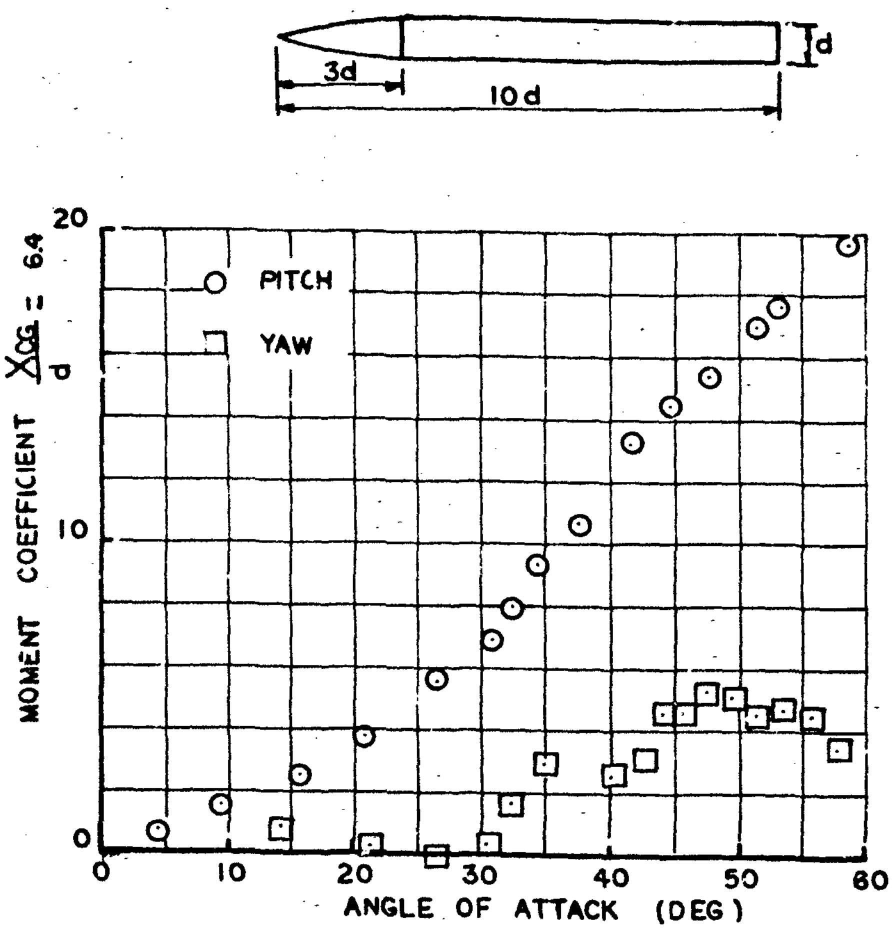

FIGURE I COMPARISON OF PITCH AND YAW MOMENTS
(ISOLATED BODY M=0.8)

number effects for bodies with and without tails. This technique is semi-empirical, drawing upon the experimental evidence referred to above, but modifying it for different flow conditions and supplementing it with analytical results and techniques. To make this technique more readily useable, it has been programmed for digital computation.

The layout of this document is as follows: first, a general description of the flowfield is presented, followed by descriptions of the techniques used to model the asymmetric vortex wake and calculate the induced forces and moments. Following these, there is a section presenting comparisons between predicted results and experimentally measured data. Finally, there is the information necessary to operate the program, i.e.,user instructions, a program flow chart and listing, sample inputs/outputs and an indication of program limitations.

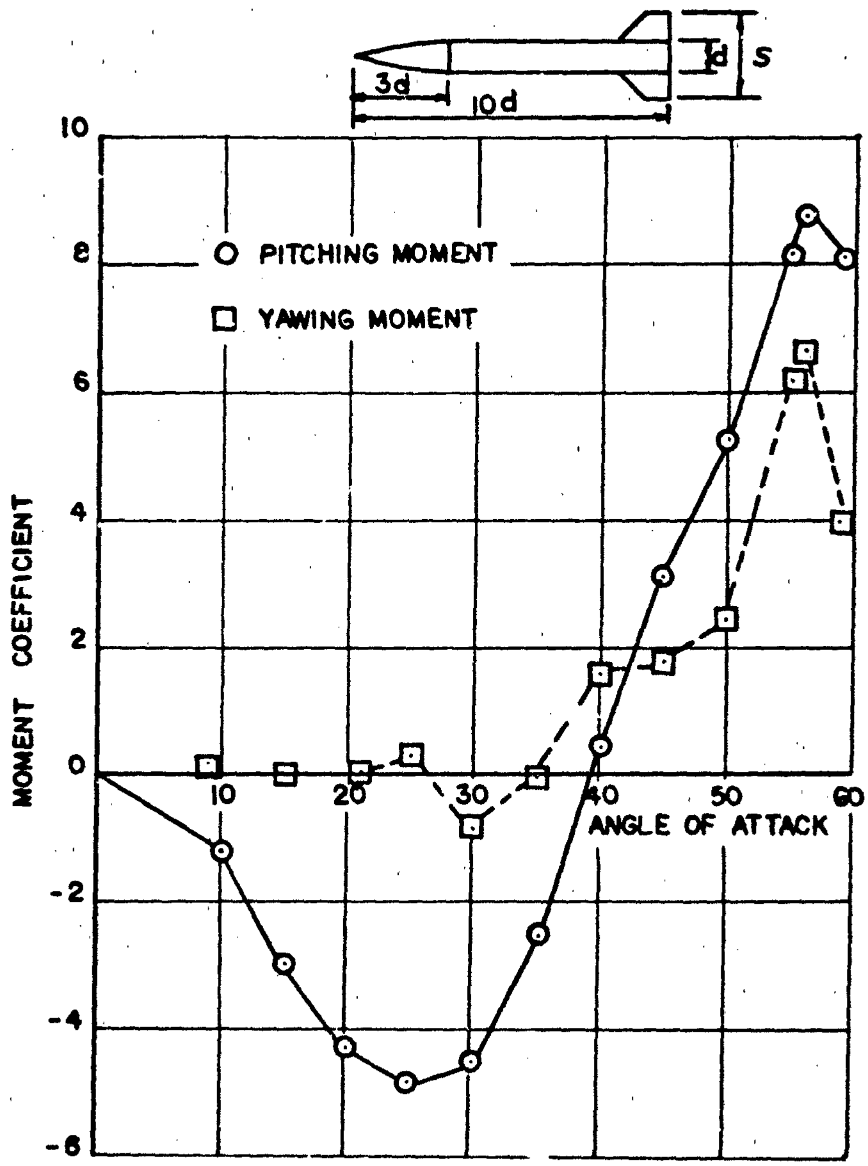

FIGURE 2 COMPARISON OF PITCHING AND YAWING MOMENTS
(BODY-TAIL M=0.8)

2.0 FLOWFIELD DESCRIPTION

When a slender missile body is placed at angle of attack in a uniform flow, the boundary layer generally separates on either side of the body and forms a lee side wake. Separation usually begins near the rear when the missile reaches about 6 degrees angle of attack. The wake takes the form of a pair of symmetrically-disposed, counter-rotating vortices fed by vorticity shed from the separating boundary layer. As angle of attack increases the axial extents, sizes and strengths of the vortex increase also.

In general, vortex size and strength also increase towards the rear of the body. Several authors have formulated descriptions of vortex development along slender bodies in terms of two-dimensional, impulsively-started flows around cylinders. These formulations relate flow development with time, measured either from the beginning of impulsive two-dimensional motion or from the instant a fluid particle makes contact with a three-dimensional body. In the latter case, time is defined by distance travelled along the body and the axial component of freestream velocity. For the two-dimensional case, the motion of the vortex cores as time passes (i.e., vortex size and strength increase) theoretically follows a path known as the Föppl line.[14] Use has been made of this result in the present work, as will be described later.

When the body angle of attack reaches about 25 degrees, the symmetric nature of the wake disappears. The two vortices are joined by a third, beginning again at the body rear, and the wake becomes asymmetric. As angle is increased further, more vortices join the flow until the wake contains several which have been shed from the body. An idealized model of the flow field is shown in Figure 3. A section taken through the wake shows

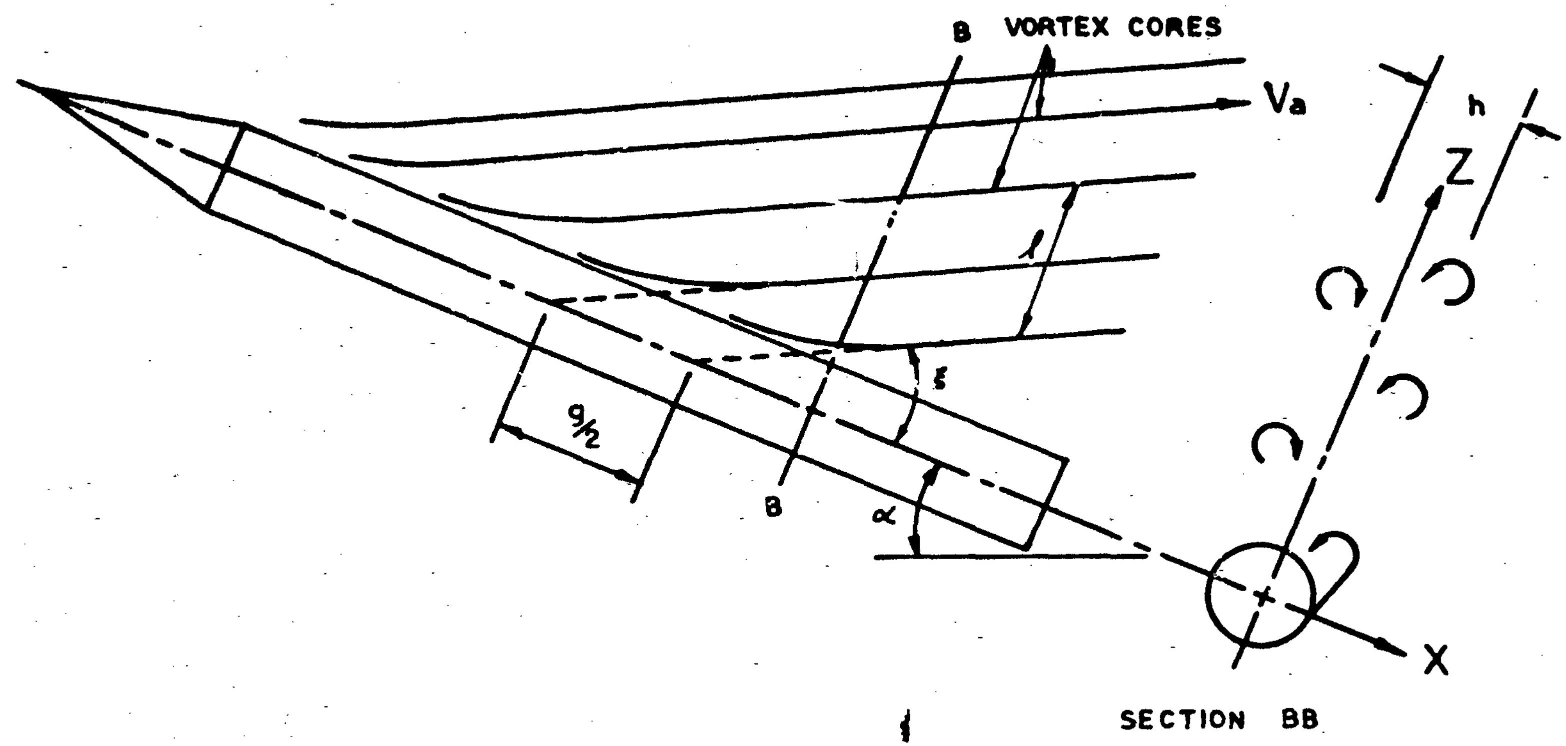

FIGURE 3 SCHEMATIC OF LEE SIDE VORTEX PATTERN

it to resemble the von Karman vortex street, well known in the literature on two-dimensional flows. Not all of the vortices are fully shed, however; two usually remain close to the body, receiving vorticity from the shedding boundary layers. If angle of attack continues to increase these, too, will be fully shed into the wake when their strength reaches some critical value. Their places will be taken by yet other growing vortices.

While a growing vortex is receiving vorticity from the boundary layer, i.e., before it reaches full strength, it tends to stay close to the body. Thomson and Morrison[1] showed schlieren photographs which implied that the vortex core is somewhat curved while it is forming. Not until full strength has been reached does the core become straight and parallel to the rest of the vortices in the street. This core behavior is indicated in Figure 3.

It has been determined that a marked similarity exists between the manifestations and effects of two- and three-dimensional asymmetric vortex wakes.[1] In fact, the von Karman street stability criterion that the ratio of lateral street dimension, h, to the distance between vortices of like sign, ℓ, given by $h = 0.281\ell$, has been shown to apply to both cases (Figure 3). However, in the wake of Figure 3 no lateral motion of the vortex cores relative to the body takes place. The two-dimensional phenomenon of increasing distance between vortex core and body as time increases is analogized in the same way as for the symmetrical vortices. That is to say, the wake is steady and the motion of a fluid particle along a (stationary) vortex core may again be described in equivalent time by its axial velocity and distance traveled. Through use of this analogy, Thomson[2] and Thomson and Morrison [1] were able to deduce the strengths of asymmetric wake vortices as well as their effects upon body crossflow drag. Thomson [8] recently extended this work to deal with induced side forces and yawing moments on bodies at subcritical crossflow Reynolds numbers.

At still higher angles of attack, say greater than 50 degrees, the wake begins to display unsteadiness. The vortex cores show definite lateral displacements relative to the body and the induced forces and moments become time-dependent. The procedure presented in this document does not consider this case. Attention is directed only to the phenomena in the angle of attack range from 25 to 50 degrees and their effects upon missile aerodynamic characteristics.

3.0 CONSTRUCTION OF FLOW FIELD MODEL

Development of a procedure to predict the effects of an asymmetric vortex wake on configuration aerodynamics requires the development of a realistic flow field model. A flow field model, reflecting the state-of-the art, can be developed using semi-empirical inputs based on the data of References 1, 2, 8 and 16 and theoretical results[14,15]

Vortex strengths and locations have been made compatible with the findings of Reference 1 and suitably scaled to broaden their ranges of applicability. In addition, theoretical results on the locations of wake vortices and their images have been introduced and the contribution of nose potential lift to vortex strength has been considered. Both shed and growing vortices are treated, making use in part, of a vorticity-conservation concept.[6] Each of the above components of the model is described in detail beginning with vortex strength.

Vortex Strength

Detailed flow surveys have shown[1,8] that not all the wake vortices are of the same strength. Generally, the first vortex from the nose originates near the nose/body junction and has the smallest strength in the wake, Γ_1, say. The second vortex separates soon after the first and has a somewhat higher strength, Γ_2. From the third vortex onwards, all have approximately the same strength, $\Gamma_s (>\Gamma_2)$, and their spacing and strength are analogous to those of the vortices in a von Karman street. While the first and second vortex strengths will contain contributions from the (potential) nose lift, the "street" vortices are wholly fed with vorticity from the separating body boundary layer. Reference 8 presents detailed information on dimensionless vortex strength, Γ_s, for various angles of attack at subcritical crossflow Reynolds number. For the first two vortices, strength is calculated using concepts from potential flow theory.

The first and second vortex strengths must contain a contribution from the potential flow lift of the nose. The strength of the first vortex, Γ_1, may be estimated if it is assumed that the nose is replaced by a horizontal lifting line of constant strength, Γ_1 located at the nose/body junction (Figure 4). All of the nose lift is assumed generated by this line and the associated trailing vortices will have its strength provided they receive no further vorticity, from the shedding boundary layer for example. The first vortex shed, near the nose body junction, will probably contain only potential-flow-generated circulation. To calculate vortex strength Γ_1 is straight forward. It can be shown[15] that the coefficients of normal and axial force acting on the nose are predicted by slender body theory to be:

$$C_N = 2 \sin \alpha \text{ and } C_A = C_{A_o} - \sin^2 \alpha$$

where the reference area is that of the body cross section. Converting these quantities to lift coefficient yields

$$C_L = C_N \cos \alpha - C_A \sin \alpha$$

If C_{A_o} is assumed negligible (as it will be, compared to the axial forces generated at the high angles of attack here) this expression becomes after some manipulation

$$L = \frac{\rho}{8} V^2 \pi d^2 (2 \sin \alpha \cos \alpha + \sin^3 \alpha)$$

$$= \rho \Gamma_1 dV$$

The latter expression is the well-known Kutta-Joukowski theorem. Finally, the equation may be rearranged to yield:

$$\frac{\Gamma_1}{Vd \sin \alpha} = \frac{\pi}{8} (2 \cos \alpha + \sin^2 \alpha) \qquad (1)$$

This dimensionless vortex strength may be compared with measurements from flow field surveys.[1] Using an angle of 30 degrees, equation (1) yields a dimensionless strength of 0.78. The corresponding measured strengths

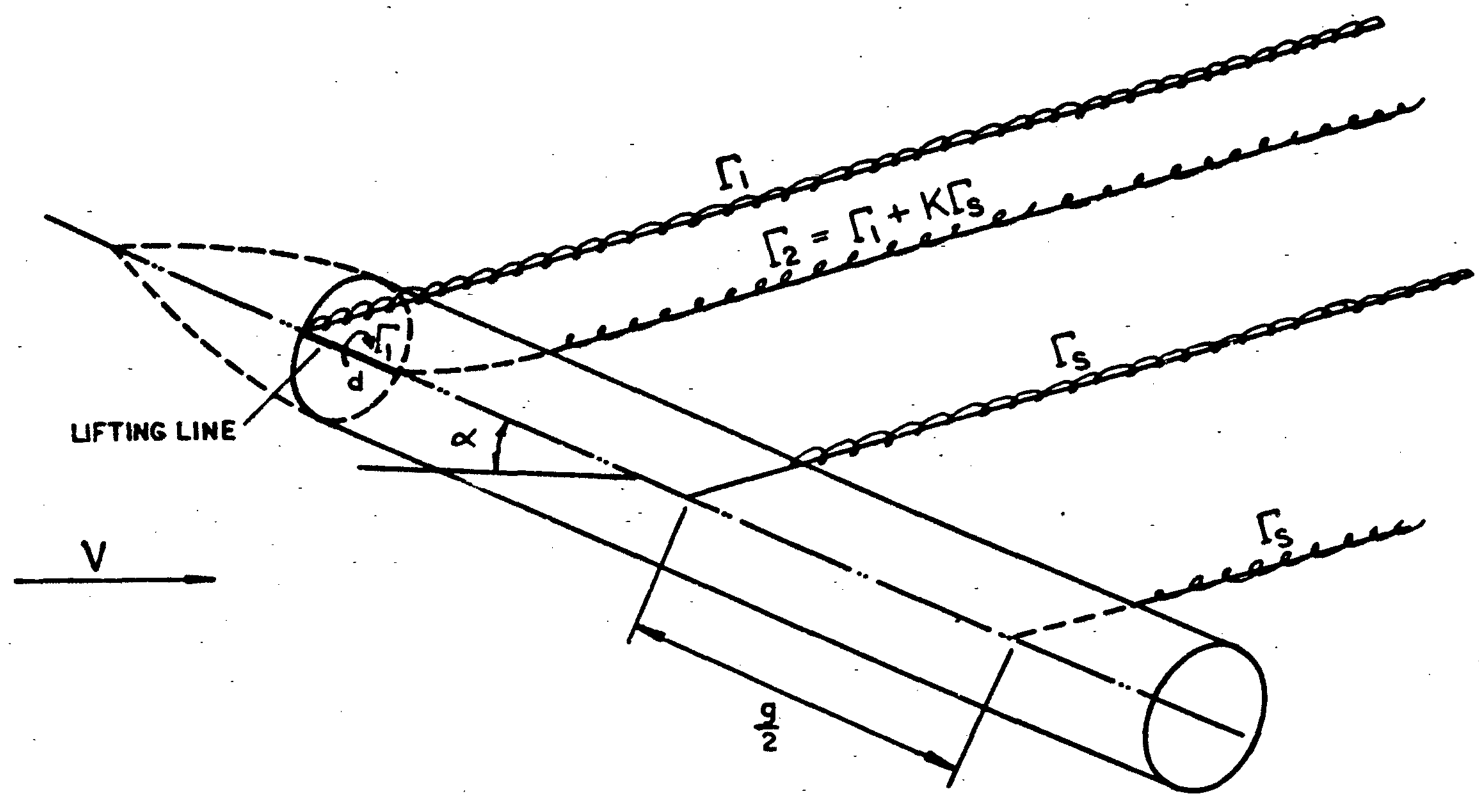

FIGURE 4 SCHEMATIC OF FLOWFIELD MODEL

from Reference 1 show a range of values from 0.3 to 1.1 with a mean value of 0.7. This compares quite well with the predicted value. Where it is found that the first vortex is shed forward of the nose/body junction, its strength is simply determined by using the local nose diameter in equation (1).

There should be little or no effect of Reynolds number on Γ_1 since the strength is determined by potential flow considerations. On the other hand, Γ_s is wholly produced by visous flow and is strongly affected by crossflow Reynolds number (R_e), which influences the characteristics of the boundary layer shed to form the street vortices. The second vortex, being shed downstream from the nose/body junction, is modeled here as a "mixed vortex," i.e., a potential flow vortex which receives additional vorticity from the shedding boundary layer just aft of the nose (Figure 4). Formally, Γ_2 is expressed as:

$$\Gamma_2 = \Gamma_1 + K\,\Gamma_s$$

K was found empirically to be about 0.22 from the wake survey data of Reference 1.

For street vortex strength at subcritical R_{e_c}, the data shown in Figure 5 were used [8]. In order to scale Γ_s for supercritical R_{e_c}, use was made of von Karman's result[14] that crossflow drag coefficient, C_{dc}, is approximately proportional to the street vortex strength, Γ_s (the expression for C_{dc} contains terms in Γ_s and Γ_s^2; however, the latter accounts for less than 10 percent of the total; hence, C_{dc} is approximately proportional to Γ_s). Data obtained from Martin Marietta investigations into crossflow drag[16] produced the information of Figure 6, which shows that for low crossflow Mach number, crossflow Reynolds number has a strong influence on crossflow drag. Above the critical crossflow Reynolds number (about 10^5), C_{dc} shows a significant decrease below the subcritical value. Hence, Γ_s, too, will be significantly reduced. An increase in crossflow Mach number, M_c, is required to increase both C_{dc} and

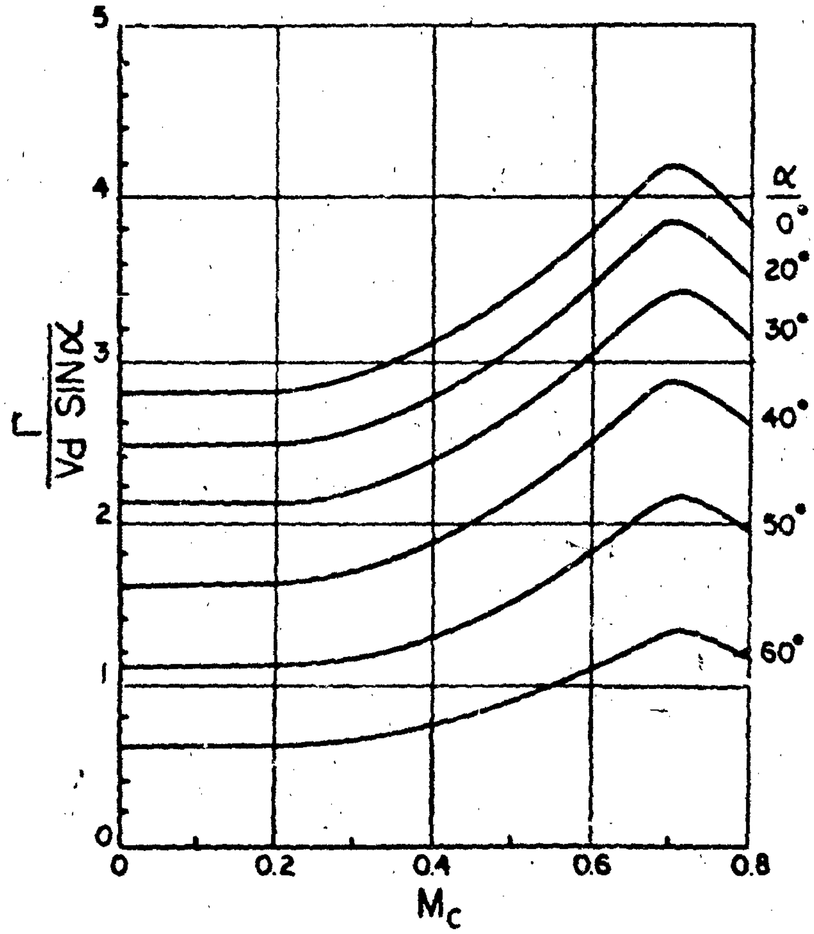

FIGURE 5 VORTEX STRENGTH PARAMETER
SUB CRITICAL R_{e_c}

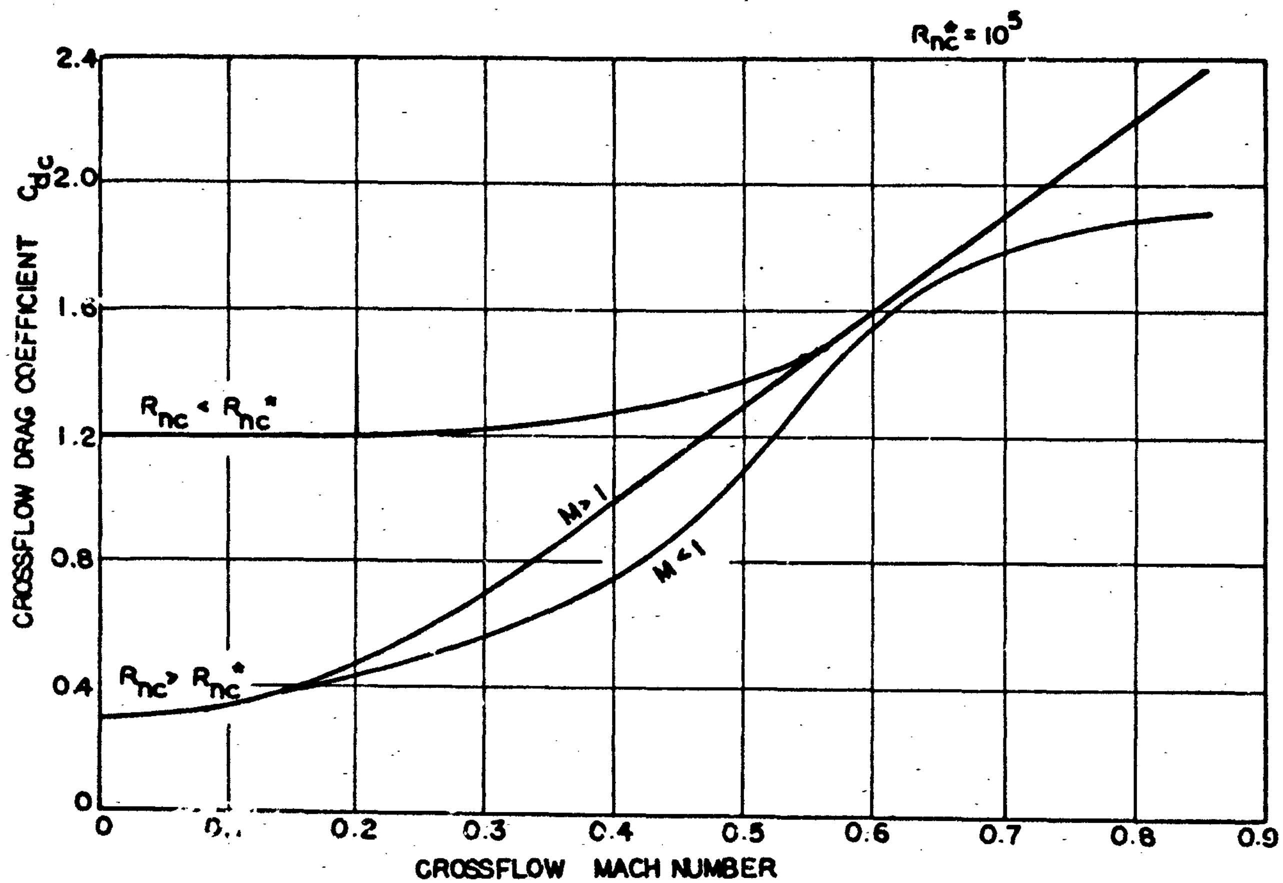

FIGURE 6 BASIC CROSSFLOW DRAG CURVES FOR Γ_S SCALING

Γ_s. Accordingly, for $R_{e_c} > 10^5$ the subcritical R_{e_c} values of Γ_s from Figure 5 are scaled in the same ratio as C_{dc} from Figure 6.

In order to illuminate further the mechanisms underlying the relationship between crossflow Reynolds number and vortex strength, recent work by Fidler[6] will be briefly described. It may be shown that the strength of a lee side asymmetric vortex can be related to the flux of crossflow vorticity leaving the body at the circumferential separation point defined by Θ_s. Further, the vorticity flux shed over axial distance g (at fixed angle of attack) in unit time is:

$$F_B = \text{const} \int_0^g U_s^2 \, dx$$

The vorticity thus shed diffuses through the vortex to produce the circulation Γ_s. Equating the flux F_B to that flowing along a wake vortex of core velocity V_a yields an expression for vortex strength:

$$\Gamma_s = \frac{\text{const}}{V_a} \int_0^g U_s^2 \, dx$$

Now U_s, the circumferential velocity at the boundary layer edge at separation, is a function of Θ_s. In the two-dimensional case [17] it has been found experimentally that when crossflow Reynolds number is subcritical, θ_s lies near the meridian of the cylinder and the associated separation velocity U_s is larger than in the supercritical Reynolds number case, where the separation point lies far over on the cylinder lee side. Continuing the analogy between two and three dimensions indicates that crossflow Reynolds number affects Γ_s through its effects; first upon θ_s, which in turn determines U_s which defines the vorticity flux **flowing** from the body and diffuses through the vortex to produce Γ_s. Hence, subcritical R_{e_c} produces larger Γ values than does supercritical R_{e_c}, provided crossflow Mach number is low.

The foregoing discussions deal with fully-developed vortices which have left the immediate vicinity of the body and joined the asymmetric wake pattern. However, consideration must be given to the street vortices while they are forming close to the body. As previously discussed, these growing vorticies are fed by vorticity from the separating body boundary layer. Assuming rapid diffusion of vorticity the local vortex strength $\Gamma(x)$ formed by shedding a boundary layer over distance x may be written (see previous equation).

$$\Gamma(x) = \text{const} \int_0^x U_s^2 \, dx$$

Furthermore, it has been experimentally determined[4] that for those portions of the body where street vortices are being formed and for given flow conditions, the circumferential location of boundary layer separation, θ_s, is approximately constant with x. Hence, U_s, the circumferential velocity at the boundary layer edge at separation is also constant. Thus the local vortex strength is seen to be directly proportional to x, i.e.,

$\Gamma(x) = \Gamma_s \, x/g$ where g is the distance over which boundary layer fluid is shed to form a street vortex.

One final item affecting the strengths of forming vortices has been considered. It has been shown by Thomson[8] that as a growing vortex nears the base of the body, the rate at which its strength increases is reduced due to base proximity. Thomson's data indicate that the growth rate is only 40 percent of normal. The axial extent of the region over which the base influence is felt is given by

$$e = \frac{d^2}{2 \, S \, \ell \tan \alpha}$$

The model contains this feature.

At any body axial station, then, the strengths of all the vortices are calculable from the combined theoretical/empirical procedures described above. The next stage in flow field model construction is to locate the vortices relative to the body so that their effects may be calculated.

Vortex Location and Spacing

The problem of locating vortex cores in space relative to the body must be handled separately for vortices growing near the body (i.e., those being fed with vorticity from the separating boundary layer) and for shed vortices which can be considered part of the wake street. In the former case, use is made of theoretical results from two-dimensional potential flow theory; in the latter, systematic experimental evidence, suitably scaled for flow parameter changes, is employed. The case of growing vortices will be described first.

Growing Vortices

In order to model the trajectory followed by a growing vortex, two reference points are required. The first is the circumferential location on the body at which the boundary layer separates. The second is the point in space at which the vortex has reached full strength and can be said to have joined the street.

The first point is located by the empirical relationship

$$\theta_s = \sin^{-1} (3 \tan \delta/2 \tan \alpha)$$

The angle thus defined places separation in the general region typical of laminar/turbulent boundary layers. Since the means of determining vortex strength does not rely upon an exact knowledge of the separation point location, the above approximation is sufficient for present purposes. If the determination of vortex strength had required use of the Kutta condition, or some estimate of vorticity flux leaving the body, the angle

θ_s would have been required with some accuracy. In the present method however, vortex strength is defined otherwise and a rough estimate of the separation angle is sufficient.

The second point for anchoring the growing vortex trajectories was taken as the intersection of the Föppl and von Karman lines along which the symmetric and asymmetric vortex cores were known to move respectively. Use of this point was justified as follows:

As discussed earlier, the appearance of vortices in the wake shows, at the earliest stage, a symmetric pair. At any axial station, increasing angle of attack produces increased vortex size and strength as well as an outward movement of the core approximately following the Föppl line. It was reasoned that at the first appearance of asymmetry, one of the vortices on the Föppl line would change its trajectory and proceed outwards along a new path defined by the von Karman stability relationship described earlier. The second vortex would perform similarly and this would then set up the spacing of vortices in the street. It was hypothesized then, that in order to continue the spacing pattern, the intersection of the Föppl and von Karman lines would denote the point at which all vortices reached full strength and were shed into the street. In order to test this hypothesis the schlieren photographs of Thomson and Morrison [1] were examined to determine the distance from the body where vortex feeding from the boundary layer ceased, i.e., the point at which the growing vortex cores became straight and joined the street. It was found that the points thus defined covered a band of values from 2 to 2.5 diameters above the body and at a lateral distance defined by the von Karman stability criterion. To determine the theoretical location of the shedding point, the following procedure was used. With the equation, (14), $2\,ry = r^2 - a^2$, the Föppl line was drawn relative to the cylinder of Figure 7. The data of Reference 1 were used in the equation $d/\ell = S/\chi$ to determine ℓ, the spacing between street vortices of like sign for subcritical crossflow Reynolds numbers. Then the von Karman relation $h = 0.281\ell$ was used to superimpose the street vortex location line on Figure 7. The intersection of the Föppl and von Karman lines was found to lie within the experimentally-determined range given above. It was concluded then, that this intersection point provided a good estimate of the location at which the vortices stopped growing and were shed to form part of the street. For the purposes of this engineering flow model the growing vortex core was assumed to move linearly between the two anchor points. The resulting core trajectory model is shown (foreshortened) in Figure 8.

Street Vortices

From the Föppl/von Karman line intersection the vortex cores stream back into the wake as straight lines, making angle ξ with the body axis. This angle was measured by Thomson and Morrison,[1] related to the rate at which a fluid particle flowing along the core increases its distance from the body, and thence analogized to the two-dimensional von Karman street. ξ is related to missile angle of attack through the parameter $\chi = \tan \xi / \tan \alpha$[1]. If the point on the body from which a vortex emanates is known, then its core location in space may be partly determined using χ. For the purposes of this work χ was assumed unaffected by changes in crossflow Reynolds number.

Vortex starting points on the body were estimated in Reference 1 as being the intersection point of the body axis and the extrapolated street vortex cores. Since these positions were obtained for tailless bodies, the

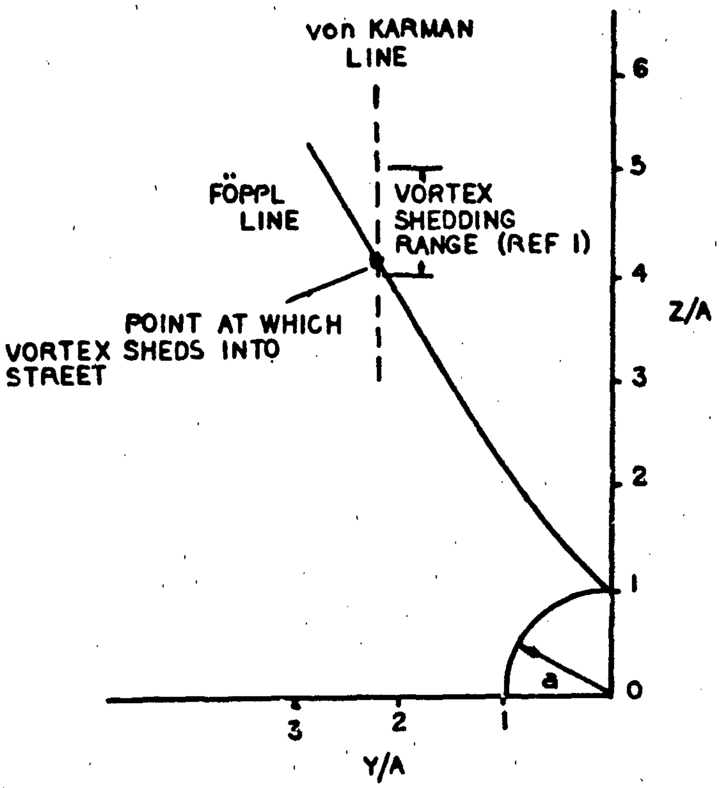

FIGURE 7 COMPARISON BETWEEN PREDICTED AND EXPERIMENTAL POINT WHERE VORTEX IS SHED INTO STREET

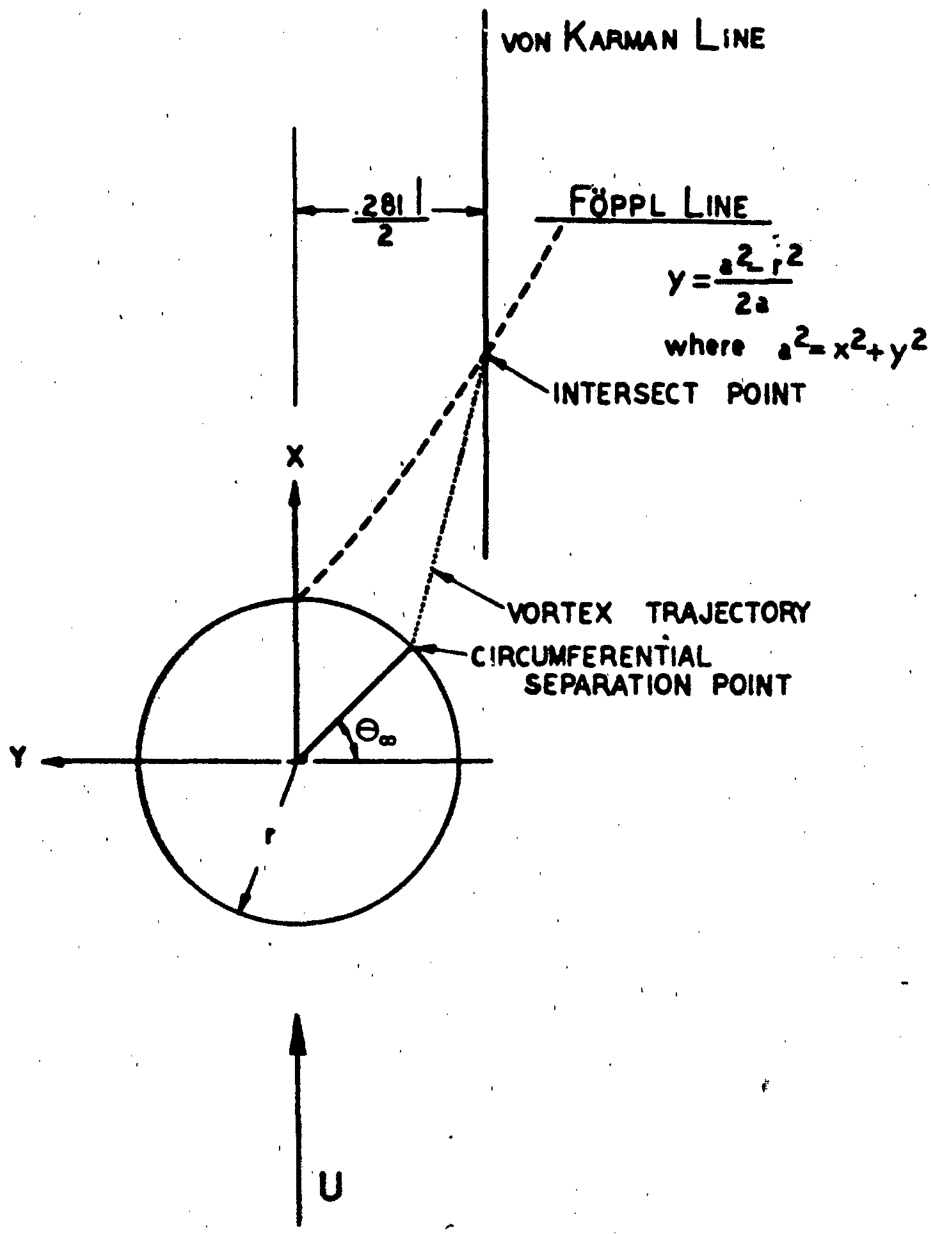

FIGURE 8 GROWING VORTEX'S TRAJECTORY

present work assumes that in the presence of tails, body vortex formation ceases at the body/tail leading edge intersection. Provided the Strouhal number, S, is known, the starting points of wake vortices can be determined. Further, using the relation[1] $d/\ell = S/\chi$, the lateral spacing, ℓ, between vortices of like sign, and hence 0.281ℓ, the von Karman-deduced criterion for lateral spacing can be determined. The vortex cores can now be located in space relative to the body at any point along their lengths. At this stage, however, the information is sufficient only for subcritical crossflow Reynolds numbers.

The quantity on which attention must be concentrated when scaling vortex locations for crossflow Reynolds number is the Strouhal number, S. This measure of the rate at which vortices of like sign are shed from the body has been shown to exhibit strong similarities between the two- and three-dimensional cases. In Reference 1, S was determined experimentally to have values near 0.2 for a wide range of crossflow Mach numbers. This compares well with the two-dimensional value at subcritical crossflow Reynolds number. It is known however,[8] that for cylinders, S varies with crossflow Reynolds number and increases to values in the range 0.3 to 0.5 at supercritical R_{e_c}. This has a direct effect on vortex spacing, both longitudinal and lateral. For bodies alone then, $S = 0.2$ is used for subcritical R_{e_c}. It has been found that a value of $S = 0.35$ gives the best results for supercritical R_{e_c}. For bodies with tails, the rate of vortex formation is influenced by the presence of the tails. Experimental evidence indicates that the effect is to reduce the rate of formation to that defined by $S = 0.2$ regardless of whether the crossflow Reynolds number is sub- or supercritical. Accordingly, for bodies with tails, $S = 0.2$ is used throughout.

Using the above empirical and theoretical inputs, a model can be constructed of the asymmetric wake produced by a slender missile configuration at high angles of attack. This model includes the number and locations of vortices in the wake and their strengths, suitably scaled for Mach number and Reynolds number effects. Both growing and shed vortices are included in the model. Having constructed a model of the wake, the next step is to consider its effect on the missile configuration.

4.0 FORCE AND MOMENT COMPUTATIONAL TECHNIQUES

Having established a technique to model the wake produced by a slender missile configuration at high angles of attack, the next step is to calculate the forces and moments induced on the configuration by the wake. This section presents a computational procedure to do this for bodies alone and then for bodies with tails. In either case, the procedure calls for the calculation of incremental effects produced on various configuration segments and then integration of these effects to determine the forces and moments induced by the wake.

This computational procedure was designed with the intent that it not be overly complicated. With this in mind, the following basic assumption was made concerning the location within the body of the image vortices required to preserve the velocity tangency condition on the surface of the body at each axial station. These image vortices are located in the body on a plane perpendicular to the vortex core; however, this raises a problem because of the inclination of the vortex cores relative to the body axis. A cross-section normal to the street cores shows an elliptical body section, inside which the location of image vortices is not simply accomplished. In keeping with the simple nature of this model it was decided that, if possible, image vortices should be located by means of the circle theorem.(14) This was accomplished by resolving the vortex circulation vectors normal and parallel to the body axis. By ignoring the former as having no relevance in the two-dimensional section model, the latter components plus their images could then be used to determine forces and moments. The use of images was not necessary for body quantities, but was, however, mandatory for tailed regions of the missiles. These points are discussed below.

Body Forces and Moments

The calculation of body forces and moments begins with the determination of the incremental force on each body segment. In order to calculate this force, the local net circulation of all the vortices in the wake must be known. Further, these vortices must have their circulation vectors resolved parallel to the body as described above. At any axial station from the nose, there are usually several wake vortices of strength Γ_s and two growing vortices, one on the left side, having strength $\Gamma_L(x)$ and another on the right, of strength $\Gamma_R(x)$. Since g is the axial distance over which a vortex grows to full strength then $x_R = x_L + g/2$ assuming $\Gamma_R > \Gamma_L$. To resolve the strengths parallel to the body axis, the angle σ for growing and ξ for street vortices were used respectively. Side force on unit length of the body was calculated using the Kutta-Joukowski expression.

$$\delta Y = \rho V \sin \alpha \left[\{\Gamma_R(x) - \Gamma_L(x)\} \cos \sigma + \left\{ \sum_{i=1}^{m} \left(\frac{\bar{R}-r_i}{\bar{R}}\right) \Gamma_{s_{R_i}} - \sum_{i=1}^{m+1} \left(\frac{\bar{R}-r_i}{\bar{R}}\right) \Gamma_{s_{L_i}} \right\} \cos \xi \right]$$

Where it has been assumed, for illustration, that there are (m+1) fully developed vortices on the left side of the body and m on the right. The term $(\bar{R}-r_i)/\bar{R}$ is an empirical factor accounting for the attenuation of fully developed vortex effects on the body as their distances from it increases. r_i is the actual distance of the vortex from the body and $\bar{R}$ is an arbitrary distance at which vortex effect is assumed to have attenuated to zero. The smallest value of r_i is defined by the Föppl/von Karman intersection point. This formulation was an attempt to model the expected vortex attenuation effect empirically. As will be shown later, it was found that the best representation of forces and moments was obtained when the street vortex strength was allowed to attenuate to zero immediately after shedding.

Total side force Y and yawing moment YM are calculated by numerically integrating along the body length. At this stage in the computerized version of the procedure, an option is provided allowing the user to calculate the effect of varying nose fineness and bluntness ratios. This option uses the data of References 3 and 19 to scale the total body side force and yawing moment for various nose fineness and bluntness ratios. The calculation of individual side forces and yawing moments outlined above, employs the flowfield model developed using the empirical data from Reference 1 to determine street vortex strength and vortex separation points. These empirical inputs were derived from wind tunnel data for a configuration having a 3.798 fineness ratio conic nose. The data of Reference 3, obtained from tests of configurations with noses of fineness ratios of 2, 3 and 4, show that the maximum absolute value of side force, $|CY|_{MAX}$, generally tended to increase with increased fineness ratio for noses with little or no bluntness (see Figure 9). To account for this effect, the data of Figure 9 were used to produce scale factors by which the basic output, based on a 3.798 fineness ratio nose, could be scaled.

The data of Reference 3 also indicated that increases in nose bluntness generally tended to reduce the maximum value of side force. Figure 10 shows the effects of blunting a fineness ratio 4.0 nose. Data were also available for fineness ratio 2.0 and 3.0 nose configurations with bluntnesses of 0, 5, 10, 20 and 50 percent. These data were used to produce scale factors by which the values of side force, already corrected for fineness ratio, could be scaled.

Schlieren photographs in Reference 3 indicate that variations in fineness ratio impact the location at which vortices are shed and that variations in

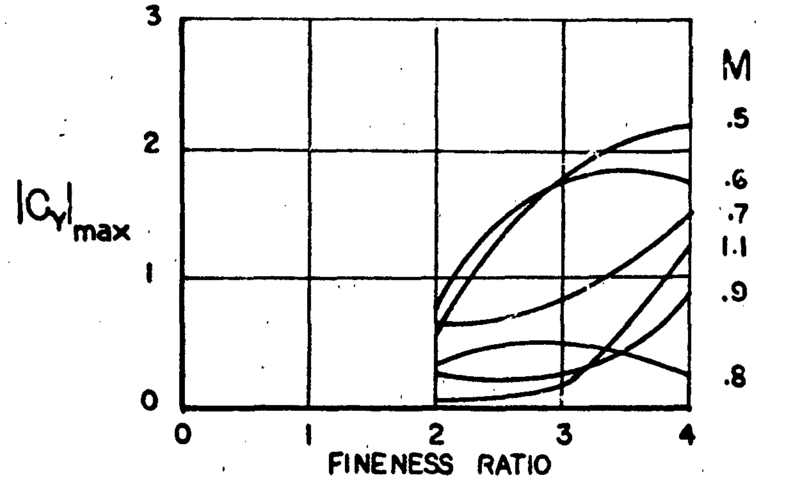

FIGURE 9 FINENESS RATIO EFFECTS

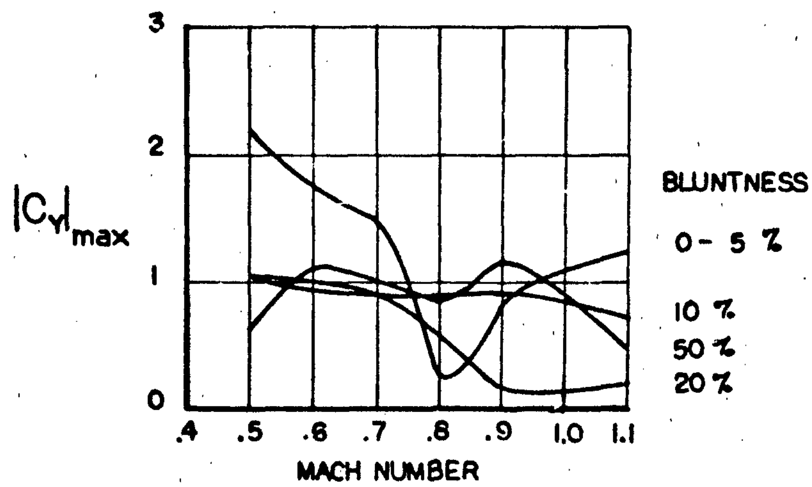

FIGURE 10 BLUNTNESS RATIO EFFECTS

fineness ratio impact the location at which vortices are shed and that variations in nose bluntness delay vortex separation. This is to say that variations in nose geometry influence the structure of the asymmetric wake. Rather than attempting to modify the flowfield model presented in Section 3.0, the scaling technique outlined above was employed in keeping with the simplified nature of the model.

Caution is advised when employing the above scaling technique for nose fineness and bluntness ratio variations. The warning is necessary because the data [3,19] used to derive the scaling factors were mean values and data showing considerable scatter. It is also possible that an independent test of these same configurations could produce considerably different data due to the dynamic nature of the vortex shedding phenomenon.

Tail Forces and Moments

Induced side forces, yawing moments and rolling moments due to the presence of tails can arise even when no asymmetry exists in the wake vortex pattern. This is because of varying net angles of attack of the various tails when the missile is rolled at arbitrary angles. Hence, in order to be certain that experimental data indicate the presence of vortex asymmetry, it is necessary to be selective in choosing missile roll attitudes. For a cruciform missile, roll angles of 0 "plus" and 45 degrees "cross" are the only attitudes where, in the absence of wake asymmetry, zero side forces, rolling moments and yawing moments occur (assuming, of course, no tail deflections). The present model has been compared against experimental data from cruciform missiles and hence the above two roll angles will be referred to exclusively.

The procedure for calculating induced tail forces will be described for a vertical lee-side tail such as could be used on a cruciform missile in "plus" attitude. The major elements of the treatment are most expeditiously described for this case, although the complete procedure will handle tails at any roll angle so that the program can treat bodies at arbitrary roll or whose tails number other than four.

The first step in the process is to determine, for each vortex, the sidewash velocity induced normal to the tail leading edge at each spanwise station. Since the effects of image vortices must be considered and it is preferred that the circle theorem be used, the wake vortex circulation vector is resolved parallel to the body axis as before. In this case, however, instead of simply resolving Γ_s through some angle analogous to ξ as was done for the body above, a new strength is defined which will produce the same values of sidewash velocity as did the original vortex. A single vortex in the wake plus its images will induce some distribution of sidewash velocity v along the tail leading edge. The average value of this sidewash is

$$\frac{1}{p} \int_a^p v dz$$

If now the average sidewash is divided by the axial velocity $V\cos\alpha$, the average angle of attack induced on the tail is obtained. Using the result from slender body theory, that for low aspect ratio tails typical of missile configurations the slope of normal force coefficient is given by $\pi AR/2$, the normal force coefficient induced on the tail due to the i^{th} vortex may be expressed formally as

$$C_{N_i} = \frac{\pi \; AR \; A_T}{2p \; V\cos\alpha \; A_B} \int_a^p v_i \, dz \tag{3}$$

In order to determine rolling moment induced on the missile due to the vertical tail, the resultant normal force is assumed to act at the centroid of the sidewash velocity distribution or, for the i^{th} vortex

$$C_{\ell_i} = C_{N_i} \left\{ a + \int_0^p v_i z dz \Big/ \int_0^p v_i dz \right\} \frac{A_T}{A_B} \tag{4}$$

The total induced forces and moments are obtained by summing the effects of all vortices in the wake.

Yawing moment induced by the tail is calculated by assuming that the resultant loading is located at the mid-point of the leading edge.

The above procedure has been generalized to handle tails at any roll angle. In this way, the contributions of all tails to side forces and yawing and rolling moments may be determined.

Since arbitrary roll angles can be considered, this raises potential problems when a vortex core intersects the leading edge. For potential vortices of the kind used here, flow velocities become extremely high near the core, resulting in unrealistically high induced sidewash angles. This problem was circumvented by introducing into each vortex a solid core of radius 0.25 body radius.[18]

When the tail intersects this core, calculations are discontinued. If the core passes over a tail while angle of attack is increasing, the forces and moments are faired across the gap within which calculations are not performed. This procedure has proved quite satisfactory in practice.

Instead of the slender body theory approach to tail force, strip theory might have been employed. It was felt, however, that the former was more appropriate for the low aspect ratio tails for which the program would probably be used. The program is flexible enough, however, that strip theory could be easily introduced if it were considered necessary.

5.0 COMPARISONS BETWEEN COMPUTED AND EXPERIMENTAL RESULTS

At this stage then, the effects of the wake vortices on bodies and tails are calculable. Comparisons will now be presented between predicted and experimental forces and moments to illustrate the performance of this engineering model. Bodies alone and with cruciform tails will be considered. The effect of varying the number of vortices considered will be shown.

Program predictions have been compared against various experimental data generated on a selection of the Martin Marietta Aerodynamic Research models.[16] The basic model used for high angle data generation was a 10 caliber tangent ogive/cylinder. This body was tested alone and with several sets of cruciform tails affixed. Each tail was individually instrumented so that program predictions of vertical tail forces and moments could be checked for "plus" attitudes. For tails other than vertical, the program would predict only the incremental force generated on them by the asymmetric wake. Freestream effects were not taken into account, and hence forces for non-vertical tails will not be discussed. However, since the differences between non-vertical tails due to asymmetric effects were presumed to be valid for "plus" and "cross" attitudes, the program was used to predict rolling moments for these attitudes.

The first comparison is shown in Figure 11. Here, program predictions of normal force on a vertical lee side tail fixed to the body are compared against experimental data. Also shown is the effect of considering all of the vortices in the wake and of using only those vortices closest to the body, i.e., the growing vortices. It will be seen that the magnitude of tail force is predicted within a few percent using only the growing vortices, while use of all vortices produces a significant discrepancy. The angle at which asymmetry begins is matched only fairly, but the angle at which the appearance of a new wake vortex drives the tail force in the opposite

INDUCED FIN FORCE

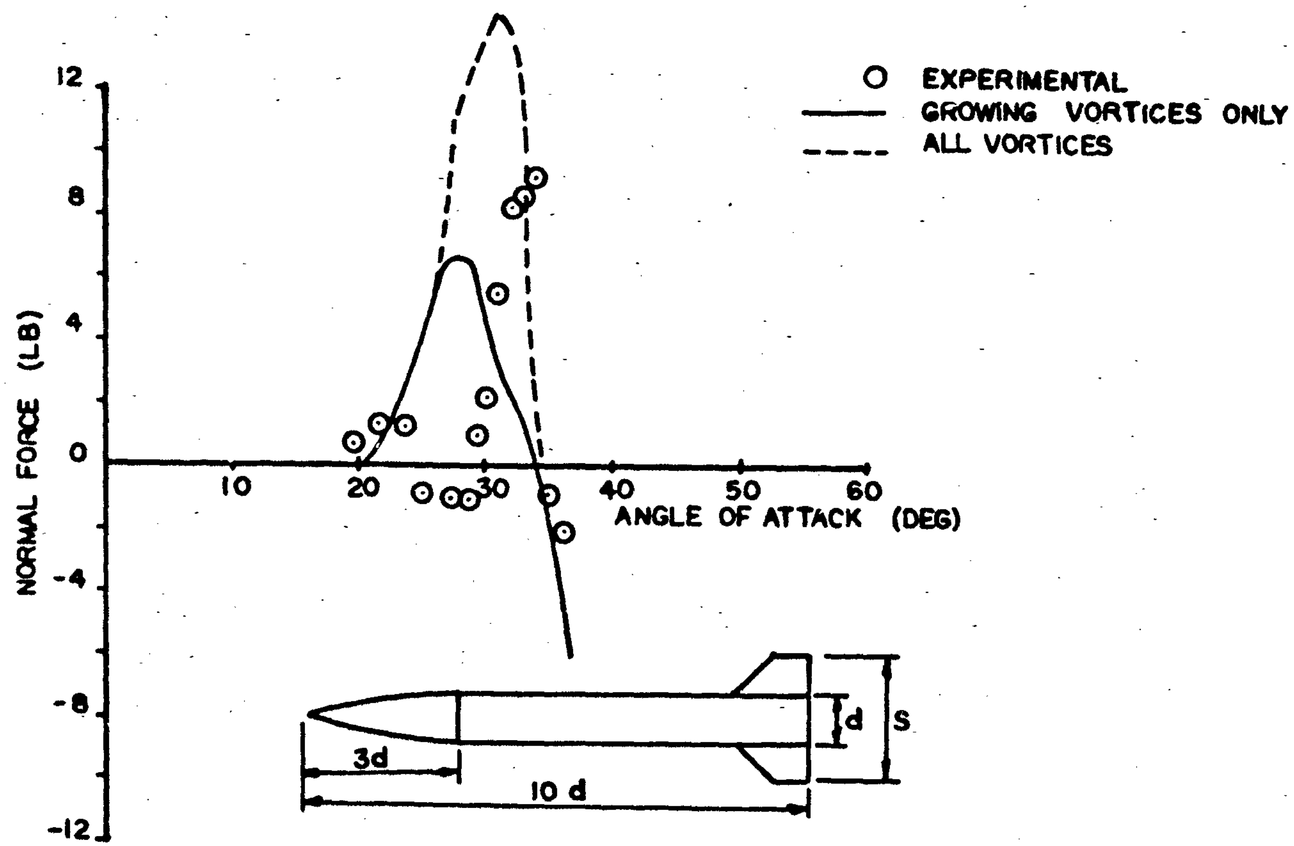

FIGURE 11 COMPARISON BETWEEN PREDICTED AND EXPERIMENTAL VERTICAL FIN NORMAL FORCE

direction is matched within a few degrees. From this evidence, it is concluded that the growing vortices tend to dominate the tail aerodynamic characteristics. The second comparison is shown in Figures 12a and b. Here, predictions of isolated body side force and yawing moments are compared against test data. Again, the effects of considering all of the wake vortices separately from the growing vortices are considered. To make the distinction clearer, no attenuation of non-growing vortex effects has been included. It will be seen that use of all the vortices produces divergent results which have none of the oscillatory character typical of asymmetric effects and evidenced by the data. This is because the net wake circulation remains unchanged in sign, regardless of the number of vortices present. Use of the growing vortices only, on the other hand, yields quite good matching of force and moment magnitudes, as well as angles of onset and new vortex appearance, at least until several vortices are present. While matching is not exact at the higher angles it is clear that use of the program will produce satisfactory preliminary design level estimates for isolated bodies.

Lastly, comparisons are shown between predictions and data for the 10 caliber body with a variety of tails. Based on the results for tails and bodies, these comparisons contain the effects of growing vortices only. Figures 13 a, b, and c show side force, yawing moment and rolling moment comparisons respectively. Prediction accuracy is generally satisfactory. In most cases the magnitudes of the quantities are predicted quite closely. On the other hand, the onset of asymmetry and the appearance of new vortices are not always so accurately reproduced.

The results of Figures 11-13 indicate that the vortices growing in the vicinity of the body dominate the induced effects. This appears intuitively correct, particularly in the context of the two-dimensional analogy. There, the vortices closest to the body would be expected to produce the pressure

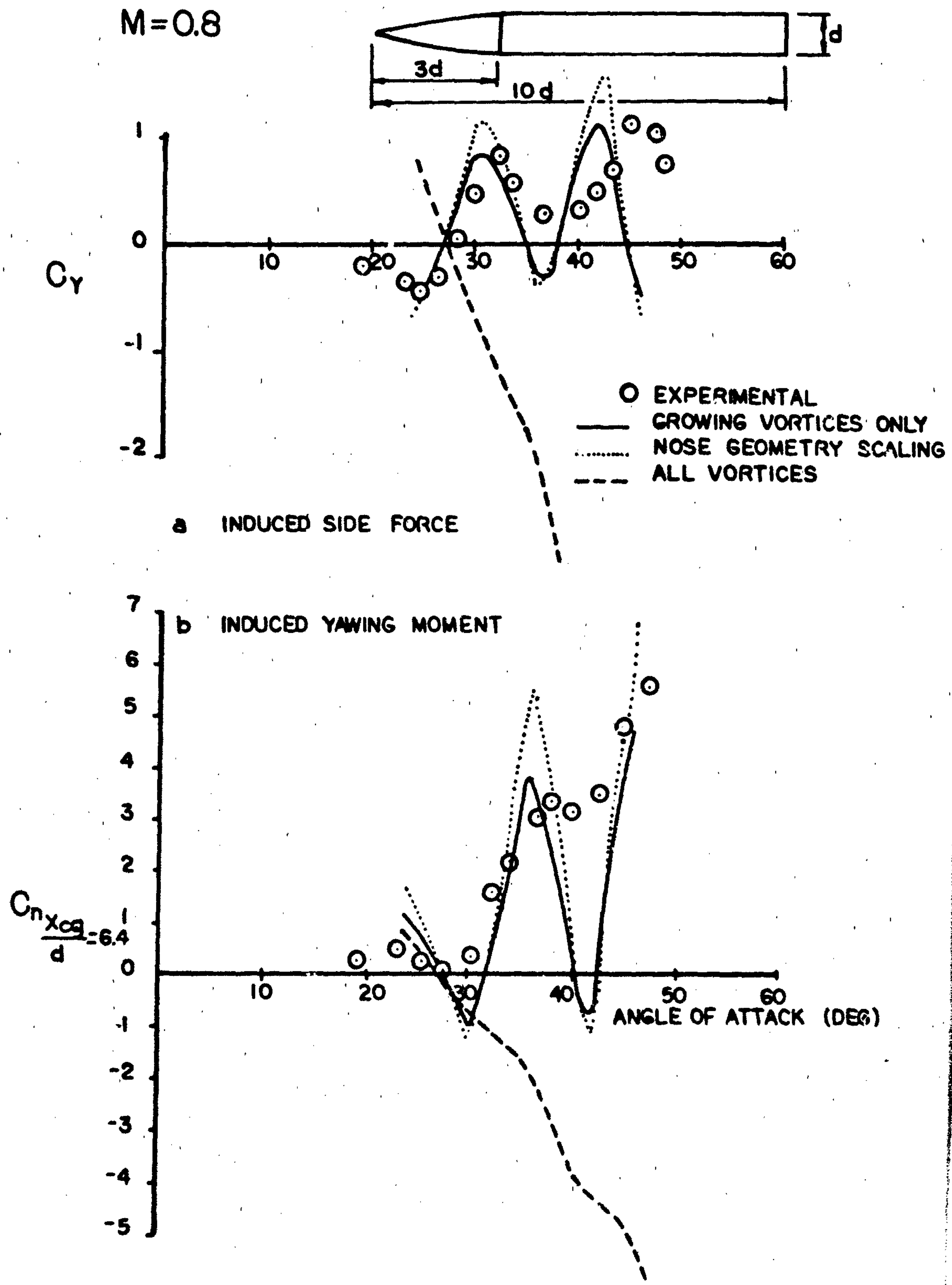

FIGURE 12 COMPARISON BETWEEN PREDICTED AND EXPERIMENTAL RESULTS (BODY ALONE)

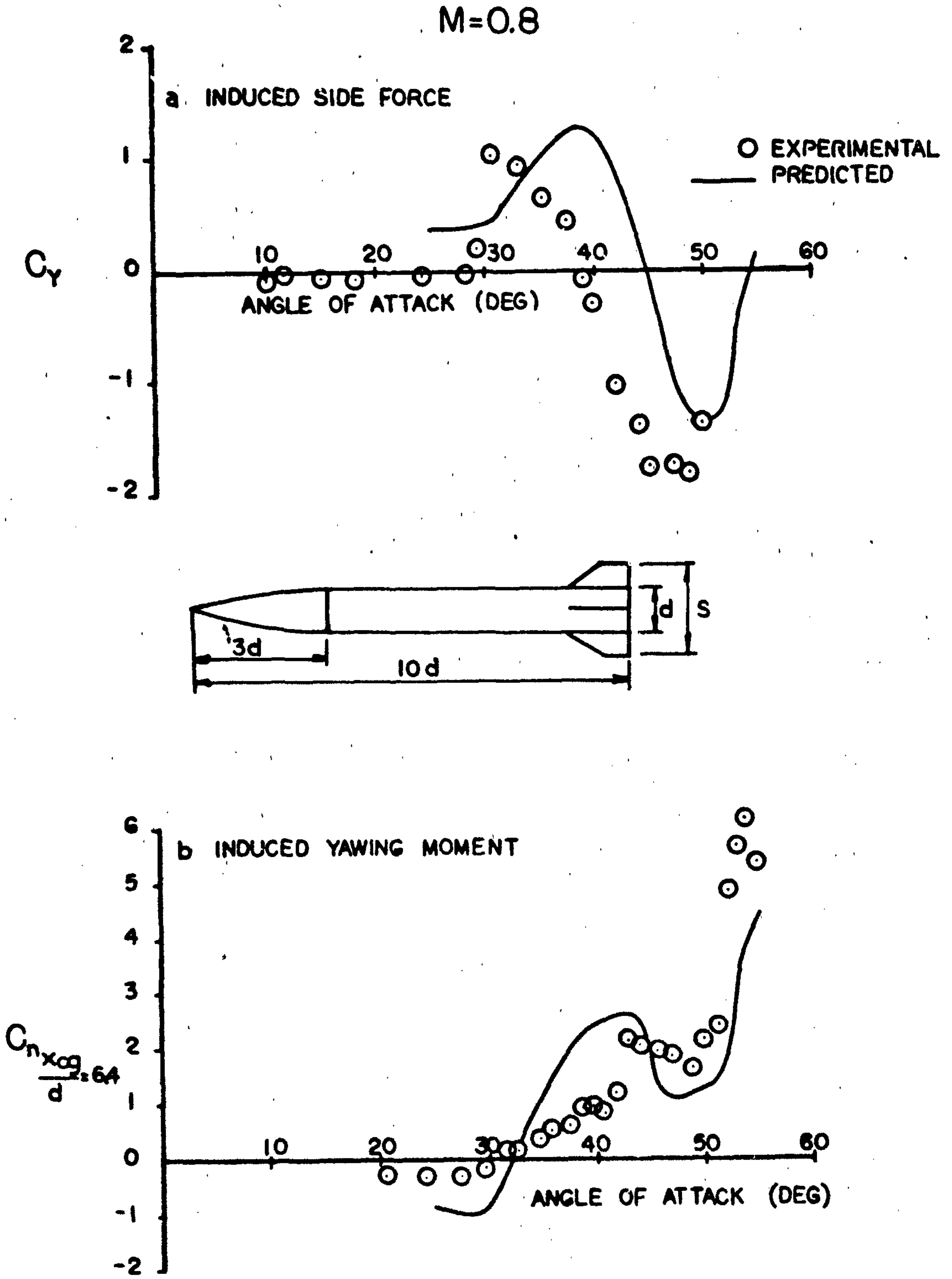

FIGURE 13 COMPARISON BETWEEN PREDICTED AND EXPERIMENTAL RESULTS (BODY+TAIL)

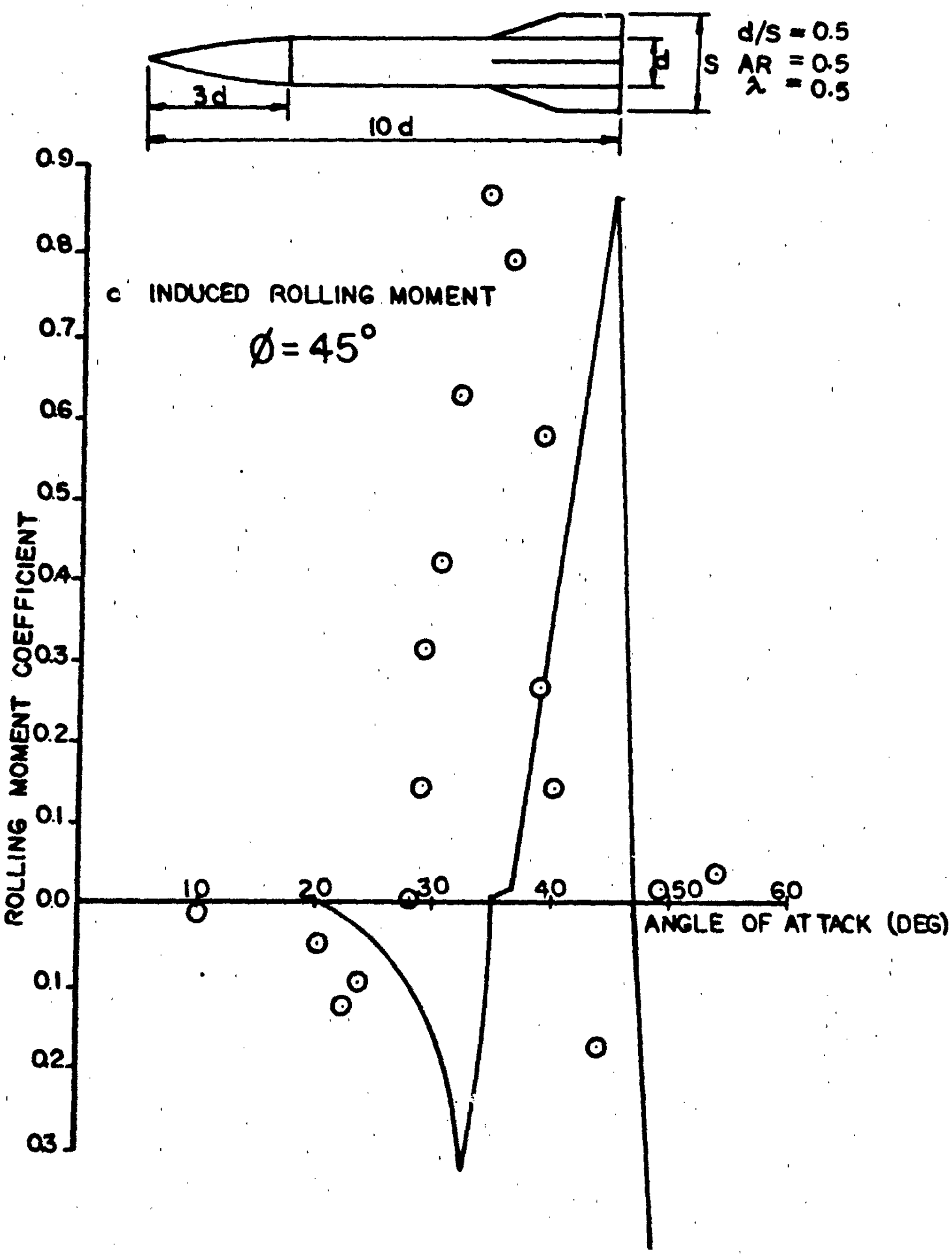

FIGURE 13 CONTINUED

and velocity distributions which generate the forces and moments, with the remainder of the vortices having little effect as they pass downstream. It is not unexpected then, that the three-dimensional case should give similar results. However, although the street vortices have been shown to have relatively little impact, the experimental information on their strengths and shedding frequencies remains of central importance since it defines the bounds of growing vortex strength and shedding frequency.

In general, the model performs quite reasonably. In view of the changes in force and moment data magnitudes and signs which can be obtained by rotation of test models, [1, 3,4] some degree of fortuitousness might be assigned to the results shown. On the other hand, it is unlikely that any measured forces and moments will be significantly greater than those calculated since the model contains all the essential elements of the vortex flowfield, both in magnitude and locations. In addition, it is felt that the means of calculating flow field effects are adequately founded in theory.

6.0 PROGRAM USERS MANUAL

6.1 Input and Output Formats

Input Format:

The input requirements for this program are relatively simple. The input can be separated into 9 basic groups. The following gives information concerning each grouping.

Group I - Flow field data

a. Format: 4F10.0

b. Variables:

VINF - Free stream velocity in ft/sec

FSMN - Free stream Mach number

RHOINF - Free stream density in $\frac{\text{lb sec}^2}{\text{ft}^4}$

ANU - Kinematic viscosity in ft^2/sec

Group II - Body Data

a. Format: 6F10.0, 2I3

b. Variables:

D - Maximum body cross sectional diameter in ft.

SREF - Body reference area in ft^2

NOSEL - Nose length in ft.

BODYL - Body length in ft.

XMC - Moment reference measured from the nose in ft. (absolute value)

DELTA - Nose half angle in deg. Delta = $\tan^{-1} \left(\frac{\text{body radius}}{\text{nose length}}\right)$

NS - Number of segments into which the finless portion of the body is to be divided. (Maximum of 100 segments)

IDCONF - Configuration Type (0 = Body, 1 = Body + Tail)

Group III - Fin Data (Input only if IDCONF = 1)

a. Format: (7F10.0)

b. Variables:

XF - Axial distance in feet from nose to physical fin root chord leading edge. Measured negative from nose aft. (See Figure 14)

YF - Distance in yaw plane from body centerline to fin root chord leading edge. Measured in feet. (See Figure 14)

ZF - Distance in pitch plane from body centerline to fin root chord leading edge. Measured in feet. (See Figure 14)

XFMAX - Axial distance in feet from nose to fin tip chord leading edge. Measured negative from nose aft. (See Figure 14)

YFMAX - Distance in yaw plane from body centerline to fin tip chord leading edge. Measured in feet. (See Figure 14)

ZFMAX - Distance in pitch plane from body centerline to fin tip chord leading edge. Measured in feet. (See Figure 14)

SREFT - Tail single panel reference area in $ft.^2$

The above measurements apply to a single lee-side fin in the pitch plane of a non-rolled missile.

Group IV - Indicators

a. Format: (3I3)

. Variables

NAOA - Number of angles of attack to be considered. As many as 30 angles of attack may be entered per run.

NTYPE - Nose type indicator

NTYPE	Nose Shape
1	Cone
2	Tangent Ogive

NLAM - Number of roll angles to be considered. As many as 30 roll angles may be entered per run.

Group V - Angles of Attack

a. Format: (8F10.0)

b. Variables:

AOAD - Angles of attack in degrees (See Figure 14)

Group VI - Roll Angles

a. Format: (8F10.0)

b. Variables:

RA* = Roll angles in degrees (See Figure 14)

*Locates fin positions relative to leeside vertical, RA = 0.0

Group VII - Radial Vortex Limit

a. Format: (F10.0)

b. Variables:

GAMLIM - Radius at which the influence of a vortex on the body goes to zero. (diameters)

Group VIII - Nose Fineness and Bluntness Ratio Option

a. Format: (I1,F10.0)

b. Variables

IOPT1 - Option indicator

(0 = Do not use option, 1 = use option)

BRN - Bluntness ratio in percent $\left(\frac{\text{Nose tip radius}}{\text{Nose base radius}} \times 100\right)$

Group IX: Run Configuration Indicator

a. Format: (I1)

b. Variables:

IRUN - Run indicator (1 - another run follows, 0 = terminate computations)

Output Format:

Output format will be determined by the nature of the configuration being analyzed. Output for isolated bodies consist of angles of attack, side force coefficients (CY) and yawing moment coefficients (CETAMC) about the moment center input by the user. If the fineness and bluntness ratio scaling option is selected, output will be scaled and repeated. Output for body plus tail configurations consist of angles of attack, induced side force coefficient (CY), yawing moment coefficient (CETAMC) about the user input moment reference center and rolling moments. Additionally, for a fin located in the leeside vertical plane (RA = 0.0), the force normal to the fin is also printed out.

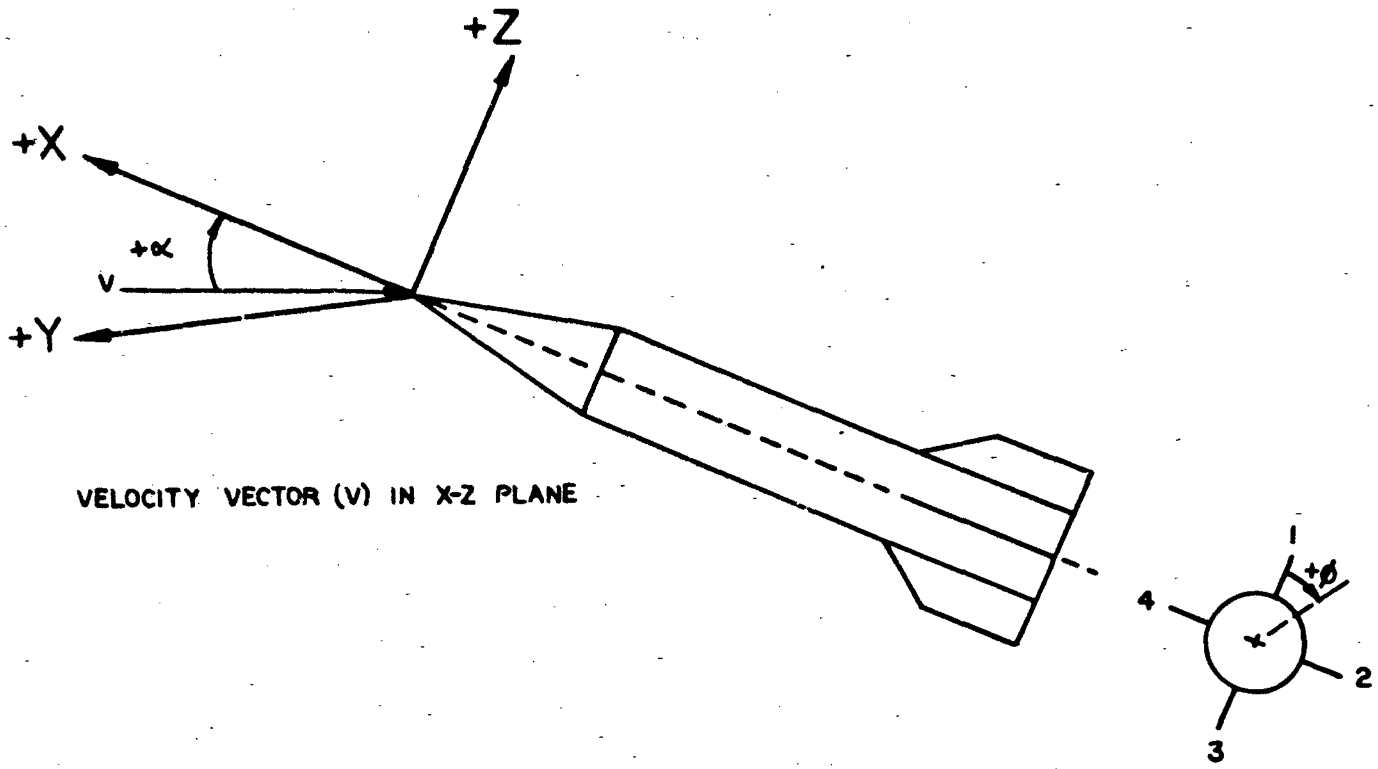

FIGURE 14 SIGN CONVENTION

6.2 Program Flow Charts

Two program flow charts are presented. The first (Chart 1) is a generalized flow chart designed to provide the user a basic map of program functions. The second flow chart (Chart 2) is designed to give the user requiring a working knowledge of program functions a more detailed breakdown of program logic.

Descriptive statements are also contained in the program listing in order to facilitate tracing the steps through the program.

Chart 1. Top Level Program Flow Chart

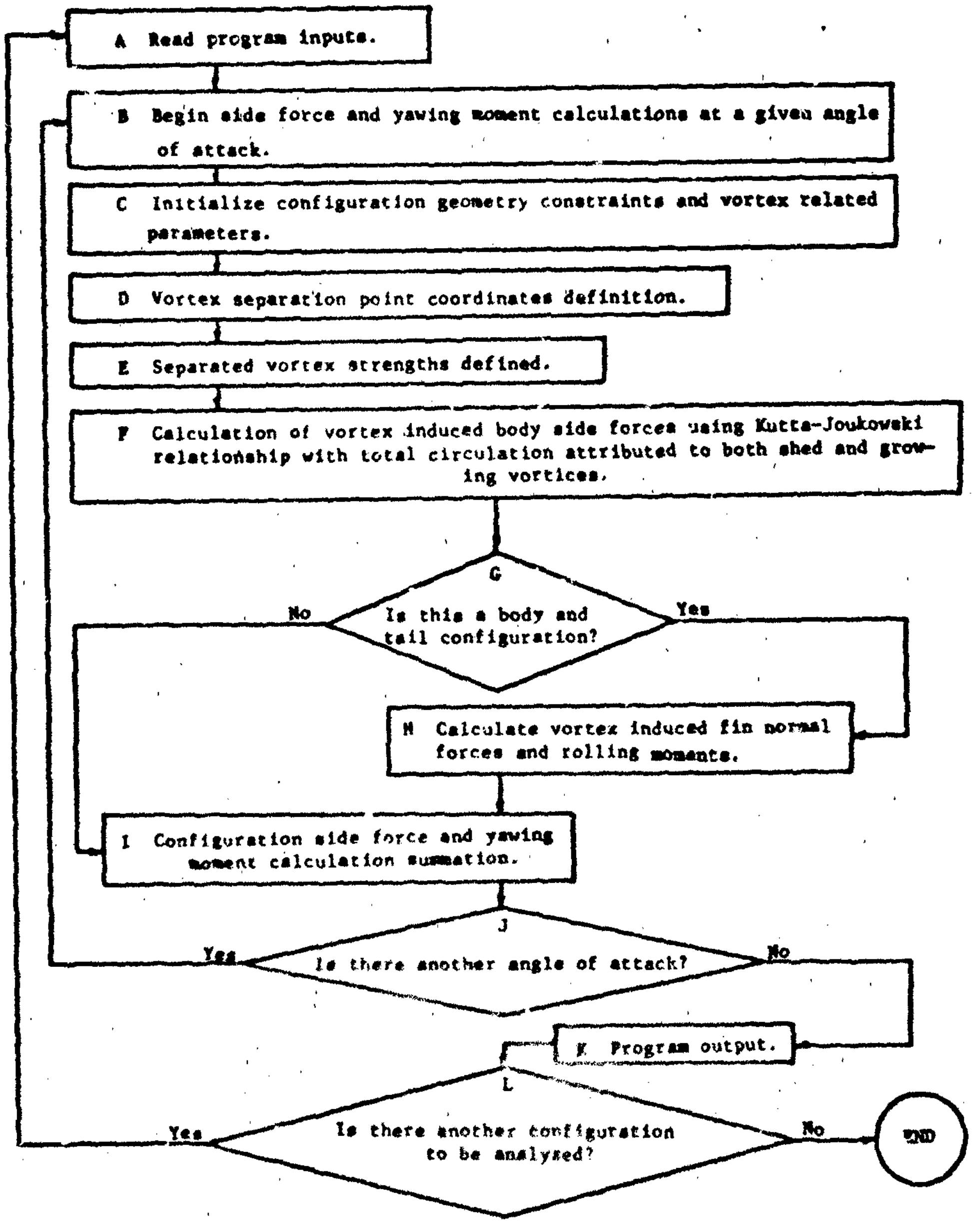

Chart 2. Detailed Program Flow Chart

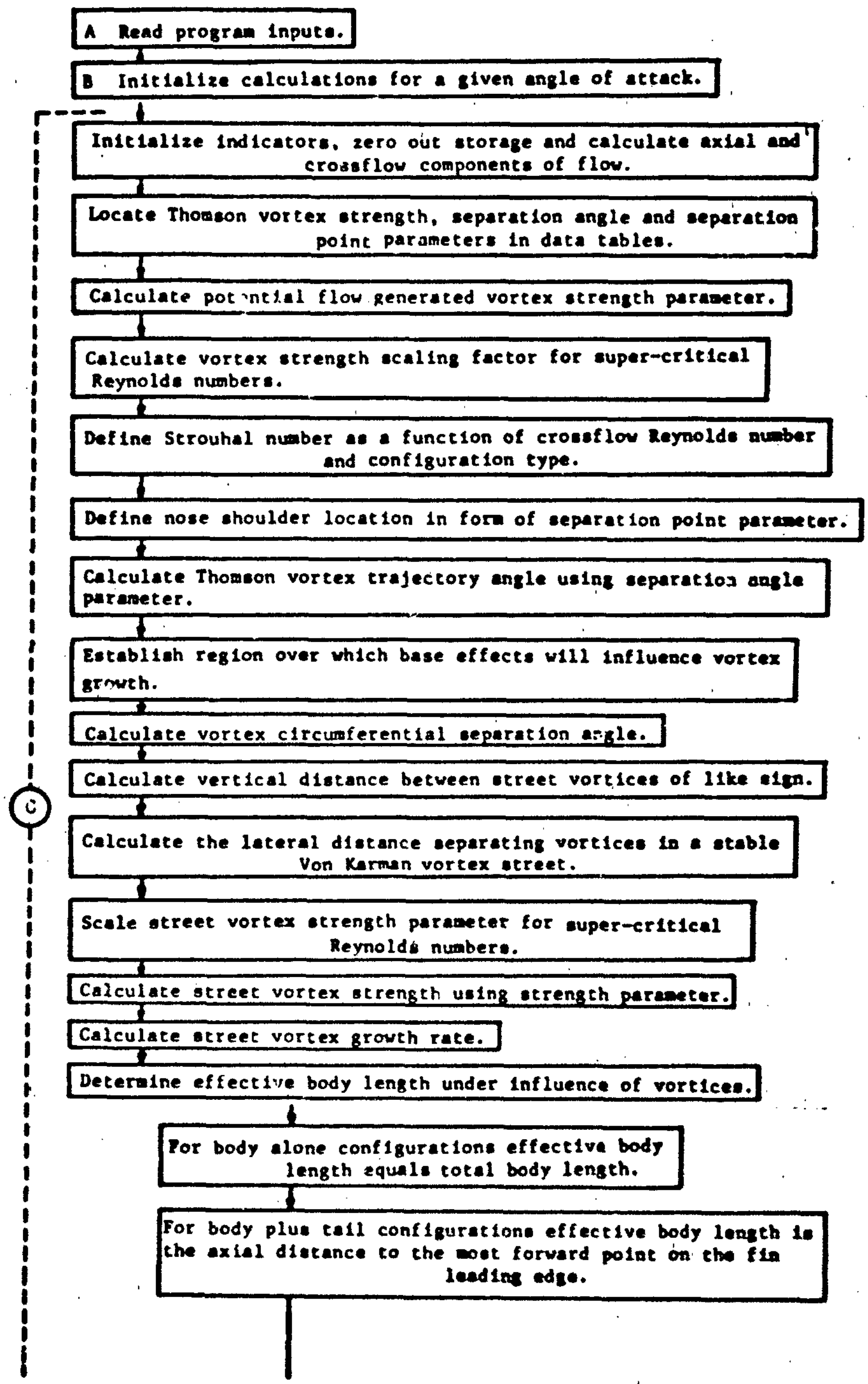

Chart 2. (continued)

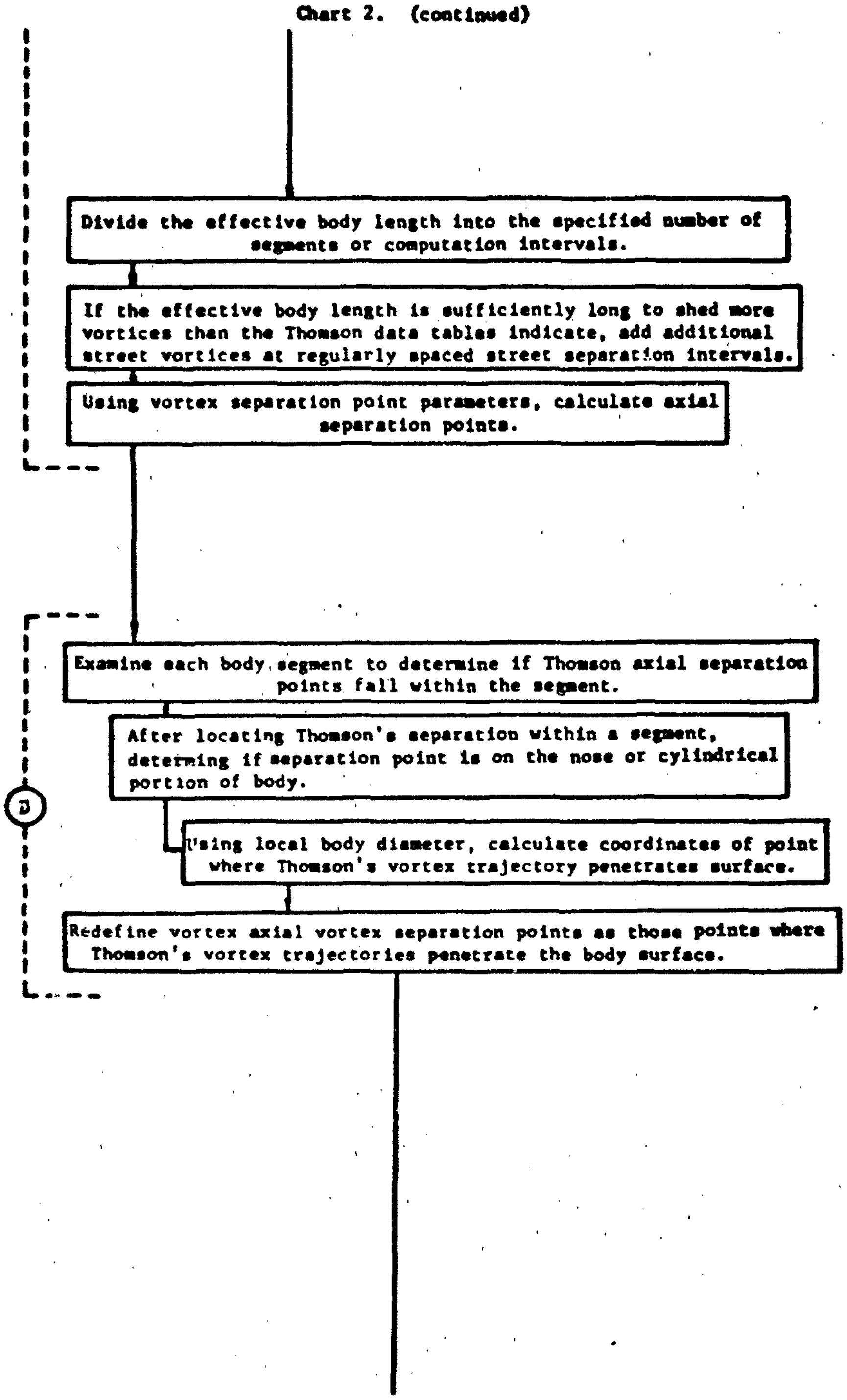

Chart 2. (continued)

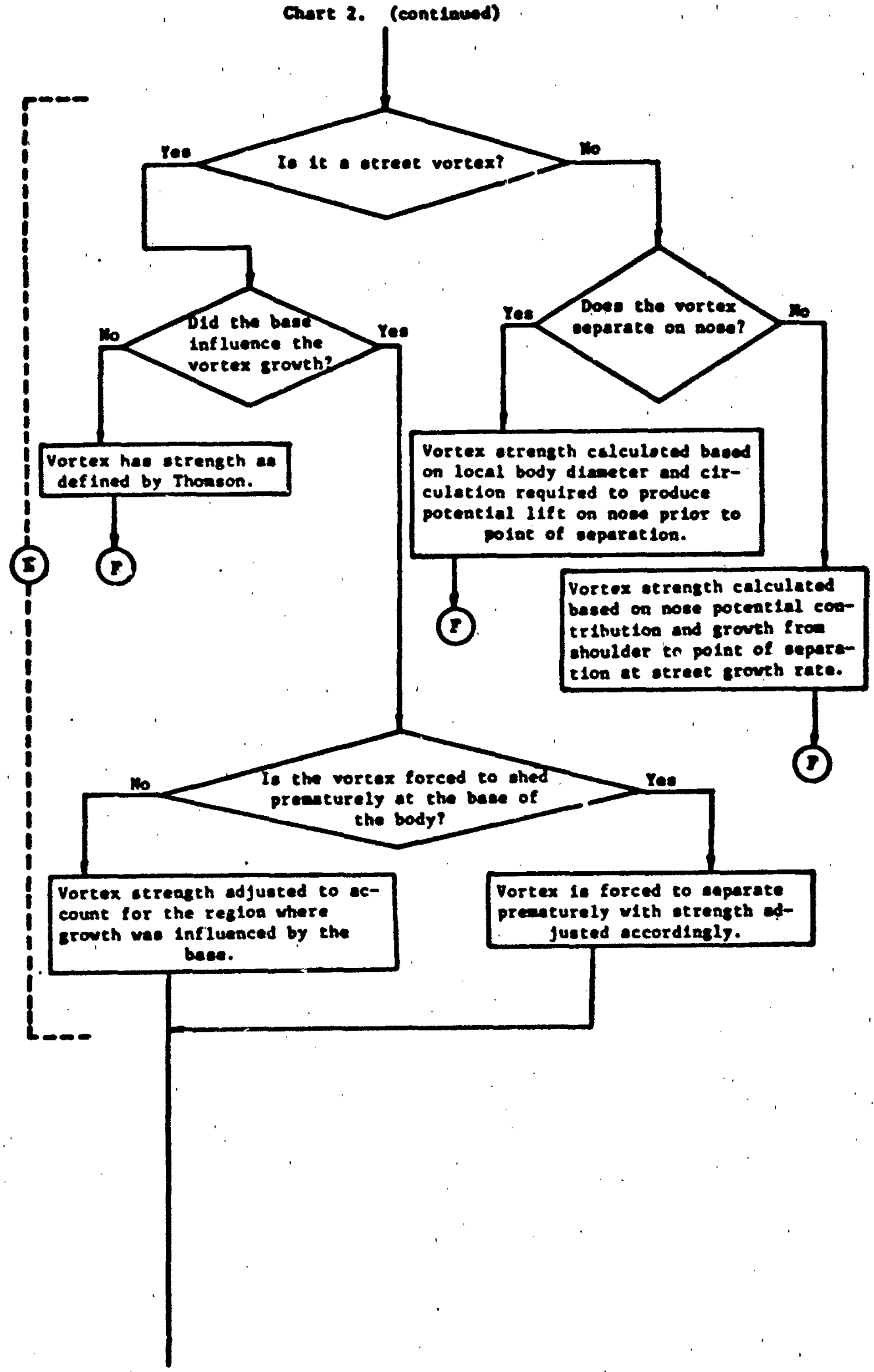

Chart 2. (continued)

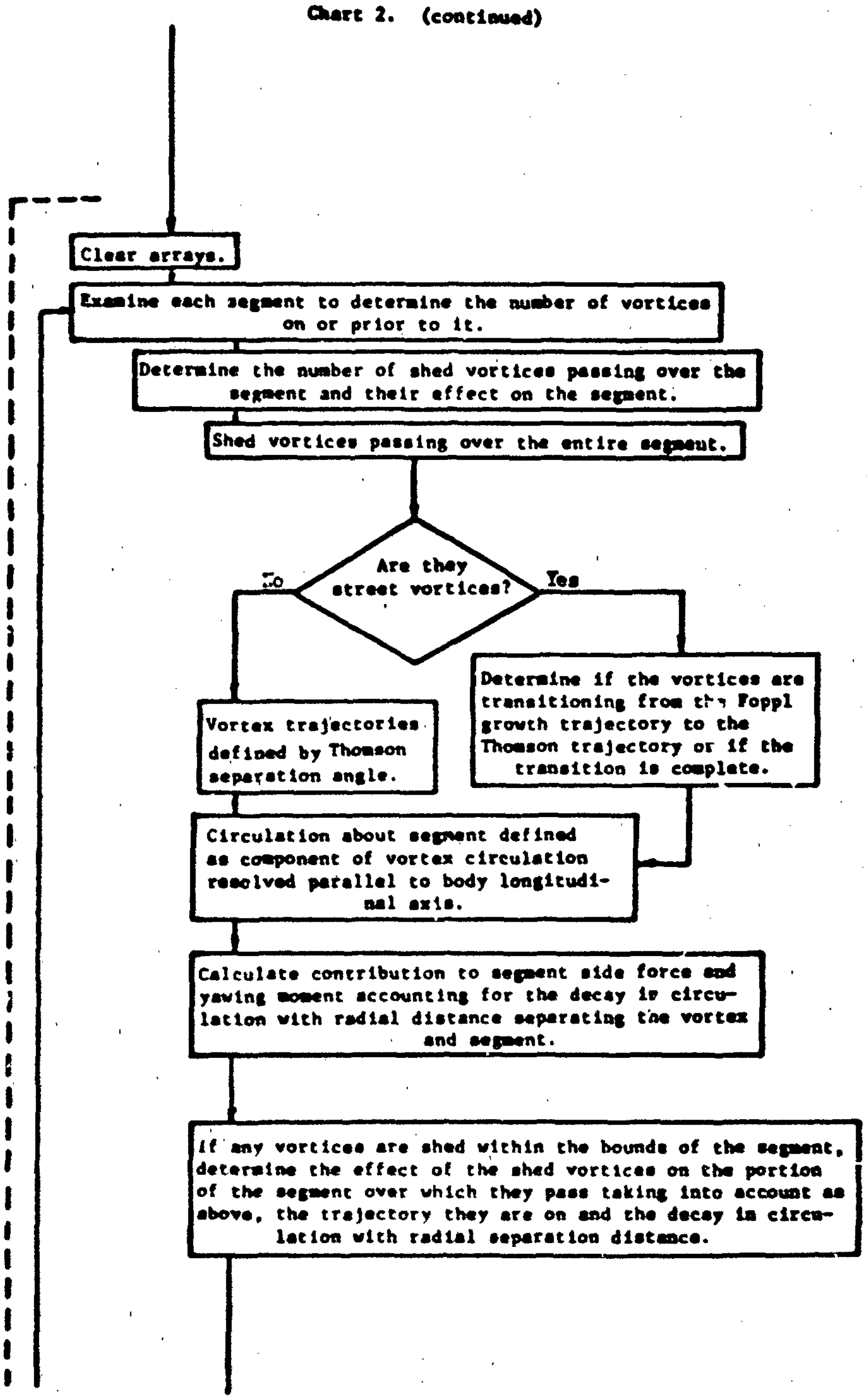

Chart 2. (continued)

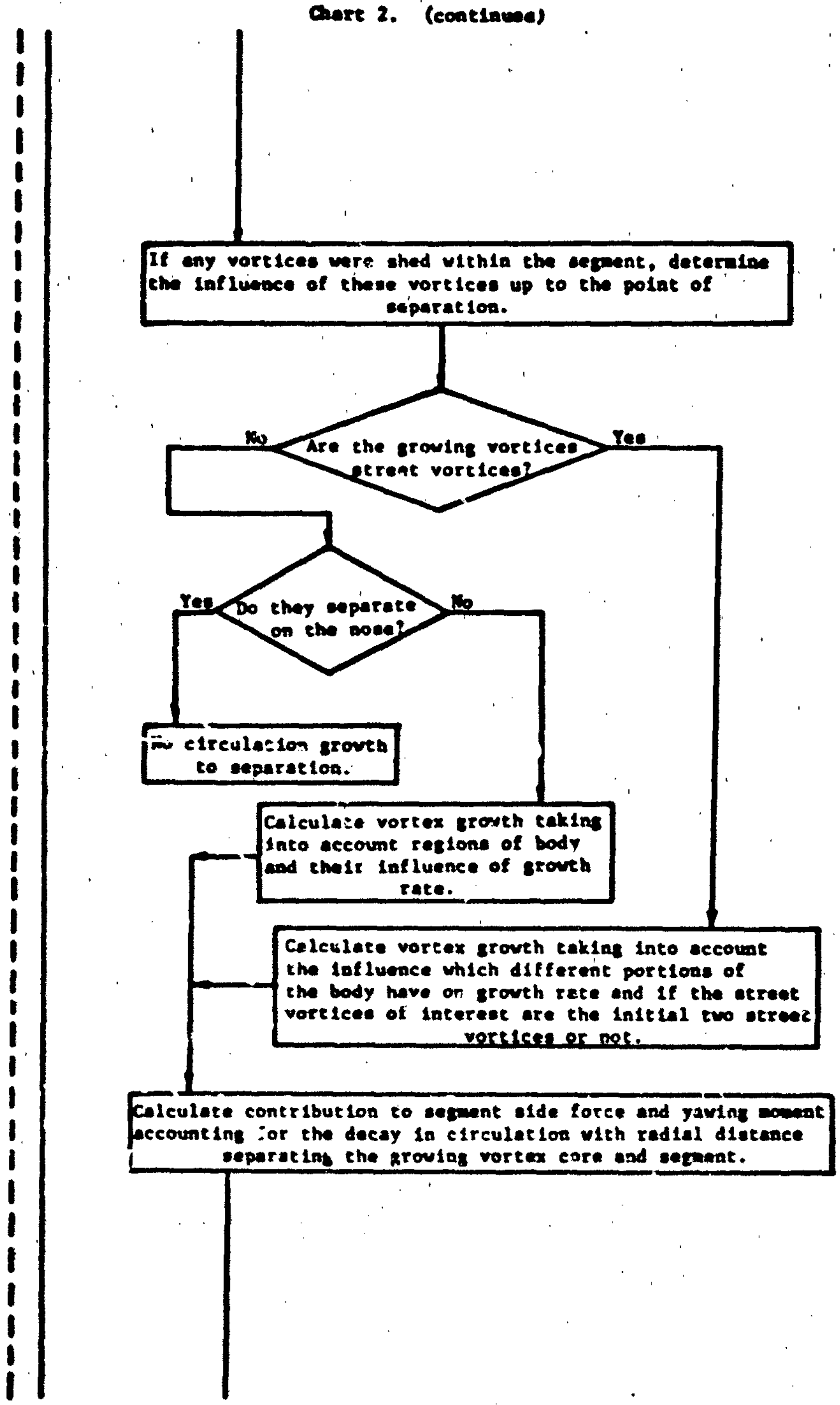

Chart 2. (continued)

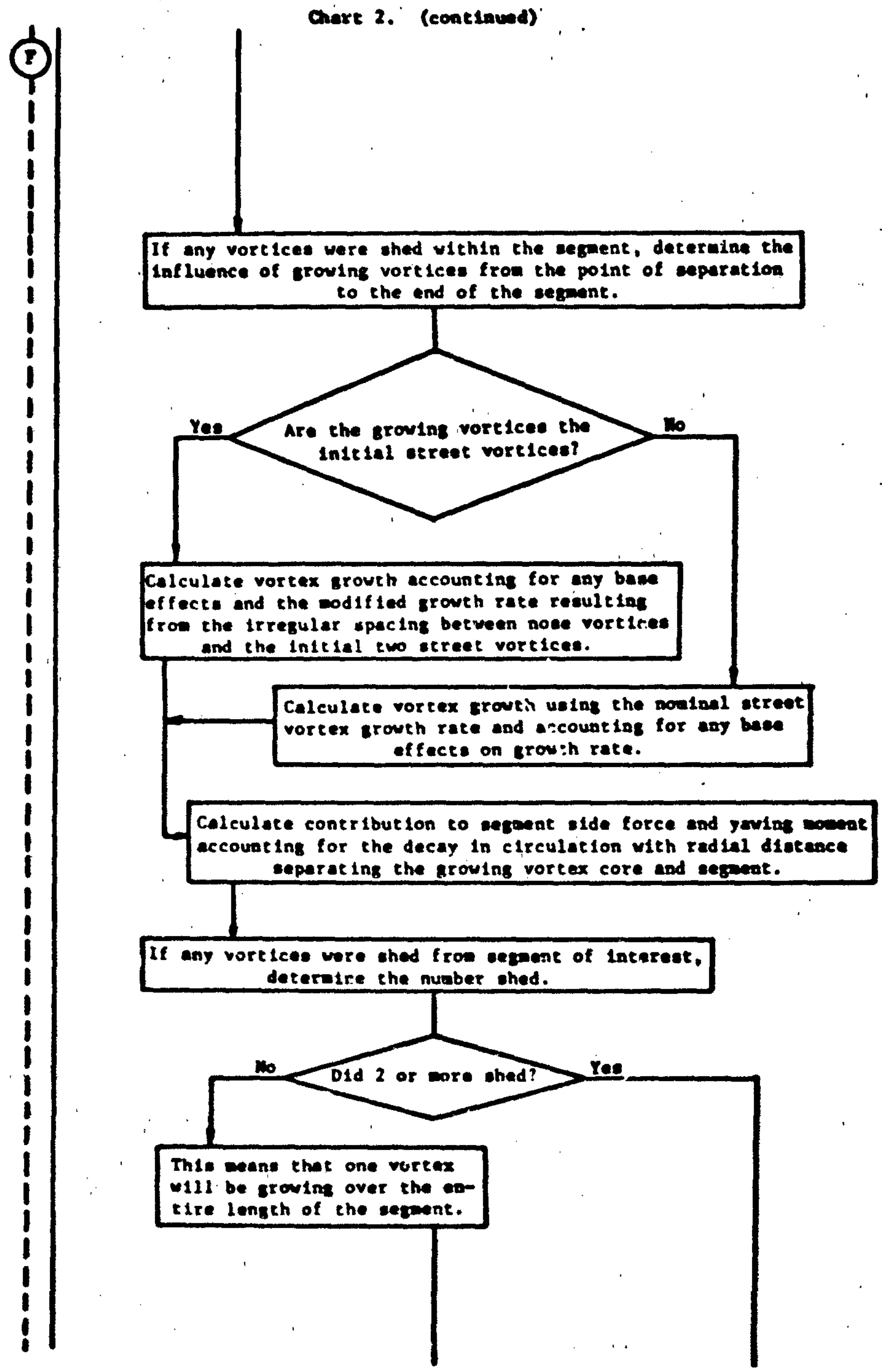

Chart 2. (continued)

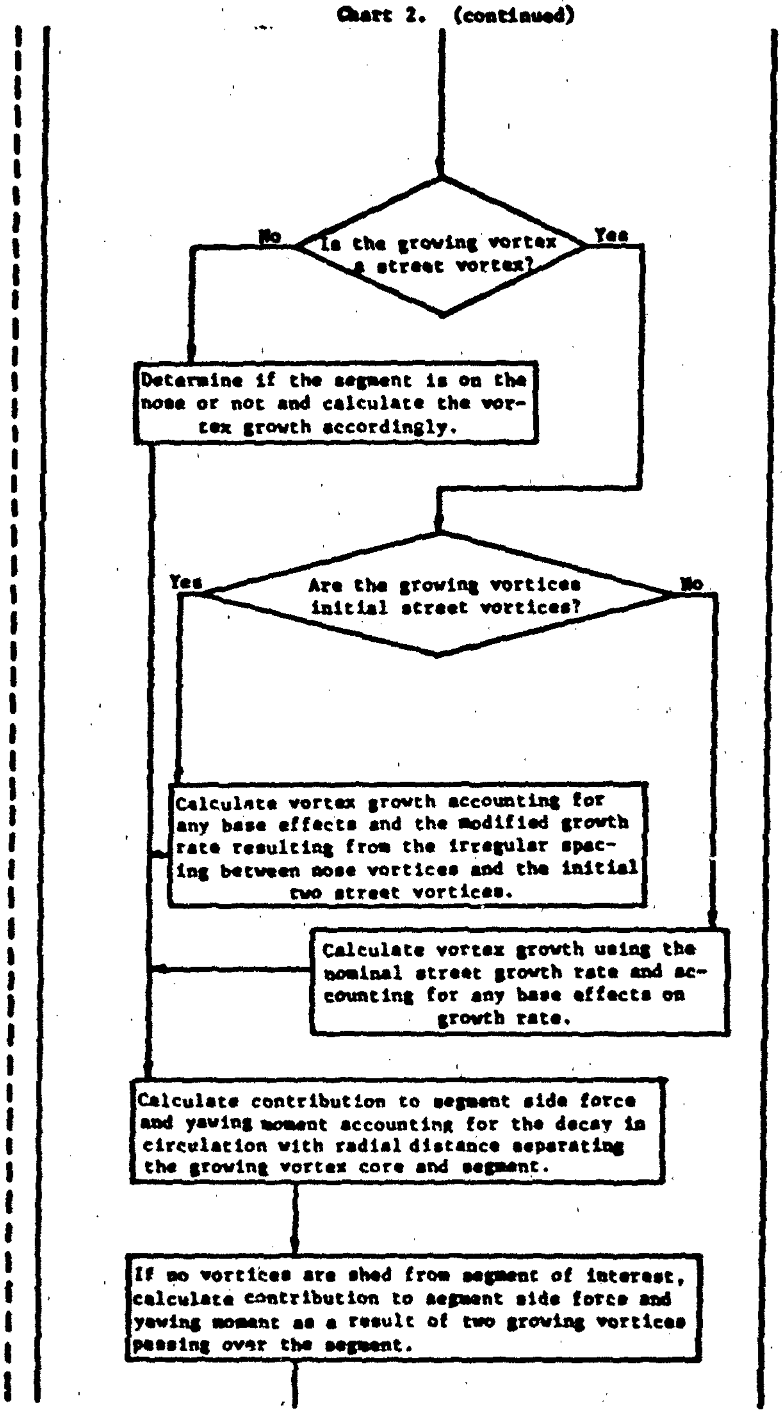

Chart 2. (continued)

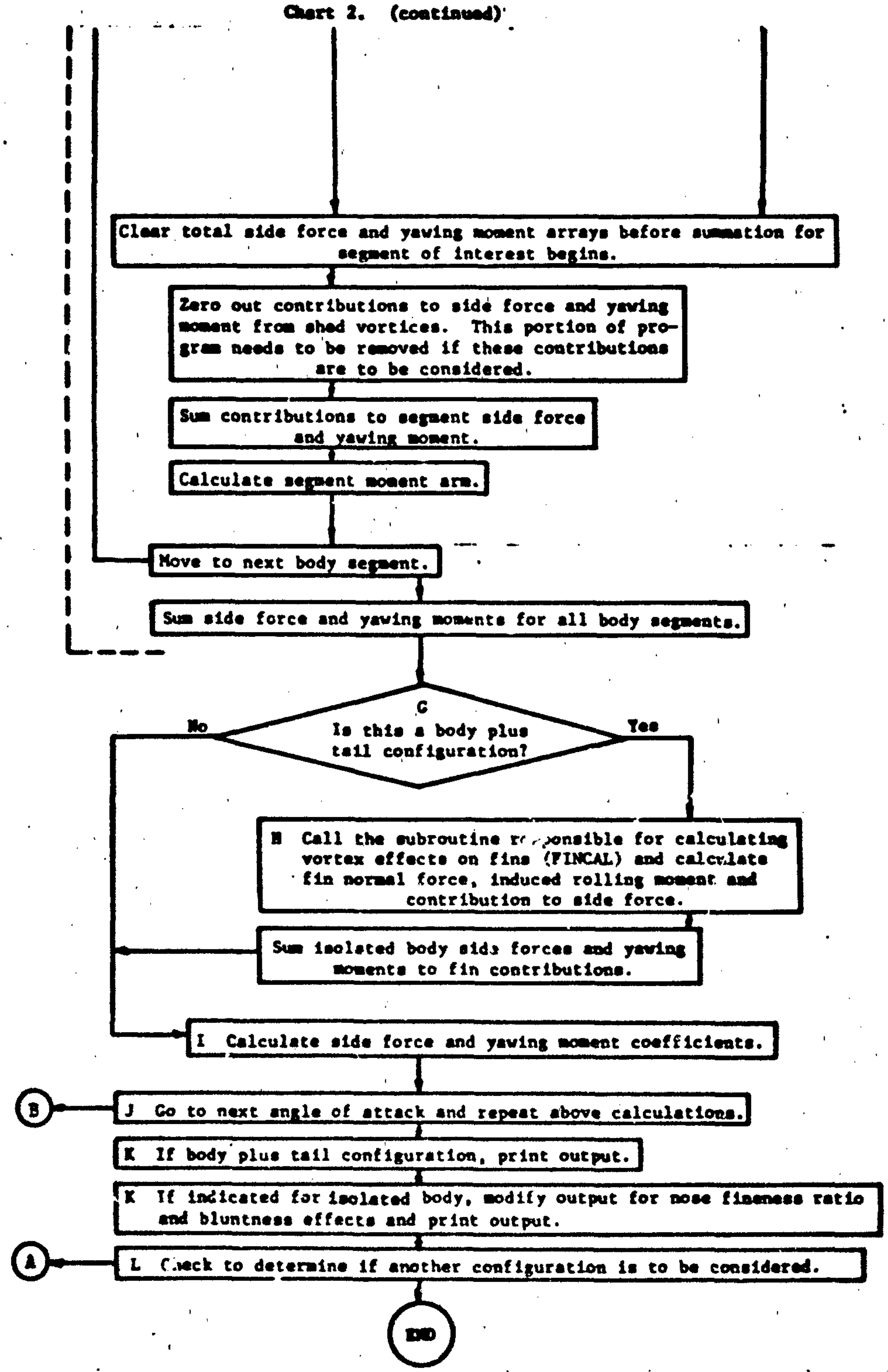

6.3 Program Listing

```
      REAL LAM,NOSE,LAMD
      DIMENSION GSEPP(20),GSEP(20),AUAR(30),ARAR(30),GAMSV(20)
      DIMENSION GAMPC(20),GAMT(100),SF(100),CY(100)
      DIMENSION YMOM(100),CETA(100),GSEPT(20),GSEPY(20),GSEPZ(20)
      DIMENSION AGSEP(20),RA(30)
      DIMENSION FMGPC(20),GPSV(20),FMGPSV(20),GOUTS(20)
      DIMENSION FMGAUT(20),GHUAS(20),FMHUAS(20),GAU(20),FMGBU(20)
      DIMENSION CETAMC(100)
      DIMENSION FMT(100),ENFQ(30)
      DIMENSION SFPC(20),SFPSV(20),SFOUTS(20),SFHUAS(20),SFGBU(20)
      DIMENSION TMACHC(17),TALPHA(6),TGAMP(17,6)
      DIMENSION ISKIP(30),SROLM(30)
      DIMENSION TXI(17),TGSEP(17,7)
      DATA TGAMP/ 2.8 , 2.8 , 2.8 ,2.8 ,2.81 , 2.84 , 2.9 , 3.0 , 3.11
     2 , 3.28 , 3.41 , 3.5 , 3.8 , 4.0 , 4.19 , 4.03 , 3.8 , 2.48 , 2.48
     3 , 2.48 , 2.49 , 2.49 , 2.5 , 2.55 , 2.65 , 2.78 , 2.92 , 3.09
     4 , 3.28 , 3.49 , 3.58 , 3.84 , 3.72 , 3.5 , 2.1 , 2.1 , 2.1 , 2.1
     5 , 2.11 , 2.13 , 2.15 , 2.26 , 2.38 , 2.51 , 2.68 , 2.85 , 3.06 ,
     6   3.27 , 3.42 , 3.35 , 3.12 , 1.5 , 1.5 , 1.6 , 1.61 , 1.62 ,
     7   1.65 , 1.69 , 1.77 , 1.88 , 2.0 , 2.12 , 2.3 , 2.5 , 2.7 ,
     8   2.88 , 2.78 , 2.5 , 1.1 , 1.1 , 1.1 , 1.1 , 1.11 , 1.13 , 1.17
     9 , 1.2 , 1.29 , 1.39 , 1.5 , 1.64 , 1.81 , 2.0 , 2.12 , 2.09 ,
     1   1.93,.61 , .61 , .61 , .62 , .63 , .64 , .67 , .7 , .75 , .81
     2 , .9 , .99 , 1.1 , 1.21 , 1.31 , 1.29 ,1.18 /
      DATA TMACHC/ 0.0 ,0.05 ,0.1 , 0.15 , 0.2 , 0.25 , 0.30 , 0.35 ,
     2            0.4 , 0.45 , 0.5 , 0.55 , 0.6 , 0.65 , 0.7  , 0.75 ,
     3            0.8 /
      DATA TALPHA/ 0.0 , 20.0 , 30.0 , 40.0 , 50.0 , 60.0 /
      DATA TGSEP/ .12 , .16 , .19 , .23 , .26 , .29 , .32 , .35 , .39 ,
     1            .42,  .45 , .47 , .50 , .52 , .53 , .56 , .58 , .23 ,
     2            .27 , .3  , .34 , .39 , .42 , .47 , .5  , .53 , .57 ,
     3            .59 , .52 , .64 , .67 , .68 , .7  , .72 , .53 , .57 ,
     4            .71 , .76 , .8  , .83 , .87 , .9  , .93 , .97 ,1.0  ,
     5           1.02 ,1.05 ,1.08 ,1.1  ,1.12 ,1.13 ,1.18 ,1.23 ,1.27 ,
     6           1.32 ,1.35 ,1.38 ,1.42 ,1.44 ,1.46 ,1.48 ,1.5  ,1.52 ,
     7           1.53 ,1.56 ,1.57 ,1.58 ,1.6  ,1.68 ,1.73 ,1.78 ,1.82 ,
     8           1.86 ,1.88 ,1.92 ,1.94 ,1.97 ,1.98 ,2.0  ,2.02 ,2.04 ,
     9           2.06 ,2.08 ,2.09 ,2.1  ,2.18 ,2.23 ,2.28 ,2.32 ,2.36 ,
     1           2.4  ,2.43 ,2.45 ,2.47 ,2.48 ,2.5  ,2.52 ,2.53 ,2.56 ,
     2           2.58 ,2.59 ,2.6  ,2.68 ,2.73 ,2.78 ,2.82 ,2.86 ,2.9  ,
     3           2.93 ,2.96 ,2.98 ,3.01 ,3.03 ,3.06 ,3.08 ,3.09 ,3.1  ,
     4           3.11 ,3.12 /
      DATA TXI /  .812, .812, .812, .812, .81 , .81 , .805, .8  , .793,
     1            .785, .775, .754, .735, .71 , .67 , .647, .57 /
C*****************************************************************
C     READ INPUT DATA AND INITIALIZE VORTEX PARAMETERS
C*****************************************************************
C     READ FREE STREAM CONDITIONS
   41 READ(5,1)VINF,FSMN,RHOINF,ANU
    1 FORMAT(8F10.0)
    2 FORMAT(6F10.0,2I3)
    3 FORMAT(3I3)
    4 FORMAT(I1,F10.0)
C     READ CONFIGURATION INFORMATION
      READ(5,2)D,SREF,NOSEL,BODYL,XMC,DELTA,NS,IDCONF
      IF(IDCONF.EQ.0)GO TO 20
C     READ FIN DATA FOR BODY PLUS TAIL CONFIGURATIONS
      READ(5,1)XF,YF,ZF,XFMAX,YFMAX,ZFMAX,SREFT
```

```
   20 DELTAR=DELTA/57.29577
C     READ NUMBER OF ANGLES OF ATTACK, NOSE TYPE AND NUMBER OF ROLL
C     ANGLES
      READ(5,3)NAOA,NTYPE,NLAM
C     READ ANGLES OF ATTACK
      READ(5,1)(AOAD(I),I=1,NAOA)
C     READ ROLL ANGLES
      READ(5,1)(RA(I),I=1,NLAM)
C     READ RADIAL LIMIT OF VORTEX INFLUENCE
      READ(5,1)GAMLIM
C     READ NOSE FINENESS AND BLUNTNESS OPTION DATA
      READ(5,4)IOPT,HRD
C     START ANGLE OF ATTACK LOOP
      DO 51 I=1,NAOA
      AOAR(I)=AOAD(I)/57.29577
   51 CONTINUE
      DO 52 I=1,NAOA
      ISKIP(I)=0
      ISTOP=0
      NORA=1
      LAM=RA(NORA)
      LAMD=LAM
      LAM=LAM/57.29577
      IF(IDCONF.EQ.0)GO TO 21
      XFR=AF
      YFR=-1.*(D/2.)*SIN(LAM)
      ZFR=(D/2.)*COS(LAM)
   21 DO 414 K=1,NS
      SF(K)=0.0
  414 CONTINUE
      DO 415 J=1,20
      AGSEP(J)=0.0
  415 CONTINUE
      CY(I)=0.0
      SROLM(I)=0.0
      CETA(I)=0.0
      CETAMC(I)=0.0
C     CROSS FLOW VELOCITY AND MACH NUMBER
      VC=VINF*SIN(AOAR(I))
      CFMN=FSMN*SIN(AOAR(I))
C     AXIAL VELOCITY AND MACH NUMBER
      AMAA=FSMN*COS(AOAR(I))
      VINFA=VINF*COS(AOAR(I))
      AOA=AOAD(I)
      IF(CFMN.GT.0.8)GO TO 52
C     GO TO NEXT ANGLE OF ATTACK IF CROSS FLOW MACH DATA EXCEEDED
      DO 30 II=1,17
      IIP1=II+1
      IF(IIP1.GT.17)GO TO 31
C     LOCATE CROSS FLOW MACH NUMBER IN DATA TABLE
      IF(CFMN.GE.TMACHC(II).AND.CFMN.LE.TMACHC(IIP1))GO TO 32
   30 CONTINUE
   32 DO 34 K=1,6
      KP1=K+1
      IF(KP1.GT.6)GO TO 31
      IF(AOA.GE.TALPHA(K).AND.AOA.LE.TALPHA(KP1))GO TO 35
   34 CONTINUE
C     INTERPOLATE FOR THOMSON VORTEX STRENGTH PARAMETER AND THOMSON
```

```
C      SEPARATION ANGLE PARAMETER
   35 A=(TMACHC(II)-CFMN)/(TMACHC(II)-TMACHC(IIP1))
      TGK=TGAMP(II,K)-(A*(TGAMP(II,K)-TGAMP(IIP1,K)))
      TGKP1=TGAMP(II,KP1)-(A*(TGAMP(II,KP1)-TGAMP(IIP1,KP1)))
      B=(TALPHA(K)-AOA)/(TALPHA(K)-TALPHA(KP1))
      GAMP=TGK-(B*(TGK-TGKP1))
      XI=TXI(II)-(A*(TXI(II)-TXI(IIP1)))
      DO 62 JJ=1,7
C      INTERPOLATE FOR THOMSON SEPARATION POINT PARAMETER
      GSEPP(JJ)=TGSEP(II,JJ)-(A*(TGSEP(II,JJ)-TGSEP(IIP1,JJ)))
   62 CONTINUE
      GO TO 36
   31 GAMP=0.0
C      CROSS FLOW REYNOLDS NUMBER
   36 RNC=VC*D/ANU
      PI=3.14159
C      VORTEX STRENGTH PARAMETER BASED ON NOSE POTENTIAL LIFT
      GAMP2=(PI/8.)*(2.*COS(AOAR(I))*(SIN(AOAR(I))**2.))
C      VORTEX STRENGTH SCALING FACTOR
      IF(FSMN.LE.1.0)RATIO=.25+(.1967*CFMN)+(1.7556*CFMN**2.)
      IF(FSMN.GT.1.0.AND.CFMN.LT.0.15)RATIO=0.25+(.1967*CFMN)+
     1(1.7556*CFMN**2.)
      IF(FSMN.GT.1.0.AND.CFMN.GE.0.15.AND.CFMN.LE.0.55)RATIO=
     10.25-(0.55754*CFMN)+(7.9698*CFMN**2.)-(8.159*CFMN**3.)
      IF(FSMN.GT.1.0.AND.CFMN.GT.0.55)RATIO=1.0
C      STROUHAL NUMBER
      S=.2
      IF(RNC.GT.1.E+05)S=0.35
      IF(IDCONF.EQ.1)S=.2
C      SHOULDER LOCATION IN TERMS OF SEPARATION POINT PARAMETER
      SNOSEL=NOSEL*TAN(AOAR(I))*S/D
C      THOMSON VORTEX SEPARATION ANGLE
      E=ATAN(XI*TAN(AOAR(I)))
C      LENGTH OF BODY INFLUENCED BY BASE EFFECTS
      EBASE=D/(2.*TAN(E))
      AXLE=BODYL-EBASE
      AGMENT=1.5*TAN(DELTAR)/TAN(AOAR(I))
      IF(AGMENT.GT.1.0)GO TO 52
C      CIRCUMFERENTIAL SEPARATION ANGLE
      THETAI=ASIN(1.5*TAN(DELTAR)/TAN(AOAR(I)))
C      VERTICAL DISTANCE BETWEEN VORTICES OF LIKE SIGN
      DL=D*XI/S
C      STABLE VORTEX STREET LATERAL SEPARATION DISTANCE
      H=.281*DL
      IF(RNC.LT.1.E+05)GO TO 55
C      SCALE THOMSON VORTEX STRENGTH FOR SUPERCRITICAL CROSS FLOW
C      REYNOLDS NUMBERS
      GAMP=GAMP*RATIO
C      THOMSON STREET VORTEX STRENGTH
   55 GAM=GAMP*VINF*D*SIN(AOAR(I))
      GAM1=GAM
C      AXIAL DISTANCE BETWEEN SEPARATION POINTS FOR STREET VORTICES OF
C      LIKE SIGN
      DG=(GSEPP(7)-GSEPP(5))*D/(TAN(AOAR(I))*S)
      DGAM=GAM1
C      STREET VORTEX GROWTH RATE
      GRATE=DGAM/DG
C      EFFECTIVE BODY LENGTH
```

```
      IF(IDCUNE.EQ.0)XF=-BODYL
      EBODYL = XF
C     BODY SEGMENT LENGTH
      SEGL=ABS(EBODYL)/NS
      DO 600 J=1,20
      IF(J.LT.8)GO TO 300
      JM2=J-2
      GSEPT(J)=GSEPT(JM2)+D3
      GO TO 600
C     VORTEX AXIAL SEPARATION POINTS AS DEFINED BY THOMSON
  300 GSEPT(J)=GSEPD(J)*D/(TAN(AUAR(I))*S)
  600 CONTINUE
C     ***************************************************************
C     CALCULATIONS TO DETERMINE COORDINATES OF ACTUAL SURFACE SEPARATION
C     POINTS USING THOMSON DATA, CIRCUMFERENTIAL SEPARATIONANGLES AND
C     LOCAL BODY DIAMETERS
C     ***************************************************************
      AXL =0.0
      J=1
  603 AXL=AXL + SEGL
      AXLMI = AXL-SEGL
  608 IF(GSEPT(J).LE.AXL.AND.GSEPT(J).GT.AXLMI)GO TO 602
      GO TO 603
  602 IF(GSEPT(J).GT.NOSEL)GO TO 604
      IF(NTYPE.EQ.2)GO TO 605
C     CONIC NOSE LOCAL RADIUS CALCULATIONS
      SIG = ASIN((D/2.)/NOSEL)
      RAXL=AXL*TAN(SIG)
      RAXLMI=AXLMI*TAN(SIG)
      Y2PRM=RAXL*SIN(THETAI)
      Y2=RAXLMI*SIN(THETAI)
      Y2BAR=(Y2+Y2PRM)/2.
      REMSEG=AXL-GSEPT(J)
      DELY=REMSEG*TAN(E)
      STEP=AXL
      IF(DELY.LT.Y2BAR)GO TO 606
      DELG=Y2BAR/TAN(E)
      GSEP(J)=GSEPT(J)+DELG
      GSEPY(J)=Y2BAR
      GSEPZ(J)=Y2BAR/TAN(THETAI)
      J=J+1
      IF(J.GT.20)GO TO 507
      GO TO 608
  606 STEP=STEP-SEGL
      STEPMI=STEP-SEGL
      RAXL=STEP*TAN(SIG)
      RAXLMI=STEPMI*TAN(SIG)
      Y2PRM=RAXL*SIN(THETAI)
      Y2=RAXLMI*SIN(THETAI)
      Y2BAR=(Y2+Y2PRM)/2.
      DELG=Y2BAR/TAN(E)
      GSEP(J)=GSEPT(J)+DELG
      IF(GSEP(J).GT.STEP)GO TO 606
      GSEPY(J)=Y2BAR
      GSEPZ(J)=Y2BAR/TAN(THETAI)
      J=J+1
      IF(J.GT.20)GO TO 507
      GO TO 608
```

```
      TANGENT OGIVE LOCAL RADIUS CALCULATIONS
  605 TORAD=(D/4.)+((NOSEL**2.)/D)
      RAXL=SQRT((TORAD**2.)-((AXL-NOSEL)**2 ))+((D/2.)-TORAD)
      RAXLM1=SQRT((TORAD**2.)-((AXLM1-NOSEL)**2 ))+((D/2.)-TORAD)
      Y2PRM=RAXL*SIN(THETAI)
      Y2=RAXLM1*SIN(THETAI)
      Y2BAR=(Y2PRM+Y2)/2.
      REMSEG=AXL-GSEPT(J)
      DELY=REMSEG*TAN(E)
      STEP=AXL
      IF(DELY.LT.Y2BAR)GO TO 609
      DELG=Y2BAR/TAN(E)
      GSEP(J)=GSEPT(J)+DELG
      GSEPY(J)=Y2BAR
      GSEPZ(J)=Y2BAR/TAN(THETAI)
      J=J+1
      IF(J.GT.20)GO TO 607
      GO TO 608
  609 STEP=STEP+SEG
      STEPM1=STEP-SEGL
      RAXL=SQRT((TORAD**2.)-((STEP-NOSEL)**2 ))+((D/2.)-TORAD)
      RAXLM1=SQRT((TORAD**2.)-((STEPM1-NOSEL)**2 ))+((D/2.)-TORAD)
      Y2PRM=RAXL*SIN(THETAI)
      Y2=RAXLM1*SIN(THETAI)
      Y2BAR=(Y2+Y2PRM)/2.
      DELG=Y2BAR/TAN(E)
      GSEP(J)=GSEPT(J)+DELG
      IF(GSEP(J).GT.STEP)GO TO 609
      GSEPY(J)=Y2BAR
      GSEPZ(J)=Y2BAR/TAN(THETAI)
      J=J+1
      IF(J.GT.20)GO TO 607
      GO TO 608
      VORTICES SEPARATE FROM CYLINDRICAL BODY SECTION
  604 Y2BAR=(D/2.)*SIN(THETAI)
      DELG=Y2BAR/TAN(E)
      GSEP(J)=GSEPT(J)+DELG
      GSEPY(J)=Y2BAR
      GSEPZ(J)=Y2BAR/TAN(THETAI)
      J=J+1
      IF(J.GT.20)GO TO 607
      GO TO 608
  607 NCOUNT=0
      ***************************************************************
      ADJUST VORTEX STRENGTHS ACCOUNTING FOR NOSE EFFECTS AND BASE
      INFLUENCE ON GROWTH RATE
      ***************************************************************
      JSTOR=0
      DO 53 J=1,20
      IF(J.GT.2)GO TO 95
      IF(J.EQ.1)GO TO 97
      IF(ABS(GSEP(1)).GE.NOSEL)GO TO 98
   97 IF(GSEP(J).GE.NOSEL)GO TO 98
      IF(NTYPE.EQ.2)GO TO 99
      SIG=ASIN((D/2.)/NOSEL)
      DCS=2.*GSEP(J)*TAN(SIG)
      GO TO 100
   99 TORAD=(D/4.)+((NOSEL**2.)/D)
```

```
      RCS=SQRT((TORAD**2.)-(ABS(GSEP(J)-NOSEL))**2.)+
     1((D/2.)-TORAD)
      DCS=2.*RCS
C     VORTEX STRENGTH FOR VORTICES SEPARATING ON NOSE SECTION
  100 GAM=GAMP2*VINF*SIN(ADAR(I))*DCS
      GO TO 96
   98 PGAM=GAMP2*VINF*SIN(ADAR(I))*D
      DELX1=GSEP(J)-NOSEL
      GAM=PGAM+DELX1*GRATE
      IF(GAM.GT.GAM1)GAM=GAM1
   96 IF(J.GT.1)GAM=-1.*GAM
      GSEP(J)=-1.0*GSEP(J)
      IF(ABS(GSEP(J)).GT.AXLE)GO TO 701
      GAMSV(J)=GAM
      GO TO 702
C     STREET VORTEX STRENGTH WHEN INFLUENCED BY BASE
  701 JM2=J-2
C     VORTEX STRENGTH ADJUSTED TO ACCOUNT FOR BASE EFFECTS
      IF(ABS(GSEP(JM2)).GT.AXLE)GAMSV(J)=0.4*GRATE*(ABS(GSEP(J))-ABS(GSE
     1P(JM2)))
      IF(ABS(GSEP(JM2)).LT.AXLE)GAMSV(J)=GRATE*(AXLE-ABS(GSEP(JM2)))+
     10.4*GRATE*(ABS(GSEP(J))-AXLE)
      IF(GAM.LT.0.0)GAMSV(J)=-GAMSV(J)
  702 IF(ABS(GSEP(J)).LE.ABS(EBODYL))GO TO 301
C     VORTEX STRENGTH CALCULATIONS FOR VORTICES FORCED TO SEPARATE
C     PREMATURELY BY THE EFFECTIVE BODY LENGTH
      JM1=J-1
      JM2=J-2
      DBODY=ABS(EBODYL)
      IF(NCOUNT.EQ.0.AND.ABS(GSEP(JM1)).EQ.ABS(EBODYL))GO TO 302
      IF(NCOUNT.EQ.1)GO TO 302
      NCOUNT = NCOUNT+1
      CALL XYZ(H,D,THETAI,AGSEP(J),GSEP(J),GSEP(JM2),DBODY,GSEPY(J),GSEP
     1Z(J),A1,A2)
      AGSEP(J)=GSEP(J)
C     SEPARATION POINT FIXED AT EFFECTIVE BODY LENGTH
      GSEP(J)=EBODYL
      IF(ABS(GSEP(JM2)).GE.AXLE)GAMSV(J)=0.4*GRATE*(ABS(GSEP(J))-
     1ABS(GSEP(JM2)))
      IF(ABS(GSEP(JM2)).LT.AXLE)GAMSV(J)=GRATE*(AXLE-ABS(GSEP(JM2)))+
     10.4*GRATE*(ABS(GSEP(J))-AXLE)
      IF(GAM.LT.0.0)GAMSV(J)=-GAMSV(J)
      GO TO 301
  302 CALL XYZ(H,D,THETAI,AGSEP(J),GSEP(J),GSEP(JM2),DBODY,GSEPY(J),GSEP
     1Z(J),A1,A2)
      AGSEP(J)=GSEP(J)
      GSEP(J)=EBODYL
      IF(ABS(GSEP(JM2)).GE.AXLE)GAMSV(J)=0.4*GRATE*(ABS(GSEP(J))-
     1ABS(GSEP(JM2)))
      IF(ABS(GSEP(JM2)).LT.AXLE)GAMSV(J)=GRATE*(AXLE-ABS(GSEP(JM2)))+
     10.4*GRATE*(ABS(GSEP(J))-AXLE)
      IF(GAM.LT.0.0)GAMSV(J)=-GAMSV(J)
      JMAX=J
      JSTOR=20
  301 IF(GAM.GT.0.0)GAM=GAM1
      IF(GAM.LT.0.0)GAM=-1.0*GAM1
      IF(JSTOR.EQ.20)GO TO 1000
   53 CONTINUE
```

```
      ***************************************************************
      AT THIS POINT ALL SHED VORTICES HAVE THEIR CORRECTED STRENGTHS
      AND SEPARATION POINTS ASSIGNED.  BEGIN CALCULATIONS TO DETERMINE
      THEIR INFLUENCE ON THE CONFIGURATION OF INTEREST.
      ***************************************************************
1000  JEND=JMAX+1
      CLEAR ARRAYS
      DO 610 J=JEND,20
      GSEP(J)=0.0
      GSEPY(J)=0.0
      GSEPZ(J)=0.0
 610  CONTINUE
      AXL=0.0
      SEGL=ABS(FBODYL)/NS
      DO 200 K=1,NS
      DO 260 II=1,JMAX
      GAMPC(II)=0.0
      SFPC(II)=0.0
      FMGPC(II)=0.0
      GPSV(II)=0.0
      SFPSV(II)=0.0
      FMGPSV(II)=0.0
      GBUTS(II)=0.0
      SFBUTS(II)=0.0
      FMGBUT(II)=0.0
      GBUAS(II)=0.0
      SFBUAS(II)=0.0
      FMBUAS(II)=0.0
      GBU(II)=0.0
      SFGBU(II)=0.0
      FMGBU(II)=0.0
  260 CONTINUE
C     EXAMINE SEGMENT OF INTEREST TO DETERMINE NUMBER OF  VORTICES
C     SEPARATING ON OR PRIOR TO IT
      AXL=AXL+SEGL
      DO 201 J=1,JMAX
      IF(AXL.GT.ABS(GSEP(J)))GO TO 201
      JM1=J-1
      GO TO 203
  201 CONTINUE
  203 IF(JM1.GT.0)GO TO 204
C     NO VORTICES SEPARATING ON OR PRIOR TO SEGMENT
      GAMT(K)=0.0
      SF(K)=0.0
      YMOM(K)=0.0
      GO TO 200
  204 AXLM1=AXL-SEGL
      ISTART=1
      DO 205 JVS=1,JM1
C     DOES VORTEX START ON OR PRIOR TO SEGMENT
      IF(ABS(GSEP(JVS)).GT.AXLM1)GO TO 206
C     ---------------------------------------------------------------
C     SEPARATED VORTICES PASSING OVER ENTIRE SEGMENT
C     ---------------------------------------------------------------
      IF(JVS.GT.2)GO TO 511
C     CIRCULATION ON SEGMENT DUE TO FIRST TWO VORTICES
      VDSP=TAN(E)*((AXLM1+(SEGL/2.))-ABS(GSEP(JVS)))
      VDCL=VDSP+((D/2.)*SIN(THETA1))
```

```
      RDIST=SQRT((VDCL**2.)+(((D/2.)*COS(THETAT))**2.))                00003670
      GAMPC(JVS)=GAMSV(JVS)*COS(E)                                     00003680
      GO TO 612                                                        00003690
C     CIRCULATION ON SEGMENT DUE TO  STREET VORTICES
  611 JVSM2=JVS-2                                                      00003700
      DSP=(AXL41+(SEGL/2.))-ABS(GSEP(JVSM2))                           00003710
      SIGMA=ATAN((SQRT((H/2.+SQRT((H/2.)**2.+                          00003720
     1(D/2.)**2.))**2.-(H/2.)**2.)-((D/2.)*                            00003730
     2SIN(THETAT))))/(ABS(GSEP(JVS))-ABS(GSEP(JVSM2))))                00003740
      XTHOM=(ABS(GSEP(JVSM2))*TAN(SIGMA)-ABS(GSEP(JVS))*TAN(E))        00003750
     1/(TAN(SIGMA)-TAN(E))                                             00003760
      XLEV=XTHOM-ABS(GSEP(JVSM2))                                      00003770
      IF(DSP.GT.XLEV)GO TO 613                                         00003780
      VDSP=TAN(SIGMA)*((AXL41+(SEGL/2.))-ABS(GSEP(JVS)))               00003790
      VDCL=VDSP+((D/2.)*SIN(THETAT))                                   00003800
      RDIST=SQRT((VDCL**2.)+((H/2.)**2.))                              00003810
C     CIRCULATION ON SEGMENT DUE TO STREET VORTEX TRANSITIONING BETWEEN
C     FOPPL AND THOMSON TRAJECTORIES
      GAMPC(JVS)=GAMSV(JVS)*COS(SIGMA)                                 00003820
      GO TO 612                                                        00003830
  613 VDSP=TAN(E)*((AXL41+(SEGL/2.))-ABS(GSEP(JVS)))                   00003840
      VDCL=VDSP+((D/2.)*SIN(THETAT))                                   00003850
      RDIST=SQRT((VDCL**2.)+((H/2.)**2.))                              00003860
C     CIRCULATION ON SEGMENT DUE TO STREET VORTICES FOLLOWING THOMSON
C     TRAJECTORY
      GAMPC(JVS)=GAMSV(JVS)*COS(E)                                     00003870
  612 RCAL=RDIST/D                                                     00003880
      IF(RCAL.GT.GAMLIM)GO TO 315                                      00003890
C     ADJUSTING INDUCED CIRCULATION FOR RADIAL DECAY
      GAMPC(JVS)=GAMPC(JVS)*((GAMLIM-RCAL)/GAMLIM)                     00003900
      GO TO 316                                                        00003910
  315 GAMPC(JVS)=0.0                                                   00003920
C     SIDE FORCE AND YAWING MOMENT CALCULATIONS
  316 SFPC(JVS)=ABS(GAMPC(JVS))*RHOINF*VC*SEGL                         00003930
      IF(GAMPC(JVS).GT.0.0)SFPC(JVS)=-SFPC(JVS)                        00003940
      FMGPC(JVS)=SFPC(JVS)*(AXL41+(SEGL/2.))                           00003950
      GO TO 205                                                        00003960
C     ----------------------------------------------------------------
C     VORTEX SEPARATES WITHIN BOUNDS OF SEGMENT
C     ----------------------------------------------------------------
  206 IF(ISTART.EQ.0)ISTART=JVS                                        00003970
      IF(JVS.GT.2)GO TO 614                                            00003980
C     CIRCULATION ON REMAINING PORTION OF SEGMENT DUE TO FIRST TWO
C     VORTICES
      VDSP=TAN(E)*(AXL-ABS(GSEP(JVS)))/2.                              00003990
      VDCL=VDSP+((D/2.)*SIN(THETAT))                                   00004000
      RDIST=SQRT((VDCL**2.)+(((D/2.)*COS(THETAT))**2.))                00004010
      GPSV(JVS)=GAMSV(JVS)*COS(E)                                      00004020
      GO TO 615                                                        00004030
C     CIRCULATION ON REMAINING PORTION OF SEGMENT DUE TO STREET VORTICES
  614 JVSM2=JVS-2                                                      00004040
      DSP=(ABS(GSEP(JVS))+((AXL-ABS(GSEP(JVS)))/2.0))-ABS(GSEP(JVSM2)) 00004050
      SIGMA = ATAN((SQRT((H/2. + SQRT((H/2.)**2. +                     00004060
     1(D/2.)**2.))**2. - (H/2.)**2.) - ((D/2.)*SIN(THETAT)))/          00004070
     2(ABS(GSEP(JVS))- ABS(GSEP(JVSM2))))                              00004080
      XTHOM = (ABS(GSEP(JVSM2))*TAN(SIGMA) - ABS(GSEP(JVS))*TAN(E))/   00004090
     1(TAN(SIGMA)- TAN(E))                                             00004100
      XLEV = XTHOM - ABS(GSEP(JVSM2))                                  00004110
```

```
      IF(DSP.GT.AXLEN)GO TO 516
      VDSP = TAN(SIGMA)* ((AXL - ABS(GSEP(JVS)))/2.)
      VDCL = VDSP +((D/2.) * SIN(THETAT))
      RDIST = SQRT((VDCL**2.) + ((H/2.)**2.))
C     CIRCULATION ON REMAINING PORTION OF SEGMENT DUE TO VORTICES
C     TRANSITIONING BETWEEN FOPPL AND THOMSON TRAJECTORIES
      GPSV(JVS) = GAMSV(JVS)*COS(SIGMA)
      GO TO 615
  616 VDSP = TAN(E) * ((AXL - ABS(GSEP(JVS)))/2.)
      VDCL = VDSP + ((D/2.) * SIN(THETAT))
      RDIST = SQRT((VDCL**2.) + ((H/2.)**2.))
C     CIRCULATION ON REMAINING PORTION OF SEGMENT DUE TO VORTICES
C     FOLLOWING THOMSON TRAJECTORY
      GPSV(JVS) = GAMSV(JVS) * COS(E)
  615 RCAL = RDIST/D
      IF(RCAL.GT.GAMLIM)GO TO 317
C     ADJUSTING INDUCED CIRCULATION TO ACCOUNT FOR RADIAL DECAY
      GPSV(JVS)=GPSV(JVS)*((GAMLIM-RCAL)/GAMLIM)
      GO TO 318
  317 GPSV(JVS)=0.0
C     SIDE FORCE AND YAWING MOMENT CALCULATIONS
  318 SFPSV(JVS)=ABS(GPSV(JVS))*RHOINF*VC*(AXL-ABS(GSEP(JVS)))
      IF(GPSV(JVS).GT.0.0)SFPSV(JVS)=-SFPSV(JVS)
      FMGPSV(JVS)=SFPSV(JVS)*(ABS(GSEP(JVS))+((AXL-ABS(GSEP(JVS)))/2.0))
  205 CONTINUE
C     GO TO 214 IF NO VORTICES SEPARATE ON SEGMENT OF INTEREST
      IF(ISTART.EQ.0)GO TO 214
C     ----------------------------------------------------------------
C     CALCULATE CIRCULATION INDUCED BY A GROWING VORTEX FROM THE
C     BEGINNING OF THE SEGMENT UP TO POINT OF SEPARATION
C     ----------------------------------------------------------------
      DO 207 N=ISTART,JH
      IF(N.GT.2)GO TO 209
      IF(N.LE.2.AND.ABS(GSEP(N)).GT.NOSEL)GO TO 209
C     NO CIRCULATION INDUCED BY POTENTIAL VORTICES UP TO POINT OF
C     SEPARATION
      GAUTS(N)=0.0
      SFAUTS(N)=0.0
      FMGAUT(N)=0.0
      GO TO 207
  209 IF(AXLM1.LT.NOSEL)GO TO 227
C     CIRCULATION INDUCED BY FIRST TWO VORTICES SEPARATING PAST THE
C     SHOULDER AND WITH THE SEGMENT LYING ENTIRELY ON THE CYLINDRICAL
C     PORTION OF BODY
      GAXLMI=((GAMP2*VINF*D*SIN(ADAR(I)))+((AXLM1-NOSEL)*GRATE))
      IF(AXLM1.GT.AXLE)GAXLMI=(GAMP2*VINF*D*SIN(ADAR(I)))+
     1((AXLE-NOSEL)*GRATE)+((AXLM1-AXLE)*GRATE*0.4)
      GSP=((GAMP2*VINF*D*SIN(ADAR(I)))+((ABS(GSEP(N))-NOSEL)*GRATE))
      IF(ABS(GSEP(N)).GT.AXLE)GSP=(GAMP2*VINF*D*SIN(ADAR(I)))+
     1((AXLE-NOSEL)*GRATE)+((ABS(GSEP(N))-AXLE)*GRATE*0.4)
  211 GAUTS(N)=(GSP+GAXLMI)/2.
      CALL EURO(N,ICASE)
      IF(ICASE.EQ.0)GO TO 237
      GO TO 238
  629 GAUTS(N)=0.0
  238 GAUTS(N)=-GAUTS(N)
C     SIDE FORCE AND YAWING MOMENT CALCULATIONS
  237 SFAUTS(N)=ABS(GAUTS(N))*RHOINF*VC*(ABS(GSEP(N))-AXLM1)
```

```
      IF(GBUTS(N).GT.0.0)SFBUTS(N)=-SFBUTS(N)
      FMGBUT(N)=SFBUTS(N)*(AXLM1+((ABS(GSEP(N))-AXLM1)/2.0))
      GO TO 207
  208 IF(N.GT.4)GO TO 210
C     CIRCULATION INDUCED BY GROWTH OF INITIAL TWO STREET VORTICES
C     EXPERIENCING MODIFIED GROWTH RATE
      NM2=N-2
      DIFF=(ABS(GSEP(N)))-(ABS(GSEP(NM2)))
      GRAD34=GAM1/DIFF
      GAXLM1=GRAD34*(AXLM1-ABS(GSEP(NM2)))
      IF(ABS(GSEP(NM2)).GT.AXLE)GAXLM1=0.4*GRAD34*(AXLM1-ABS(GSEP(NM2)))
      IF(AXLM1.GT.AXLE.AND.ABS(GSEP(NM2)).LT.AXLE)GAXLM1=((AXLE-
     1ABS(GSEP(NM2)))*GRAD34)+((AXLM1-AXLE)*GRAD34*0.4)
      GSP=GRAD34*(ABS(GSEP(N))-ABS(GSEP(NM2)))
      IF(ABS(GSEP(NM2)).GT.AXLE)GSP=0.4*GRAD34*(ABS(GSEP(N))-ABS(GSEP(NM
     12)))
      IF(ABS(GSEP(N)).GT.AXLE.AND.ABS(GSEP(NM2)).LT.AXLE)GSP=((AXLE
     1-ABS(GSEP(NM2)))*GRAD34)+((ABS(GSEP(N))-AXLE)*GRAD34*0.4)
      XPOINT = AXLM1 + ((ABS(GSEP(N)) - AXLM1)/2.)
      CALL XYZ(HD,THETA1,ASEP(N),GSEP(N),GSEP(NM2),XPOINT,Y,Z,A1,A2)
      RDIST = SQRT((Y**2.) + (Z**2.))
      RCAL = RDIST/D
      IF(RCAL.GT.GAMLIM)GO TO 620
C     ADJUSTING CIRCULATION TO ACCOUNT FOR RADIAL DECAY
      GAXLM1 = GAXLM1 * ((GAMLIM - RCAL)/GAMLIM)
      GSP = GSP * ((GAMLIM - RCAL)/GAMLIM)
      GAXLM1 = GAXLM1 *COS(A1) * COS(A2)
      GSP = GSP * COS(A1) * COS(A2)
      GO TO 211
  210 NM2=N-2
C     CIRCULATION INDUCED BY GROWTH OF STREET VORTICES HAVING NOMINAL
C     GROWTH RATE
      GAXLM1=GRATE*(AXLM1-ABS(GSEP(NM2)))
      IF(ABS(GSEP(NM2)).GT.AXLE)GAXLM1=0.4*GRATE*(AXLM1-ABS(GSEP(NM2)))
      IF(AXLM1.GT.AXLE.AND.ABS(GSEP(NM2)).LT.AXLE)GAXLM1=((AXLE
     1-ABS(GSEP(NM2)))*GRATE)+((AXLM1-AXLE)*GRATE*0.4)
      GSP=GRATE*(ABS(GSEP(N))-ABS(GSEP(NM2)))
      IF(ABS(GSEP(NM2)).GT.AXLE)GSP=0.4*GRATE*(ABS(GSEP(N))-ABS(GSEP(NM2
     1)))
      IF(ABS(GSEP(N)).GT.AXLE.AND.ABS(GSEP(NM2)).LT.AXLE)GSP=((AXLE-
     1ABS(GSEP(NM2)))*GRATE)+((ABS(GSEP(N))-AXLE)*GRATE*0.4)
      XPOINT = AXLM1 + ((ABS(GSEP(N)) - AXLM1)/2.)
      CALL XYZ(HD,THETA1,ASEP(N),GSEP(N),GSEP(NM2),XPOINT,Y,Z,A1,A2)
      RDIST = SQRT((Y**2.) + (Z**2.))
      RCAL = RDIST/D
      IF(RCAL.GT.GAMLIM)GO TO 620
      GAXLM1 = GAXLM1 * ((GAMLIM - RCAL)/GAMLIM)
C     ADJUSTING CIRCULATION TO ACCOUNT FOR RADIAL DECAY
      GSP = GSP * ((GAMLIM - RCAL)/GAMLIM)
      GAXLM1 = GAXLM1 *COS(A1) * COS(A2)
      GSP = GSP * COS(A1) * COS(A2)
      GO TO 211
C     CIRCULATION INDUCED BY FIRST TWO VORTICES SEPARATING PAST THE
C     SHOULDER BUT WITH A PORTION OF THE SEGMENT ON THE NOSE
  227 GAXLM1=0.0
      GNOSEL=GAMP2*VINF*D*SIN(AOAR(I))
      GSP=((GAMP2*VINF*D*SIN(AOAR(I)))+((ABS(GSEP(N))-NOSEL)*GRATE))
      IF(ABS(GSEP(N)).GT.AXLE)GSP=(GAMP2*VINF*D*SIN(AOAR(I)))+(
```

```
     1(AXLE-NOSEL)*GRATE)+((ABS(GSEP(N))-AXLE)*0.4*GRATE)            0A005030
      GBUTS(N)=(GNOSEL+GSP)/2.                                         0A005040
      CALL EORO(N,ICASE)                                               0A005050
      IF(ICASE.EQ.0)GO TO 240                                          0A005060
  241 GBUTS(N)=-GBUTS(N)                                               0A005070
C     SIDE FORCE AND YAWING MOMENT CALCULATIONS
  240 SFBUTS(N)=ABS(GBUTS(N))*RHOINF*VC*(ABS(GSEP(N))-NOSEL)          0A005080
      IF(GBUTS(N).GT.0.0)SFBUTS(N)=-SFBUTS(N)                          0A005090
      FMGBUT(N)=SFBUTS(N)*(NOSEL+((ABS(GSEP(N))-NOSEL)/2.0))          0A005100
  207 CONTINUE                                                         0A005110
C     ----------------------------------------------------------------
C
C     CALCULATE CIRCULATION INDUCED BY A GROWING VORTEX FROM THE POINT
C     OF SEPARATION TO THE END OF THE SEGMENT
C
C     ----------------------------------------------------------------
      DO 212 L=ISTART,JM1                                              0A005120
      IF(L.GT.2)GO TO 214                                              0A005130
      IF(L.LE.2.AND.ABS(GSEP(L)).GT.NOSEL)GO TO 214                    0A005140
      IF(L.EQ.2)GO TO 215                                              0A005150
C     CIRCULATION INDUCED BY GROWTH OF THIRD VORTEX
      DIFF=ABS(GSEP(3))-ABS(GSEP(1))                                   0A005160
      GRAD3=GAM1/DIFF                                                  0A005170
      GAXL=GRAD3*(AXL-ABS(GSEP(1)))                                    0A005180
      IF(ABS(GSEP(1)).GE.AXLE)GAXL=0.4*GRAD3*(AXL-ABS(GSEP(1)))        0A005190
      IF(ABS(GSEP(1)).LT.AXLE.AND.AXL.GT.AXLE)GAXL=((AXLE-ABS(GSEP(1)))*0A005200
     1GRAD3)+(0.4*GRAD3*(AXL-AXLE))                                    0A005210
      GSP=0.0                                                          0A005220
      LP2=L+2                                                          0A005230
      XPOINT = ABS(GSEP(L))+((AXL-ABS(GSEP(L)))/2.)                    0A005240
      CALL XYZ(H,D,THETAI,ABSEP(LP2),GSEP(LP2),GSEP(L),XPOINT,Y,Z,A1,A2)0A005250
      RDIST = SQRT((Y**2.)+(Z**2.))                                    0A005260
      RCAL = RDIST/D                                                   0A005270
      IF(RCAL.GT.GAMLIM)GO TO 621                                      0A005280
C     ADJUSTING INDUCED CIRCULATION TO ACCOUNT FOR RADIAL DECAY
      GAXL = GAXL*((GAMLIM-RCAL)/GAMLIM)                               0A005290
      GAXL = GAXL * COS(A1) * COS(A2)                                  0A005300
  216 GBUAS(LP2)=(GAXL+GSP)/2.                                         0A005310
      CALL EORO(LP2,ICASE)                                             0A005320
      IF(ICASE.EQ.0)GO TO 242                                          0A005330
      GO TO 243                                                        0A005340
  621 GBUAS(LP2)=0.0                                                   0A005350
  243 GBUAS(LP2)=-GBUAS(LP2)                                           0A005360
C     SIDE FORCE AND YAWING MOMENT CALCULATIONS
  242 SFBUAS(LP2)=ABS(GBUAS(LP2))*RHOINF*VC*(AXL-ABS(GSEP(L)))         0A005370
      IF(GBUAS(LP2).GT.0.0)SFBUAS(LP2)=-SFBUAS(LP2)                    0A005380
      FMBUAS(LP2)=SFBUAS(LP2)*(ABS(GSEP(L))+((AXL-ABS(GSEP(L)))/2.))  0A005390
      GO TO 212                                                        0A005400
C     CIRCULATION INDUCED BY GROWTH OF FORTH VORTEX
  215 DIFF2=ABS(GSEP(4))-ABS(GSEP(2))                                  0A005410
      GRAD4=GAM1/DIFF2                                                 0A005420
      GAXL=GRAD4*(AXL-ABS(GSEP(2)))                                    0A005430
      IF(ABS(GSEP(2)).GE.AXLE)GAXL=0.4*GRAD4*(AXL-ABS(GSEP(2)))        0A005440
      IF(ABS(GSEP(2)).LT.AXLE.AND.AXL.GT.AXLE)GAXL=((AXLE-ABS(GSEP(2)))*0A005450
     1GRAD4)+(0.4*GRAD4*(AXL-AXLE))                                    0A005460
      GSP=0.0                                                          0A005470
      LP2=L+2                                                          0A005480
      XPOINT = ABS(GSEP(L))+((AXL-ABS(GSEP(L)))/2.)                    0A005490
      CALL XYZ(H,D,THETAI,ABSEP(LP2),GSEP(LP2),GSEP(L),XPOINT,Y,Z,A1,A2)0A005500
      RDIST = SQRT((Y**2.)+(Z**2.))                                    0A005510
```

```
      RCAL = RDIST/D
      IF(RCAL.GT.GAMLIM)GO TO 621
C     ADJUSTING INDUCED CIRCULATION TO ACCOUNT FOR RADIAL DECAY
      GAXL = GAXL*((GAMLIM-RCAL)/GAMLIM)
      GAXL = GAXL * COS(A1) * COS(A2)
      GO TO 216
C     CIRCULATION INDUCED BY STREET VORTEX EXPERIENCING NOMINAL GROWTH
C     RATE
  214 GAXL=GRATE*(AXL-ABS(GSEP(L)))
      LP2=L+2
      IF(ABS(GSEP(L)).GT.AALE)GAXL=0.4*GRATE*(AXL-ABS(GSEP(L)))
      IF(ABS(GSEP(L)).LT.AALE.AND.AXL.GT.AXLE)GAXL=((AXLE-ABS(GSEP(L)))*
     1GRATE)+(0.4*GRATE*(AXL-AXLE))
      GSP=0.0
      XPOINT = ABS(GSEP(L))+((AXL-ABS(GSEP(L)))/2.)
      CALL XYZ(H,D,THETAI,AGSEP(LP2),GSEP(LP2),GSEP(L),XPOINT,Y,Z,A1,A2)
      RDIST = SQRT((Y**2.)+(Z**2.))
      RCAL = RDIST/D
      IF(RCAL.GT.GAMLIM)GO TO 621
      GAXL = GAXL*((GAMLIM-RCAL)/GAMLIM)
      GAXL = GAXL * COS(A1) * COS(A2)
      GO TO 216
  212 CONTINUE
C     ****************************************************************
C     IF ISTART DOES NOT EQUAL JM1, THIS MEANS THAT NO GROWING VORTICES
C     CAN PASS OVER THE FULL LENGTH OF THE SEGMENT.  THEREFORE ALL
C     CIRCULATION CALCULATIONS FOR THE SEGMENT ARE COMPLETE.  GO TO 221
C     ****************************************************************
      IF(ISTART.NE.JM1)GO TO 221
C     ----------------------------------------------------------------
C     CALCULATE GROWTH OVER SEGMENT DUE TO A SINGLE VORTEX GROWING
C     OVER THE ENTIRE SEGMENT LENGTH
C     ----------------------------------------------------------------
      JNEXT=ISTART+1
      IF(JNEXT.EQ.2)GO TO 219
      IF(JNEXT.GT.2)GO TO 220
  219 IF(AAL.GT.NOSEL.AND.AALM1.GE.NOSEL)GO TO 223
      IF(AAL.GT.NOSEL)GO TO 226
C     SEGMENT ENTIRELY ON NOSE
      GBU(JNEXT)=0.0
      GO TO 224
C     CIRCULATION INDUCED ON SEGMENT BY GROWTH OF SECOND VORTEX WITH
C     THE SEGMENT STARTING ON THE NOSE
  226 GAXLM1=0.0
      GNOSEL=GAMP2*VINF*D*SIN(ADAR(I))
      GAXL=((GAMP2*VINF*D)*SIN(ADAR(I)))+((AXL-NOSEL)*GRATE))
      IF(AAL.GT.AXLE)GAXL=(GAMP2*VINF*D*SIN(ADAR(I)))+
     1((AXLE-NOSEL)*GRATE)+((AXL-AALE)*GRATE*0.4)
      GBU(JNEXT)=(GAXL+GNOSEL)/2.
      CALL FORD(JNEXT,ICASE)
      IF(ICASE.EQ.0)GO TO 246
  247 GBU(JNEXT)=-GBU(JNEXT)
C     SIDE FORCE AND YAWING MOMENT CALCULATIONS
  246 SFGBU(JNEXT)=ABS(GBU(JNEXT))*RHO*VINF*VC*(AXL-NOSEL)
      IF(GBU(JNEXT).GT.0.0)SFGBU(JNEXT)=-SFGBU(JNEXT)
      FMGBU(JNEXT)=SFGBU(JNEXT)*(NOSEL+((AXL-NOSEL)/2.))
      GO TO 221
C     CIRCULATION INDUCED ON SEGMENT BY GROWTH OF SECOND VORTEX WITH
```

```
      THE ENTIRE SEGMENT WING ON THE CYLINDRICAL BODY SECTION
  223 GAXLMI=((GAMP2*VINF*D*SIN(ADAR(I)))+((AXLMI-NOSEL)*GRATE))
      IF(AXLMI.GT.AXLE)GAXLMI=(GAMP2*VINF*D*SIN(ADAR(I)))+
     1((AXLE-NOSEL)*GRATE)+((AXLMI-AXLE)*GRATE*0.4)
      GAXL=((GAMP2*VINF*D*SIN(ADAR(I)))+((AXL-NOSEL)*GRATE))
      IF(AXL.GT.AXLE)GAXL=(GAMP2*VINF*D*SIN(ADAR(I)))+
     1((AXLE-NOSEL)*GRATE)+((AXL-AXLE)*GRATE*0.4)
  225 GBU(JNEXT)=(GAXL+GAXLMI)/2.
      CALL EORU(JNEXT,ICASE)
      IF(ICASE.EQ.0)GO TO 224
      GO TO 245
  622 GBU(JNEXT)=0.0
  245 GBU(JNEXT)=-GBU(JNEXT)
:     SIDE FORCE AND YAWING MOMENT CALCULATIONS
  224 SFGBU(JNEXT)=ABS(GBU(JNEXT))*RHOINF*VC*SEGL
      IF(GBU(JNEXT).GT.0.0)SFGBU(JNEXT)=-SFGBU(JNEXT)
      FMGBU(JNEXT)=SFGBU(JNEXT)*(AXLMI+(SEGL/2.))
      GO TO 221
  220 IF(JNEXT.GT.4)GO TO 222
:     CIRCULATION INDUCED BY INITIAL TWO STREET VORTICES HAVING A
:     MODIFIED GROWTH RATE
      JNM2=JNEXT-2
      IF(ABS(GSEP(JNM2)).GT.NOSEL)GO TO 222
      DIFF=ABS(GSEP(JNEXT))-ABS(GSEP(JNM2))
      GRAD34=GAMI/DIFF
      GAXLMI=GRAD34*(AXLMI-ABS(GSEP(JNM2)))
      IF(ABS(GSEP(JNM2)).GT.AXLE)GAXLMI=0.4*GRAD34*(AXLMI-ABS(GSEP(JNM2))
     1))
      IF(AXLMI.GT.AXLE.AND.ABS(GSEP(JNM2)).LT.AXLE)GAXLMI=((AXLE
     1-ABS(GSEP(JNM2)))*GRAD34)+((AXLMI-AXLE)*GRAD34*0.4)
      GAXL=GRAD34*(AXL-ABS(GSEP(JNM2)))
      IF(ABS(GSEP(JNM2)).GT.AXLE)GAXL=0.4*GRAD34*(AXL-ABS(GSEP(JNM2)))
      IF(AXL.GT.AXLE.AND.ABS(GSEP(JNM2)).LT.AXLE)GAXL=((AXLE-
     1ABS(GSEP(JNM2)))*GRAD34)+((AXL-AXLE)*GRAD34*0.4)
      XPOINT = AXLMI + (SEGL/2.)
      CALL XYZ(H,D,THETAT,ABSEP(JNEXT),GSEP(JNEXT),GSEP(JNM2),XPOINT,Y,Z
     1,A1,A2)
      RDIST = SQRT((Y**2.)+(Z**2.))
      RCAL = RDIST/D
      IF(RCAL.GT.GAMLIM)GO TO 622
      GAXLMI = GAXLMI * ((GAMLIM - RCAL)/GAMLIM)
:     ADJUSTING CIRCULATION TO ACCOUNT FOR RADIAL DECAY
      GAXL = GAXL * ((GAMLIM - RCAL)/GAMLIM)
      GAXLMI = GAXLMI * COS(A1) *COS(A2)
      GAXL = GAXL * COS(A1) *COS(A2)
      GO TO 225
  222 JNM2=JNEXT-2
:     CIRCULATION INDUCED BY STREET VORTICES HAVING REGULAR GROWTH RATE
      GAXLMI=GRATE*(AXLMI-ABS(GSEP(JNM2)))
      IF(ABS(GSEP(JNM2)).GT.AXLE)GAXLMI=0.4*GRATE*(AXLMI-ABS(GSEP(JNM2))
     1)
      IF(AXLMI.GT.AXLE.AND.ABS(GSEP(JNM2)).LT.AXLE)GAXLMI=((AXLE-
     1ABS(GSEP(JNM2)))*GRATE)+((AXLMI-AXLE)*GRATE*0.4)
      GAXL=GRATE*(AXL-ABS(GSEP(JNM2)))
      IF(ABS(GSEP(JNM2)).GT.AXLE)GAXL=0.4*GRATE*(AXL-ABS(GSEP(JNM2)))
      IF(AXL.GT.AXLE.AND.ABS(GSEP(JNM2)).LT.AXLE)GAXL=((AXLE-
     1ABS(GSEP(JNM2)))*GRATE)+(AXL-AXLE)*GRATE*0.4
      XPOINT = AXLMI + (SEGL/2.)
```

```
      CALL XYZ(H,D,THETA1,ABSEP(JNEXT),BSEP(JNEXT),GSEP(JNM2),XPOINT,Y,Z0
     1,A1,A2)
      RDIST = SQRT((Y**2.)+(Z**2.))
      RCAL = RDIST/D
      IF(RCAL.GT.GAMLIM)GO TO 622
      GAXLMI = GAXLMI * ((GAMLIM - RCAL)/GAMLIM)
      GAXL = GAXL * ((GAMLIM - RCAL)/GAMLIM)
      GAXLMI = GAXLMI * COS(A1) *COS(A2)
      GAXL = GAXL * COS(A1) *COS(A2)
      GO TO 225
C     ******************************************************************
C     COME TO 218 WHEN NO VORTICES SEPARATE WITHIN BOUNDS OF SEGMENT
C     OF INTEREST.  TWO GROWING VORTICES PASS OVER THE  ENTIRE SEGMENT.
C     ******************************************************************
  218 JP1=J+1
      DO 228 J1=J,JP1
      IF(J1.EQ.2)GO TO 229
      IF(J1.GT.2)GO TO 230
  229 IF(AXL.GT.NOSEL.AND.AXLMI.GE.NOSEL)GO TO 231
      IF(AXL.GT.NOSEL)GO TO 232
C     SEGMENT ENTIRELY ON NOSE
      GBU(J1)=0.0
      GO TO 233
C     CIRCULATION INDUCED BY SECOND VORTEX WHEN SEGMENT STARTS ON NOSE
  232 GAXLMI=0.0
      GNOSEL=GAMP2*VINF*D*SIN(ADAR(I))
      GAXL=((GAMP2*VINF*D*SIN(ADAR(I)))+((AXL-NOSEL)*GRATE))
      IF(AXL.GT.AXLE)GAXL=(GAMP2*VINF*D*SIN(ADAR(I)))+((AXLE-NOSEL)*
     1GRATE)+((AXL-AXLE)*0.4*GRATE)
      GBU(J1)=(GAXL+GNOSEL)/2.
      CALL EURO(J1,ICASE)
      IF(ICASE.EQ.0)GO TO 233
  249 GBU(J1)=-GBU(J1)
C     SIDE FORCE AND YAWING MOMENT CALCULATIONS
  233 SFGBU(J1)=ABS(GBU(J1))*RHOINF*VC*(AXL-NOSEL)
      IF(GBU(J1).GT.0.0)SFGBU(J1)=-SFGBU(J1)
      FMGBU(J1)=SFGBU(J1)*(NOSEL+((AXL-NOSEL)/2.))
      GO TO 228
C     CIRCULATION INDUCED BY SECOND VORTEX WHEN ENTIRE SEGMENT IS ON
C     CYLINDRICAL PORTION OF BODY
  231 GAXLMI=((GAMP2*VINF*D*SIN(ADAR(I)))+((AXLMI-NOSEL)*GRATE))
      IF(AXLMI.GT.AXLE)GAXLMI=(GAMP2*VINF*D*SIN(ADAR(I)))+
     1((AXLE-NOSEL)*GRATE)+((AXLMI-AXLE)*GRATE*0.4)
      GAXL=((GAMP2*VINF*D*SIN(ADAR(I)))+((AXL-NOSEL)*GRATE))
      IF(AXL.GT.AXLE)GAXL=(GAMP2*VINF*D*SIN(ADAR(I)))+
     1((AXLE-NOSEL)*GRATE)+((AXL-AXLE)*GRATE*0.4)
  236 GBU(J1)=(GAXL+GAXLMI)/2.
      CALL EURO(J1,ICASE)
      IF(ICASE.EQ.0)GO TO 250
      GO TO 251
  623 GBU(J1)=0.0
  251 GBU(J1)=-GBU(J1)
C     SIDE FORCE AND YAWING MOMENT CALCULATIONS
  250 SFGBU(J1)=ABS(GBU(J1))*RHOINF*VC*SEGL
      IF(GBU(J1).GT.0.0)SFGBU(J1)=-SFGBU(J1)
      FMGBU(J1)=SFGBU(J1)*(AXLMI+(SEGL/2.))
      GO TO 228
  230 IF(J1.GT.4)GO TO 235
```

```
C      CIRCULATION INDUCED BY INITIAL TWO STREET VORTICES HAVING MODIFIED
C      GROWTH RATE
       J1M2=J1-2
       DIFF=ABS(GSEP(J1))-ABS(GSEP(J1M2))
       GRAD34=GAM1/DIFF
       GAXLM1=GRAD34*(AXLM1-ABS(GSEP(J1M2)))
       IF(ABS(GSEP(J1M2)).GT.AXLE)GAXLM1=0.4*GRAD34*(AXLM1-ABS(GSEP(J1M2)
      1))
       IF(AXLM1.GT.AXLE.AND.ABS(GSEP(J1M2)).LT.AXLE)GAXLM1=((AXLE
      1-ABS(GSEP(J1M2)))*GRAD34)+((AXLM1-AXLE)*GRAD34*0.4)
       GAXL=GRAD34*(AXL-ABS(GSEP(J1M2)))
       IF(ABS(GSEP(J1M2)).GT.AXLE)GAXL=0.4*GRAD34*(AXL-ABS(GSEP(J1M2)))
       IF(AXL.GT.AXLE.AND.ABS(GSEP(J1M2)).LT.AXLE)GAXL=((AXLE
      1-ABS(GSEP(J1M2)))*GRAD34)+((AXL-AXLE)*GRAD34*0.4)
       XPOINT = AXLM1 + (SEGLV2.)
       CALL XYZ(H,D,THETAI,ABSEP(J1),GSEP(J1),GSEP(J1M2),XPOINT,Y,Z,A1,A2
      1)
       RDIST=SQRT((Y**2.)+(Z**2.))
       RCAL = RDIST/D
       IF(RCAL.GT.GAMLIM)GO TO 623
C      ADJUSTING CIRCULATION TO ACCOUNT FOR  RADIAL DECAY
       GAXLM1 = GAXLM1 * ((GAMLIM - RCAL)/GAMLIM)
       GAXL = GAXL * ((GAMLIM - RCAL)/GAMLIM)
       GAXLM1 = GAXLM1 * COS(A1) * COS(A2)
       GAXL = GAXL * COS(A1) *COS(A2)
       GO TO 236
  234  J1M2=J1-2
C      CIRCULATION INDUCED ON SEGMENT BY STREET VORTICES HAVING NOMINAL
C      GROWTH RATE
       GAXLM1=GRATE*(AXLM1-ABS(GSEP(J1M2)))
       IF(ABS(GSEP(J1M2)).GT.AXLE)GAXLM1=0.4*GRATE*(AXLM1-ABS(GSEP(J1M2))
      1)
       IF(AXLM1.GT.AXLE.AND.ABS(GSEP(J1M2)).LT.AXLE)GAXLM1=((AXLE-
      1ABS(GSEP(J1M2)))*GRATE)+((AXLM1-AXLE)*GRATE*0.4)
       GAXL=GRATE*(AXL-ABS(GSEP(J1M2)))
       IF(ABS(GSEP(J1M2)).GT.AXLE)GAXL=0.4*GRATE*(AXL-ABS(GSEP(J1M2)))
       IF(AXL.GT.AXLE.AND.ABS(GSEP(J1M2)).LT.AXLE)GAXL=((AXLE-
      1ABS(GSEP(J1M2)))*GRATE)+((AXL-AXLE)*GRATE*0.4)
       XPOINT = AXLM1 + (SEGLV2.)
       CALL XYZ(H,D,THETAI,ABSEP(J1),GSEP(J1),GSEP(J1M2),XPOINT,Y,Z,A1,A2
      1)
       RDIST=SQRT((Y**2.)+(Z**2.))
       RCAL = RDIST/D
       IF(RCAL.GT.GAMLIM)GO TO 623
C      ADJUSTING CIRCULATION TO ACCOUNT FOR RADIAL DECAY
       GAXLM1 = GAXLM1 * ((GAMLIM - RCAL)/GAMLIM)
       GAXL = GAXL * ((GAMLIM - RCAL)/GAMLIM)
       GAXLM1 = GAXLM1 * COS(A1) * COS(A2)
       GAXL = GAXL * COS(A1) *COS(A2)
       GO TO 236
  228  CONTINUE
  221  SF(K)=0.0
       FMT(K)=0.0
C      ZEROING OUT CONTRIBUTIONS FROM SHED VORTICES
       DO 239 JT=1,JMAX
       SFPC(JT)=0.0
       FMGPC(JT)=0.0
       SFPSV(JT)=0.0
```

```
      FMGPSV(JT)=0.0                                                    0n007440
C     SUM CONTRIBUTIONS TO SIDE FORCE AND YAWING MOMENT ON EACH SEGMENT
      SF(K)=SF(K)+SFPC(JT)+SFPSV(JT)+SFBUTS(JT)+SFBUAS(JT)+SF3BU(JT)    0n007450
      FMT(K)=FMT(K)+FMGPC(JT)+FMGPSV(JT)+FMGBUT(JT)+FMBUAS(JT)          0n007460
     1+FM3BU(JT)                                                        0n007470
  239 CONTINUE                                                          0n007480
C     CALCULATE SEGMENT CENTER OF PRESSURE
      XARM=ABS(FMT(K))/ABS(SF(K))                                       0n007490
      YMOM(K)=SF(K)*XARM                                                0n007500
C     GO TO NEXT SEGMENT AND REPEAT CALCULATIONS
  200 CONTINUE                                                          0n007510
      TSF=0.0                                                           0n007520
      TYMOM=0.0                                                         0n007530
C     SUM SIDE FORCE AND YAWING MOMENT CONTRIBUTIONS FROM ALL SEGMENTS
      DO 312 K=1,NS                                                     0n007540
      TSF=TSF+SF(K)                                                     0n007550
      TYMOM=TYMOM+YMOM(K)                                               0n007560
  312 CONTINUE                                                          0n007570
C     GO TO 59 IF ISOLATED BODY
      IF(IDCONF.EQ.0)GO TO 59                                           0n007580
      JMAX1=JMAX
      DO 350 K=1,JMAX                                                   0n007590
      IF(ABS(GSEP(K)).LE.ABS(EBODYL))GO TO 350                          0n007600
      JMAX1=K-1
      GO TO 352                                                         0n007620
  350 CONTINUE                                                          0n007630
  352 NFF1=0                                                            0n007640
      JMAX=JMAX1
      FNF1(I)=0.0                                                       0n007650
      SROLM(I)=0.0                                                      0n007660
C     CALL FINCAL TO CARRY OUT VORTEX/FIN INTERACTION CALCULATIONS
  351 CALL FINCAL(JMAX,GAMSV(1),XFR,YFR,ZFR,XFMAX,XF,ZFMAX,ZF,LAM,      0n007670
     1GSEPY(1),GSEPZ(1),H,E,PI,D,VINFA,SREFT,RHOINF,GSEP(1),RNFY,ISTOP, 0n007680
     2RNF,HYCP,ROLM)                                                    0n007690
      IF(ISTOP.EQ.1)ISKIP(I)=1                                          0n007700
C     IF ISTOP=1 A VORTEX PASSES WITHIN 1/4 BODY RADIUS OF FIN,
C     DISCONTINUE CALCULATIONS,GO TO NEXT ANGLE OF ATTACK
      IF(ISTOP.EQ.1)GO TO 55                                            0n007710
      SROLM(I)=SROLM(I)+ROLM                                            0n007720
C     SUM SIDE FORCE AND YAWING MOMENT
      TSF=TSF+RNFY                                                      0n007730
      TYMOM=TYMOM+((ABS(EBODYL)+(ABS(XFMAX-XF)/2.))*RNFY)               0n007740
      IF(LAM.EQ.0.0)NFF1=1                                              0n007750
      IF(LAM.EQ.0.0)FNF1(I)=RNF                                         0n007760
      NORA=NORA+1                                                       0n007770
C     GO TO 58 WHEN CONTRIBUTIONS FROM ALL FINS HAVE BEEN CALCULATED
      IF(NORA.GT.NLAM)GO TO 58                                          0n007780
      LAM=RA(NORA)                                                      0n007790
      LAMD=LAM                                                          0n007800
      LAM=LAM/57.29577                                                  0n007810
C     CALCULATE COORDINATES OF FIN ROOT CHORD LEADING EDGE
      XFR=XF                                                            0n007820
      YFR=-1.*(D/2.)*SIN(LAM)                                           0n007830
      ZFR=(D/2.)*COS(LAM)                                               0n007840
      GO TO 351                                                         0n007850
C     CALCULATE FREE STREAM DYNAMIC PRESSURE
   58 Q=.5*RHOINF*(VINF**2.)                                            0n007860
C     CALCULATE SIDE FORCE AND YAWING MOMENT COEFFICIENTS
```

```
      CY(I)=TSF/(Q*SREF)                                                 00007870
      CETA(I)=TYMOM/(Q*SREF*D)                                           00007880
C     TRANSFER OF YAWING MOMENT
      CETAMC(I)=((CETA(I)/CY(I))-(XMC/D))*CY(I)                          00007890
   52 CONTINUE                                                           00007900
      IF(IDCONF.EQ.0)GO TO 23                                            00007910
C     PRINT BODY PLUS TAIL OUTPUT
      IF(NFF1.NE.0)WRITE(5,8)XMC                                         00007920
    8 FORMAT(3X,15HANGLE OF ATTACK,4X,2HCY,6X,6HCETAMC,7X,9HROLL MOM.,
     24X,12HNORMAL FORCE,/,
     36X,9H(DEGREES),14X,3HCG=,F5.2,2HFT,5X,7H(FT-LB),4X,
     416H(FIN NO. 1 (LB)))
      IF(NFF1.EQ.0)WRITE(5,10)XMC                                        00007970
   10 FORMAT(3X,15HANGLE OF ATTACK,4X,2HCY,6X,6HCETAMC,7X,9HROLL MOM.,/,
     2 6X,9H(DEGREES),14X,3HCG=,F5.2,2HFT,5X,7H(FT-LB))
      DO 313 I=1,NAOA                                                    00008000
      IF(ISKIP(I).NE.0)GO TO 313                                         00008010
      IF(NFF1.NE.0)WRITE(5,9)AOAD(I),CY(I),CETAMC(I),SROLM(I),FNFI(I)    00008020
    9 FORMAT(7X,F5.2,6X,F7.3,5X,F7.3,6X,F7.3,7X,F8.3)                    00008030
      IF(NFF1.EQ.0)WRITE(5,11)AOAD(I),CY(I),CETAMC(I),SROLM(I)           00008040
   11 FORMAT(7X,F6.2,6X,F7.3,5X,F7.3,6X,F7.3)                            00008050
  313 CONTINUE                                                           00008060
      GO TO 24                                                           00008070
C     PRINT ISOLATED BODY OUTPUT
   23 WRITE(6,25)XMC                                                     00008080
   25 FORMAT(3X,15HANGLE OF ATTACK,4X,2HCY,6X,6HCETAMC,/,
     26X,9H(DEGREES),14X,3HCG=,F5.2,2HFT)
      DO 26 I=1,NAOA                                                     00008110
      WRITE(6,27)AOAD(I),CY(I),CETAMC(I)                                 00008120
   27 FORMAT(7X,F6.2,6X,F7.3,5X,F7.3)                                    00008130
   26 CONTINUE                                                           00008140
      IF(IOPT.NE.1)GO TO 24                                              00008150
C     IF IOPT=1  SCALE ISOLATED BODY OUTPUT FOR NOSE FINENESS RATIO AND
C     BLUNTNESS RATIO EFFECTS
      CALL OPT1(FSMN,NOSE,BOWBRN,XMC,CY(1),CETA(1),CETAMC(1),            00008160
     2IPASS,NAOA)                                                        00008161
      IF(IPASS.EQ.0)GO TO 24                                             00008170
      WRITE(6,800)                                                       00008180
  800 FORMAT(1X,12HPICKS OPTION)
      WRITE(6,25)XMC                                                     00008200
      DO 801 I=1,NAOA                                                    00008210
      WRITE(6,27)AOAD(I),CY(I),CETAMC(I)                                 00008220
  801 CONTINUE                                                           00008230
   24 READ(5,4)IRUN                                                      00008270
C     CHECK TO SEE IF ANOTHER RUN IS TO BE MADE
      IF(IRUN.EQ.1)GO TO 41                                              00008280
      CALL EXIT                                                          00008290
      END                                                                00008300
```

XYZ

```
      SUBROUTINE XYZ(H,D,THETAI,AJ,XJ,XJM2,X,Y,Z,PI,DELTA)              00008310
C     ****************************************************************
C     SUBROUTINE XYZ CALCULATES COORDINATES OF POINTS ALONG VORTEX
C     GROWTH TRAJECTORY
C     ****************************************************************
      IF(ABS(AJ).GT.ABS(XJ))GO TO 100                                    00008320
C     CALCULATE COORDINATES OF POINTS ALONG GROWTH TRAJECTORY OF A
C     NORMAL STREET VORTEX
      PI =ATAN(((H/2.)-((D/2.)*COS(THETAI)))/(ABS(XJ)-ABS(XJM2)))       00008330
      CEBAR=(ABS(XJ) -X)/COS(PI)                                         00008340
      ACBAR = SQRT((((H/2.)-((D/2.)*COS(THETAI)))**2 )+                  00008350
     1((ABS(XJ)-ABS(XJM2))**2 ))                                         00008360
      Z=(H/2.) - ((ABS(XJ)- X)*TAN(PI))                                  00008370
  101 DELTA = ATAN((SQRT(((H/2.)+SQRT(((H/2.)**2.)+((D/2.)**2.)))**2.    00008380
     1-((H/2.)**2.))-((D/2.)*SIN(THETAI)))/ACBAR)                        00008390
      Y = ((ACBAR-CEBAR)*TAN(DELTA))+((D/2.)*COS(THETAI))                00008400
      GO TO 102                                                          00008410
C     CALCULATE COORDINATES OF POINTS ALONG GROWTH TRAJECTORY OF A
C     VORTEX FORCED TO SEPARATE AT THE BASE OF THE BODY
  100 PI = ATAN(((H/2.)-((D/2.)*COS(THETAI)))/(ABS(AJ)-ABS(XJM2)))      00008420
      CEBAR =(ABS(AJ)-X)/COS(PI)                                         00008430
      ACBAR =SQRT((((H/2.)-((D/2.)*COS(THETAI)))**2 )+                   00008440
     1((ABS(AJ)-ABS(XJM2))**2 ))                                         00008450
      Z= (H/2.)-((ABS(AJ)-X)*TAN(PI))                                    00008460
      GO TO 101                                                          00008470
  102 RETURN                                                             00008480
      END                                                                00008490
```

```
SUBROUTINE EORO(INT,IEO)
*************************************************************************
SUBROUTINE EORO DETERMINES IF A VORTEX IS NUMBERED EVEN OR ODD..
THIS DETERMINES THE SIGN APPLIED TO THE CIRCULATION
*************************************************************************
INTD2=INT/2
INP1=INT+1
INP1D2=INP1/2
IEO=1
IF(INP1D2.GT.INTD2)IEO=0
ODD IEO=0
EVEN IEO=1
RETURN
END
```

```
      SUBROUTINE FINCAL(JMAX,GAMSV,XFR,YFR,ZFR,XFMAX,XF,ZFMAX,ZF,LAM,
     1GSEPT,GSEPZ,H,E,PHI,D,VINFA,SREF,RHOINF,GSEP,RNFY,ISTOP,
     2RNF,RYCP,ROLM)
      REAL LAM
      DIMENSION GAMSV(1),GSEPT(1),GSEPZ(1),GSEP(1),X(10),Y(10),Z(10),
     1VNT(10),VT(10),AOAOS(10),VNBAR(20),FN(20)
      DIMENSION YCP(20)
C     SUBROUTINE FINCAL CALCULATES THE NORMAL FORCE INDUCED ON FINS BY
C     SHED VORTICES  IN THE BODY LEE SIDE WAKE
C     ******************************************************************
      JSTART=JMAX-1
      DO 53 J=JSTART,JMAX
C     SHED VORTEX STRENGTH
      GAM=GAMSV(J)
C     CALCULATION OF COORDINATES ON FIN LEADING EDGE WHERE CALCULATIONS
C     ARE TO BE MADE
      X(1)=XFR
      Y(1)=YFR
      Z(1)=ZFR
      FLES=(XFMAX-XF)/(ZFMAX-ZF)
      DELZ=(ZFMAX-ZF)/10.
      DO 51 I=1,10
      IF(I.GT.1)GO TO 56
      X(I)=FLES*(DELZ/2.)+X(I)
      Z(I)=Z(I)+(DELZ/2.)*COS(LAM)
      Y(I)=Y(I)-(DELZ/2.)*SIN(LAM)
      GO TO 57
   56 K=I-1
      X(I)=FLES*DELZ+X(K)
      Z(I)=Z(K)+DELZ*COS(LAM)
      Y(I)=Y(K)-DELZ*SIN(LAM)
C     AXIAL DISTANCE FROM POINT OF VORTEX SEPARATION TO POINT ON FIN
   57 DELX=ABS(X(I)+GSEPT(J))
C     DEFINITION OF VORTEX LATERAL DISPLACEMENT
      IF(GAM.GT.0.0.AND.J.LE.2)YVCL=-GSEPZ(J)
      IF(GAM.GT.0.0.AND.J.GT.2)YVCL=-H/2.
      IF(GAM.GT.0.0.AND.J.EQ.JSTART.OR.J.EQ.JMAX)YVCL=-GSEPZ(J)
       IF(GAM.LT.0.0.AND.J.LE.2)YVCL=GSEPZ(J)
      IF(GAM.LT.0.0.AND.J.GT.2)YVCL=H/2.
      IF(GAM.LT.0.0.AND.J.EQ.JSTART.OR.J.EQ.JMAX)YVCL=GSEPZ(J)
      A1=(ABS(Z(I)-DELX*TAN(E)))*COS(E)
      B1=ABS(YVCL-Y(I))
      ANGLE=ATAN(A1/B1)
      BBAR=DELX/COS(E)
      DBBAR=(ABS(DELX*TAN(E)-Z(I)))*SIN(E)
      BBAR=BBAR-DBBAR
      ZADJ=BBAR*SIN(E)
      PHII=ANGLE
C     RADIAL DISTANCE FROM VORTEX CORE TO POINT ON FIN MEASURED ALONG
C     A LINE PERPENDICULAR TO THE VORTEX CORE
   67 RI=(ABS(Z(I)-DELX*TAN(E)))*COS(E)/SIN(PHII)
      RID=RI/(D/2.)
C     IF VORTEX PASSES WITHIN 1/4 BODY RADIUS OF POINT ON FIN
C     DISCONTINUE CALCULATIONS
      IF(RID.LE.0.25)GO TO 21
C     VELOCITY INDUCED AT POINT ON FIN BY VORTEX
      VTI=GAM/(2.*PI*RI)
C     COMPONENTS OF VELOCITY
```

```
      VYI=VTI*SIN(PHII)
      VZI=VTI*COS(PHII)*COS(E)
      IF(ZADJ.LT.Z(I))GO TO 86
      IF(YVCL.LT.Y(I))GO TO 87
      VYI=-1.*VYI
      GO TO 69
   87 VYI=-1.*VYI
      VZI=-1.*VZI
      GO TO 69
   86 IF(YVCL.LT.Y(I))VZI=-1.*VZI
   69 VYNI=VYI*COS(LAM)
      VZNI=VZI*SIN(LAM)
C     NORMAL COMPONENT OF VELOCITY INDUCED ON FIN BY VORTEX
      VNI=VYNI+VZNI
      A2=ABS(Z(I)-DELX*TAN(E))
      B2=ABS(YVCL-Y(I))
      ANGLE2=ATAN(A2/B2)
      ZADJ2=DELX*TAN(E)
      PHI2=ANGLE2
   70 R2=(ABS(Z(I)-DELX*TAN(E)))/SIN(PHI2)
      IF(YVCL.GT.Y(I).AND.ZADJ2.GT.Z(I))GO TO 88
      IF(YVCL.LT.Y(I).AND.ZADJ2.GT.Z(I))GO TO 89
      IF(YVCL.GT.Y(I).AND.ZADJ2.LT.Z(I))GO TO 90
      IF(YVCL.LT.Y(I).AND.ZADJ2.LT.Z(I))GO TO 91
C     DEFINITION OF EQUIVALENT VORTEX STRENGTH
   88 GAM2=VNI*(2.*PHI*R2)/(COS(PHI2)*SIN(LAM)-SIN(PHI2)*COS(LAM))
      GO TO 73
   89 GAM2=-1.*VNI*(2.*PHI*R2)/(SIN(PHI2)*COS(LAM)+COS(PHI2)*SIN(LAM))
      GO TO 73
   90 GAM2=VNI*(2.*PHI*R2)/(SIN(PHI2)*COS(LAM)+COS(PHI2)*SIN(LAM))
      GO TO 73
   91 GAM2=VNI*(2.*PHI*R2)/(SIN(PHI2)*COS(LAM)-COS(PHI2)*SIN(LAM))
C     LOCATION OF IMAGE VORTEX
   73 F=SQRT((ABS(YVCL))**2.)+(DELX*TAN(E))**2.)
      GI=((D/2.)**2.)/F
      THETA=ATAN((ABS(YVCL))/(DELX*TAN(E)))
      IF(GAM2.GT.0.0)THETA=-1.*THETA
      YI=GI*SIN(THETA)
      ZI=GI*COS(THETA)
      RI=SQRT(((ABS(Y(I)-YI))**2.)+(ABS(Z(I)-ZI))**2.)
      GAMI=-1.*GAM2
C     CALCULATE VELOCITY INDUCED AT POINT ON FIN BY IMAGE VORTEX
      VTI=GAMI/(2.*PHI*RI)
      A2I=ABS(Z(I)-ZI)
      B2I=ABS(YI-Y(I))
      ANGLEI=ATAN(A2I/B2I)
      PHI2I=ANGLEI
      VYI=VTI*SIN(PHI2I)
      VZI=VTI*COS(PHI2I)
      IF(ZI.LT.Z(I))GO TO 92
      IF(YI.LT.Y(I))GO TO 93
      VYI=-1.*VYI
      GO TO 76
   93 VYI=-1.*VYI
      VZI=-1.*VZI
      GO TO 76
   92 IF(YI.LT.Y(I))VZI=-1.*VZI
   76 VYNI=VYI*COS(LAM)
```

```
      VZNI=VZI*SIN(LAM)                                                  00009580
C     NORMAL COMPONENT OF VELOCITY INDUCED AT POINT ON FIN BY IMAGE
C     VORTEX
      VNI=VYNI+VZNI                                                      00009590
      RC=SQRT(ABS(Y(I))**2.+ABS(Z(I))**2.)                               00009600
C     CALCULATION OF NORMAL COMPONENT OF VELOCITY INDUCED AT POINT
C     ON FIN BY CENTRAL VORTEX
      VNC=GAM2/(2.*PHI*RC)                                               00009610
C     SUMMATION OF NORMAL VELOCITY COMPONENTS FOR ALL SEGMENTS
      VNT(I)=VNI+VNI+VNC                                                 00009620
   51 CONTINUE                                                           00009630
      VT(J)=0.0                                                          00009640
      DO 52 I=1,10                                                       00009650
      VT(J)=VT(J)+VNT(I)                                                 00009660
   52 CONTINUE                                                           00009670
      DO 83 I=1,10                                                       00009680
C     EFFECTIVE ANGLE OF ATTACK INDUCED AT POINT ON FIN
      AOADS(I)=ATAN(ABS(VNT(I))/VINFA)                                   00009690
      IF(VNT(I).GT.0.0)AOADS(I)=-1.*AOADS(I)                             00009700
   83 CONTINUE                                                           00009710
      SYADY=0.0                                                          00009720
      SADY=0.0                                                           00009730
      DO 84 I=1,10                                                       00009740
      IF(I.EQ.1)YCPI=D/2.+DELZ/2.                                        00009750
      IF(I.GT.1)YCPI=YCPI+DELZ                                           00009760
      SYADY=AOADS(I)*YCPI*DELZ+SYADY                                     00009770
      SADY=AOADS(I)*DELZ+SADY                                            00009780
   84 CONTINUE                                                           00009790
C     FIN SPANWISE CENTER OF PRESSURE
      YCP(J)=SYADY/SADY                                                  00009800
C     AVERAGE VELOCITY INDUCED AT FIN LEADING EDGE
      VNBAR(J)=ABS(VT(J)/10.)                                            00009810
      AIND=ATAN(VNBAR(J)/VINFA)                                          00009820
      VELR=SQRT((VINFA**2.)+(VNBAR(J)**2.))                              00009830
      AR=2.*(ZFMAX-ZF)**2./SREF                                          00009840
      CNA=PHI*AR/2.                                                      00009850
      Q=0.5*RHOINF*(VELR**2.)                                            00009860
C     NORMAL FORCE INDUCED ON FIN BY A VORTEX
      FN(J)=CNA*AIND*Q*SREF                                              00009870
      AIND=AIND*57.29                                                    00009880
      IF(VT(J).LT.0.0)FN(J)=-1.*FN(J)                                    00009890
C     LOOP AND CALCULATE NORMAL FORCE INDUCED BY ALL OTHER VORTICES IN
C     WAKE
   53 CONTINUE                                                           00009900
      RNF=0.0                                                            00009910
C     RESULTANT FIN NORMAL FORCE
      DO 54 I=JSTART,JMAX                                                00009920
      RNF=RNF+FN(I)                                                      00009930
   54 CONTINUE                                                           00009940
      RNFY=RNF*COS(LAM)                                                  00009950
      RNFZ=RNF*SIN(LAM)                                                  00009960
      RM=0.0                                                             00009970
C     CALCULATE ROLLING MOMENT
      DO 85 I=JSTART,JMAX                                                00009980
      RM=RM+YCP(I)*FN(I)                                                 00009990
   85 CONTINUE                                                           00010000
      RYCP=ABS(RM)/ABS(RNF)                                              00010010
      ROLM=-1.*RNF*RYCP                                                  00010020
```

```
      GO TO 23
   21 ISTOP=1
   23 RETURN
      END
```

OPT1

```
      SUBROUTINE OPT1(FSMN,AN,D,BRN,AIC,CY,CETA,CETAMC,IPASS,NADA)
      DIMENSION FRK(6,4),TMACH(6),TFR(4),TBR(5),BRK2(6,5),
     2BRK3(6,5),BRK4(6,5),CY(1),CETA(1),CETAMC(1)
C     ******************************************************************
C     SUBROUTINE OPT1 SCALES ISOLATED BODY SIDE FORCE AND YAWING
C     MOMENT FOR FINENESS RATIO AND BLUNTNESS RATIO EFFECTS
C     ******************************************************************
      DATA TMACH/0.5,0.5,0.6,0.8,0.9,1.1/
      DATA TFR/2.0,3.0,3.759,4.0/
      DATA FRK/0.267,0.555,1.081,1.037,0.603,0.089,
     2         0.839,0.989,1.339,1.429,0.373,0.180,
     3         1.000,1.000,1.000,1.000,1.000,1.000,
     4         1.014,0.957,0.406,0.714,1.269,1.389/
      DATA TBR/0.0,0.5,10.0,20.0,50.0/
      DATA BRK2/1.000,1.000,1.000,1.000,1.000,1.000,
     2          1.000,1.000,1.000,1.000,1.000,1.000,
     3          0.130,0.224,0.239,0.343,0.222,2.750,
     4          3.261,2.134,2.194,3.257,2.815,2.875,
     5          1.000,0.776,1.119,1.543,0.222,2.250/
      DATA BRK3/1.000,1.000,1.000,1.000,1.000,1.000,
     2          1.000,1.000,1.000,1.000,1.000,1.000,
     3          0.703,0.495,0.940,2.440,0.720,1.667,
     4          0.736,0.522,1.450,2.000,2.920,1.778,
     5          0.796,0.431,0.255,0.220,1.000,0.778/
      DATA BRK4/1.000,1.000,1.000,1.000,1.000,1.000,
     2          1.000,1.000,1.000,1.000,1.000,1.000,
     3          0.477,0.575,0.600,3.440,1.082,0.502,
     4          0.477,0.545,0.613,2.320,0.212,0.176,
     5          0.295,0.551,0.700,3.440,1.412,0.376/
      IF(FSMN.LT.0.5.OR.FSMN.GT.1.1)GO TO 1
      FRN=AN/D
      IF(FRN.LT.2.0.OR.FRN.GT.4.0)GO TO 1
      IF(BRN.GT.50.0)GO TO 1
      IPASS=1
      DO 2 I=1,3
      J=I+1
      IF(FRN.GE.TFR(I).AND.FRN.LE.TFR(J))GO TO 3
    2 CONTINUE
    3 IFR=I
      IFR1=J
      DO 4 I=1,5
      J=I+1
      IF(FSMN.GE.TMACH(I).AND.FSMN.LE.TMACH(J))GO TO 5
    4 CONTINUE
    5 IM=I
      IM1=J
      RATIO=(TMACH(IM)-FSMN)/(TMACH(IM)-TMACH(IM1))
      F1=FRK(IM,IFR)-(RATIO*(FRK(IM,IFR)-FRK(IM1,IFR)))
      F2=FRK(IM,IFR1)-(RATIO*(FRK(IM,IFR1)-FRK(IM1,IFR1)))
      FRKI=F1-(F1-F2)*((TFR(IFR)-FRN)/(TFR(IFR)-TFR(IFR1)))
      IF(BRN.LE.5.0)GO TO 9
      DO 7 I=2,4
      J=I+1
      IF(BRN.GE.TBR(I).AND.BRN.LE.TBR(J))GO TO 8
    7 CONTINUE
    8 IBR=I
      IBR1=J
      F1=BRK3(IM,IBR)-(RATIO*(BRK3(IM,IBR)-BRK3(IM1,IBR)))
```

OPT1

```
      F2=BRK3(IM,IBR1)-(RATIO*(BRK3(IM,IBR1)-BRK3(IM1,IBR1)))
      FI=F1-(F1-F2)*((TBR(IBR)-BRN)/(TBR(IBR)-TBR(IBR1)))
      IF(FRN.GE.3.0.AND.FRN.LE.4.0)GO TO 10
      G1=BRK2(IM,IBR)-(RATIO*(BRK2(IM,IBR)-BRK2(IM1,IBR)))
      G2=BRK2(IM,IBR1)-(RATIO*(BRK2(IM,IBR1)-BRK2(IM1,IBR1)))
      RATIO1=(2.0-FRN)/(2.0-3.0)
      GO TO 11
   10 G1=BRK4(IM,IBR)-(RATIO*(BRK4(IM,IBR)-BRK4(IM1,IBR)))
      G2=BRK4(IM,IBR1)-(RATIO*(BRK4(IM,IBR1)-BRK4(IM1,IBR1)))
      RATIO1=(4.0-FRN)/(4.0-3.0)
   11 GI=G1-(G1-G2)*((TBR(IBR)-BRN)/(TBR(IBR)-TBR(IBR1)))
      BRKI=GI-(GI-FI)*RATIO1
      GO TO 12
    9 BRKI=1.0
   12 DO 13 I=1,NADA
      CY(I)=CY(I)*FRKI*BRKI
      CETA(I)=CETA(I)*FRKI*BRKI
      CETAMC(I)=((CETA(I)/CY(I))-(XMC/D))*CY(I)
   13 CONTINUE
      GO TO 14
    1 IPASS=0
   14 RETURN
      END
```

6.4 Sample Inputs/Outputs

Isolated Bodies

Input:

VINF	=	890.0	ft/sec
FSMN	=	0.8	
RHOINF	=	0.000642	lb sec^2/ft^4
ANU	=	0.000575	ft^2/sec
D	=	0.312	ft
SREF	=	0.0768	ft^2
NOSEL	=	0.936	ft
BODYL	=	3.12	ft
XMC	=	2.0	ft
DELTA	=	9.45	deg
NS	=	50	
IDCONF	=	0	
NAOA	=	15	
NTYPE	=	2	
NLAM	=	1	
AOAD	=	24., 25., 26., 28., 30., 32., 34., 36., 38., 40., 42., 44., 46., 48., 50.	
RA	=	0.0	
GAMLIM	=	100.	
IOPT1	=	1	
BRN	=	0.0	
IRUN	=	0	

Output:

ANGLE OF ATTACK (DEGREES)	CY	CETAMC CG= 2.00FT
24.00	0.486	1.209
25.00	0.342	0.891
26.00	0.155	0.537
28.00	-0.287	-0.255
30.00	-0.791	-0.909
32.00	-0.705	0.308
34.00	-0.241	2.254
36.00	0.251	3.872
38.00	-0.069	2.334
40.00	-0.693	0.319
42.00	-1.137	-0.774
44.00	-0.389	2.218
46.00	0.455	4.772
48.00	-0.324	1.495
50.00	-1.163	-1.341

PICKS OPTION

ANGLE OF ATTACK (DEGREES))	CY	CETAMC CG= 2.00FT
24.00	0.694	1.728
25.00	0.489	1.273
26.00	0.222	0.767
28.00	-0.410	-0.365
30.00	-1.130	-1.299
32.00	-1.008	0.441
34.00	-0.344	3.221
36.00	0.358	5.573
38.00	-0.099	3.336
40.00	-0.991	0.456
42.00	-1.625	-1.105
44.00	-0.556	3.169
46.00	0.651	6.819
48.00	-0.463	2.136
50.00	-1.662	-1.916

Body Plus Tail

Input:

VINF	=	921.0	ft/sec
FSMN	=	0.8	
RHOINF	=	0.00059	lb sec^2/ft^4
ANU	=	0.000574	ft^2/sec
D	=	0.312	ft
SREF	=	0.0768	ft^2
NOSEL	=	0.938	ft
BODYL	=	3.12	ft
XMC	=	2.0	ft
DELTA	=	9.45	deg
NS	=	50	
IDCONF	=	1	
XF	=	-2.709	ft
YF	=	0.0	ft
ZF	=	0.1561	ft
XFMAX	=	-2.917	ft
YFMAX	=	0.0	ft
ZFMAX	=	0.312	ft
SREFT	=	0.049	ft^2
NAOA	=	18	
NTYPE	=	2	
NLAM	=	4	
AOAD	=	25., 27., 29., 31., 33., 35., 37.,39., 41., 43., 45., 47., 49., 51., 53., 55., 57., 59.	
RA	=	0.0, 90., 180., 270.	
GAMLIM	=	100.	
IOPTI	=	0	
BRN	=	0	
IRUN	=	0	

OUTPUT

ANGLE OF ATTACK (DEGREES)	CY	CETAMC CG= 2.00 FT	ROLL MOM. (FT-LB)	NORMAL FORCE FIN NO. 1 (LB)
25.00	0.355	-0.820	-0.607	0.939
29.00	0.353	-1.026	-0.797	1.767
31.00	0.490	-0.484	0.001	1.120
33.00	0.767	0.376	0.116	1.208
35.00	1.013	1.171	0.487	0.594
37.00	1.190	1.856	1.199	-0.964
39.00	1.285	2.314	2.215	-3.388
43.00	0.651	2.669	-0.155	-1.884
45.00	-0.096	1.650	-0.839	-0.640
47.00	-0.804	1.111	-2.174	2.498
51.00	-1.315	1.445	0.374	1.705
53.00	-0.522	3.404	2.680	-0.899
55.00	0.176	4.468	3.296	-5.729
57.00	-0.238	3.576	-0.470	-1.280
59.00	-0.538	1.324	-2.087	2.631

The results of these two sample outputs, are compared against experimental data in Figures 12a and b and 13a and b

6.5 Program Limitations

There are certain limits which apply to the application of the procedures and program described in this document. Following is a list of the program limitations which the user must be familiar with before trying to use the program.

a. The program is crossflow Mach number limited to values between 0.15 and 0.8.

b. Due to the large side wash velocities and correspondingly large fin normal forces produced when a vortex core passes close to a fin, the program has been set up to discontinue calculations at angles of attack when a vortex core passes within 1/4 body radius of a fin and proceed to the next angle of attack. The 1/4 body radius limitation was selected after comparing the results of numerous runs against experimental data.

A potential vortex model is used in the program. The velocity produced by such a vortex at a radius R is given by the following equation:

$$V_t = \frac{\Gamma}{2\pi r}$$

It is because of this that the induced side wash velocities becomes so large when a vortex core passes close to a fin. In actuality a vortex has a viscous core beyond which the vortex can be modeled by a potential vortex. In the viscous core the velocity goes to zero at the center. In order to retain as simple a model as possible, it was decided to place the limitation described above on the program.

c. The program should only be applied to configurations which have $\phi = 0°$ or 45°. This is because the program only calculates fin forces induced by the presence of an asymmetric vortex system. Only at these roll angles do the forces on the fins produced by flow conditions other than vortices cancel themselves out due to opposite senses of direction.

d. Physically it is logical that the side force induced on the finless portion of a body is contributed to by both feeding sheets and shed vortices. However, comparisons between predictions and experimental data have indicated that the best results will be obtained when the contributions from shed vortices are neglected. The program logic predicts both contributions but prior to the point at which total side force is calculated the contributions from shed vortices are set equal to zero. This is accomplished by inserting the following

SFPC (JT) = 0.0	FMPGC (JT) = 0.0	Side force and yawing moment induced by a shed vortex passing over a complete segment
SFPSV (JT) = 0.0	FMGPSV (JT) = 0.0	Side force and yawing moment induced by a vortex shedding within the bounds of a segment

within the do-loop ending with statement 239.

These cards may be removed at anytime in order to study the effects of shed vortices on body side forces.

e. Caution is advised when employing the option to correct for nose fineness and bluntness ratios. The reason for this being that the scaling factors were derived from data showing considerable scatter. Also due to the unsteady nature of the vortex phenomenon, it is possible that considerably different scaling factors could be derived using other data sources.

REFERENCES

1. Thomson, K. D. and Morrison, D. F., "The Spacing, Position and Strength of Vortices in the Wake of Slender, Cylindrical Bodies at Large Incidence," Journal Fluid Mech., 50, 1971
2. Thomson, K. D., "The Estimation of the Drag of Circular Cylinders at Sub-Critical Reynolds Numbers and Subsonic Speeds," Journal R. Ae. Society, September 1970
3. Pick, G. S., "Investigation of Side Forces on Ogive-Cylinder Bodies at High Angles of Attack in the M=0.5 to 1.1 Range," AIAA Paper 71-570, 1971
4. Briggs, M. M., Clark, W. H., and Peoples, J. R., "Occurrence and Inhibition of Large Yawing Moments During High Incidence Flight of Slender Missile Configurations," AIAA Second Atmosphere Flight Conference, Palo Alto, California, September 1972
5. Fleeman, E. L. and Nelson, R. C., "Aerodynamic Forces and Moments on a Slender Body with a Jet Plume for Angles of Attack up to 180 Degrees," AIAA Paper 74-110
6. Fidler, J. E., "Approximate Method for Estimating Wake Vortex Strength," AIAA Journal, May 1974
7. Kubin, J. F., "An Analysis of Steady Asymmetric Vortex Shedding from a Missile at High Angles of Attack," Thesis, U.S.A.F. Institute of Technology, GAM/AE/73A-13, Wright-Patterson AFB, Ohio, December 1973
8. Thomson, K. D., "The Estimation of Viscous Normal Force, Pitching Moment, Side Force and Yawing Moment on Bodies of Revolution at Incidences up to 90 Degrees," Australian Weapons Res. Est. WRE-Report-782, 1972

9. Wardlaw, A. B., "Prediction of Yawing Force at High Angle of Attack," AIAA Journal, August 1974

10. Allen, H. J. and Perkins, E. W., "Characteristics of Flow over Inclined Bodies of Revolution," NACA RM A50L07, 1951

11. Perkins, E. W. and Jorgensen, L. H., "Comparison of Experimental and Theoretical Normal Force Distributions (including Reynolds Number Effects) on an Ogive-Cylinder at Mach 1.98," NACA TN3716, 1956

12. Kelley, H. R., "The Estimation of Normal-Force and Pitching-Moment Coefficients for Blunt-Based Bodies of Revolution at Large Angles of Attack," J. Aerospace Sci. 21, August 1954

13. Hill, J. A. F., "A Non-Linear Theory of the Life on Slender Bodies of Revolution," Proceedings, U.S. Navy Symposium on Aerolsallistics, U.S. Naval Ordnance Test Station Rpt. 5338, 1954

14. Milne-Thomson, L. M., Theoretical Hydrodynamics, Third Ed., MacMillian Company, New York, 1955

15. Liepmann, H. W. and Roshko, A., Elements of Gasdynamics, John Wiley and Sons Inc., New York, 1966

16. Fidler, J. E., "A Systematic Experimental Approach to Upgrading Missile Aerodynamic Technology," Ninth U.S. Navy Symposium on Aeroballistics, 1972

17. Achenbach, E., "Distribution of Local Pressure and Skin Friction around a Circular Cylinder in Cross-Flow up to Re = 5×10^6," Journal Fluid Mech. 34, 1968

18. Jorgensen, L. H. and Perkins, E. W., "Investigation of Some Wake Vortex Characteristics of an Inclined Ogive-Cylinder Body at Mach Number 2," NACA Report 1371, 1958.

19. Pick, G. Personal Communication, October 1975, NSRDC

END 7-79